Adsorption Removal of Arsenic from Water Using Iron Hydroxide Loaded Cellulose Beads

By

Chuan Liang

A Thesis

In

Chemical Engineering

Submitted to the Graduate Faculty
of Texas Tech University in
Partial Fulfillment of
the Requirements for
the Degree of

MASTER OF SCIENCE

Approved

Danny Reible
Chair of Committee

Chongzheng Na

Nurxat Nuraje

Mark Sheridan
Dean of the Graduate School

December 2017

ACKNOWLEDGMENTS

First and foremost, I would like to express my sincere gratitude to my advisor, Prof. Danny Reible for the continuous support of my Master's study and research, for his patience, kindness and immense knowledge. It has been my honor to be offered this opportunity to come to his group. His guidance helped me under how research should be done, solve the problems arisen in research, promote the research progress and be aware of the importance of mathematics.

My sincere thanks also go to Prof. Chongzheng Na, the co-advisor. Every discussion with him has refreshed my knowledge and helped me better understand the topic. His wisdom and enthusiasm in this project have greatly help me successfully finish my research and thesis.

I would like to thank the postdocs Haitao Wang, who greatly helped me in preparing the materials, designing experiments and analyzing data; Balaji Rao and Magdalena who helped me deal with lab management and use of instrument; and Xiaolong Shen who helped me solve the modeling problems.

I would like to give my thanks to Brad, the unit manager. Only with his management of lab security and kind help using ICP-MS can I finish my experiments and obtain all the data I need.

I would like to thank my fellow labmates in the Reible research group: Tianyu Chen, Songjing Yan, Xin Zhang, Tariq, Ilektra, Alex Smith, Giovanna, Dimitri, Tea, Michelle for their kind help in the lab.

Last but not least, I would like to thank my wife for her support in all the difficulties and our parents for their understanding and support.

TABLE OF CONTENTS

ABSTRACT

Arsenic contamination in groundwater has posed global challenges to drinking water supply. Due to the awareness of its toxicity and chronic effects on human health, removal of arsenic from water using adsorptive materials has been extensively studied. Iron-based composite materials are a group of promising adsorbents due to their high affinity to arsenic species.

In the present research, iron hydroxide loaded bead cellulose adsorbents have been synthesized through a one-step hydrolysis and coating procedure using five different loading percentages ranging from 3.8% to 21.7% in terms of mass of iron. Adsorption kinetics at various concentrations of arsenite (As(III)) and arsenate (As(V)) were tested in batch experiments. The adsorption competition by coexisting phosphate and sulphate and the regeneration performance were also investigated. The adsorption kinetics were modeled using the Pseudo-second-order kinetics equation and the calculated equilibrium concentrations and adsorption capacities were used to build the adsorption isotherms, which were then fitted using Langmuir and Freundlich equations. The Langmuir adsorption capacity (in terms of mg arsenic per g dry mass of bead) of As(III) increased from 49.9 mg/g to 92.0 mg/g when the iron content increased from 3.84% to 17.7%, followed by a slight decrease to 86.1 mg/g when the iron content continued increasing to 21.7%. The adsorption capacity for As(V) showed a linear increasing, reaching 26.9 mg/g, with the increase of iron content. The coexisting PO_4^{3-} of 5 mg P/L and 500 mg SO_4^{2-}/L reduced the equilibrium adsorption capacity for As(III) by 14.5% and 24.4%, respectively. After two cycles of regeneration by 2.0 M NaOH solutions, the adsorbent showed 99.2% of the original adsorption capacity for As(III).

The breakthrough behavior of As(III) and As(V) were investigated in packed

bed column experiments. To determine the dispersion coefficients of arsenic in the column, the breakthrough curve of methylene blue as a tracer was obtained and modeled using the equilibrium convection diffusion equation. The estimated dispersion coefficient was 1.9 cm^2/h at a flow rate of 361.4 cm/h for As(III) and 2.9 cm^2/h at 561.1 cm/h for As(V), respectively. Parameters controlling the breakthrough behavior of arsenic were then estimated by fitting the Two-sites nonequilibrium convection diffusion equation to the experimental data using the Stanmod modeling package. The results showed that almost all the adsorption sites (96.46% for As(III) and 99.56% for As(V)) were at nonequilibrium adsorption state. The first order kinetics controlled the adsorption of As(III) and As(V) in the column at a rate of 0.0017 h^{-1} and 0.0018 h^{-1}, respectively. The estimated partition coefficient for As(III) and As(V) was 99812.7 L/kg and 200721.8 L/kg, respectively.

LIST OF TABLES

LIST OF FIGURES

CHAPTER 1
GENERAL INTRODUCTION

1.1 Background

The contamination of groundwater by arsenic is a global environmental issue threatening safe drinking water supply. The magnitude of arsenic problem is often expressed in terms of the affected population. Even though it is impossible to assess the accurate population influenced by arsenic polluted groundwater worldwide, various reports have given estimates based on regional surveys. For example, an estimation of over 100 million people in Bangladesh, India, China, Myanmar, Pakistan, Vietnam, Nepal and Cambodia are exposed to high levels of arsenic by consuming untreated well water as long-term drinking water (Berg et al. 2001, Fendorf et al. 2010, Nordstrom 2002, Rahman et al. 2015, Rodríguez-Lado et al. 2013, Smith et al. 2000)rf et al. 2010, Nordstrom 2002, Rahman et al. 2015, Rodríguez-Lado et al. 2013, Smith et al. 2000). Directly seen from the map of arsenic in groundwater of the United States, as shown in Fig. 1.1, concentrations above 10 $\mu g / L$ and even higher than 50 $\mu g / L$ can be found in states including Texas, Arizona, California, Nevada, Maine, Michigan, Minnesota, South Dakota (Smedley and Kinniburgh 2002, Welch et al. 2000). Bangladesh faces the most severe groundwater arsenic pollution problems. Approximately 21 million people are relying on well water with arsenic concentrations greater than its national permitted level of 50 $\mu g / L$. If the World Health Organization (WHO) recommended maximum contaminant level (MCL) of 10 $\mu g / L$ for arsenic is applied, the population exposing to high levels of arsenic is over 45 million. It was predicted by the WHO that 10% of the deaths in Bangladesh could be directly related to cancers caused by arsenic (Chowdhury et al. 2000, Nickson et al. 1998, Smith et al. 2000). With regard to China,

a risk model has estimated that 19.6 million people are exposing to dangerous levels of arsenic, mainly located in arid and semi-arid areas including Xinjiang, Inner Mongolia, Henan, Shandong and Jiangsu Provinces (Rodríguez-Lado et al. 2013). In Latin American countries including Chile, Argentina and Mexico, an estimated 4.5 million people are at long-term risks of consuming arsenic with concentrations higher than 50 $\mu g / L$ (Bundschuh et al. 2012, McClintock et al. 2012).

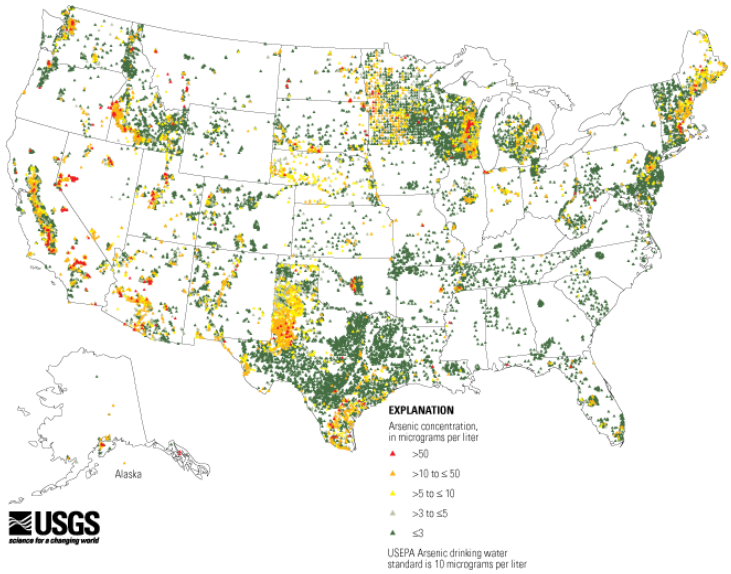

Fig. 1.1 Map of arsenic concentrations in groundwater of the United States (USGS (United States Geological Survey) 2000).

Another way to delineate the magnitude of arsenic contamination of groundwater is to use the probability of exposure to high levels of arsenic (Ayotte et al. 2006, Dai et al. 2014). Rahman et al. 2015. Based on field measured arsenic concentration data, Amini et al. (Amini et al. 2008) developed a global probability map to depict the probability to be affected by arsenic of over 10 $\mu g / L$ in reducing and oxidizing geological conditions. This research provided an overview of global arsenic pollution situation, as shown in Fig. 1.2. Rodriguez et al. have developed a probability map to illustrate the potential magnitude of arsenic contamination in groundwater of

China using a threshold of 10 $\mu g / L$, as shown in Fig. 1.3 (Rodríguez-Lado et al. 2013).

Elevated concentrations of arsenic in groundwater can be attributed to both natural release and industrial activities. The mobilization mechanisms vary largely under specific environmental conditions. (Neumann et al. 2010, Nordstrom 2002, Polizzotto et al. 2005, Polizzotto et al. 2008, Winkel et al. 2008). Generally, the predominant species of arsenic in groundwater are pentavalent arsenate [As(V) as $H_2AsO_4^-$, $HAsO_4^{2-}$ and AsO_4^{3-}], trivalent arsenite [As(III) as $HAsO_3^0$ and $H_2AsO_3^-$] and organic arsenic compounds such as monomethylarsonic acid (MMA), dimenthylarsonic acid (DMA) trimethylarsonic acid and arsenobetaine (Cullen and Reimer 1989, Mandal and Suzuki 2002). The toxicity of arsenic varies largely across its different speciation. Generally, inorganic arsenic is more toxic to humans than inorganic species and arsenite is more toxic than arsenate (Sharma and Sohn 2009).

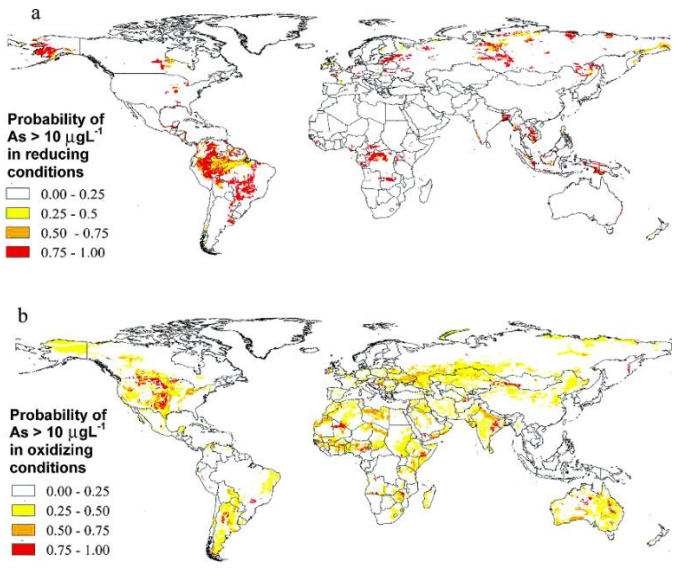

Fig. 1.2 Global map of probability of exposure to groundwater containing arsenic with concentrations above 10 $\mu g / L$ in a) reducing conditions and b) oxidizing conditions (Amini et al. 2008).

Poisoning and deaths caused by exposure to inorganic arsenic through water,

food and air have been widely reported in many countries. The acute symptoms due to arsenic ingestion include vomiting, abdominal pain and diarrhea, which may be followed by numbness and even death in extreme cases. These poisoning symptoms could happen in 30 minutes after ingestions of high concentrations of arsenic. The chronic effects caused by arsenic has attracted great attention because in many countries and regions groundwater containing low levels of arsenic is the long-term drinking water sources. This can lead to bladder cancer, lung cancer, liver cancer and skin pigmentation or lesions that finally lead to skin cancer within 5 to 15 years of exposure. In addition to its carcinogenic properties, long-term intake of arsenic may lead to diabetes, impaired development and cardiovascular diseases (Abernathy et al. 1999, Hong et al. 2014, Lin et al. 2013, Sharma and Sohn 2009, Smith and Steinmaus 2009). Therefore, the WHO and the International Agency for Research on Cancer (IARC) have classified arsenic as a Group 1 contaminant carcinogenic to human (IARC 1980). Also, the WHO has regarded arsenic as one of the top 10 chemicals causing major public health concerns.

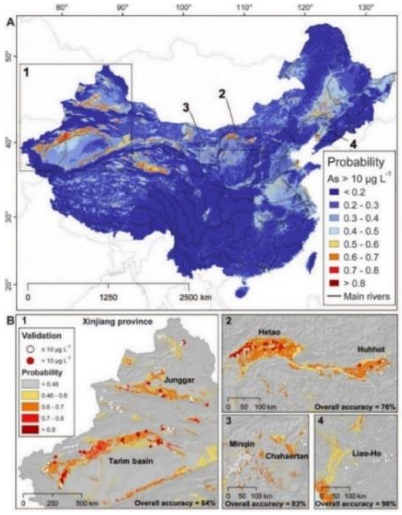

Fig. 1.3 Predictive probability map of arsenic exceeding 10 $\mu g / L$ in A) overview of China and B) major affected regions in China (Rodríguez-Lado et al. 2013).

Arsenic has been posing long-term challenges to drinking water supply to millions of people all over the world who are consuming groundwater. There is still no known effective treatment for arsenic poisoning. Therefore, the removal of arsenic from contaminated water is urgent to provide clean and safe water to human. In the past decades, various treatment technologies have been developed for treatment of arsenic polluted water. The commonly employed techniques include coagulation, precipitation, oxidation, ion-exchange, reverse osmosis, lime softening and adsorption (Chandra et al. 2010, Choong et al. 2007a, Han et al. 2002, Janet et al. 1997, Yuan et al. 2003).

Adsorption has become the most promising technique compared to the other methods due to its high efficiency, low cost and simplicity in operation (Ali and Gupta 2007, Mondal et al. 2006, Wu et al. 2012). Adsorption can be easily applied in both batch reactors and fixed bed column filters. These filters are easy to be installed in rural areas of many developing countries where most severe arsenic contamination occurs. In addition, the availability of various adsorbent materials has made adsorption suitable for water treatment. The widely reported efficient adsorbents for arsenic removal are composites combining surface metal oxides/hydroxides such as aluminum oxides/hydroxides, manganese oxide and iron oxides/hydroxides with other materials such as activated carbon, graphene oxide, chitosan and cellulose. These composites can take advantages of both metal oxide offering effective adsorption sites and the other materials serving as ideal supporting matrixes (Ali 2012, Carpenter et al. 2015, Mohan and Pittman Jr 2007). The selection of proper metal oxides, the surface loading of the metal oxides, surface area of the supporting material and the particle size of the synthesized adsorbents are key factors affecting the performance of the prepared adsorbents. It is generally accepted that the higher the loading of metal oxides and

surface area, the better of the adsorption performance. Emphasis of recent research is focused on achieving high surface area and high surface loading of metal oxides. Therefore, various of nanoscale adsorbents have been developed and tested for arsenic removal, such as the magnetic-maghemite nanoparticles, Fe_2O_3 nanoparticles and nanoscale zero-valent iron (Chowdhury and Yanful 2010, Kanel et al. 2005, Yu et al. 2013). However, the small particles are not suitable for water treatment because they can hardly be separated from the solution after adsorption due to the poor sedimentation properties. Additionally, it is difficult to implement the small particles into fixed bed columns as the porosity will be very small so that the flow through of solution will cause extremely high pressure in the columns. The flexibility of utilizing the adsorbents into fixed bed columns is a critical factor affecting the performance of the designed adsorbents. Another disadvantage for the recent studies is that the influence of iron contents on arsenic adsorption capacity has not been investigated systematically. Despite the recent studies have spared no efforts to develop highly efficient adsorbents for arsenic removal, little attention has been paid on the cost-effectiveness. For example, activated carbon is largely used as the supporting matrix for the composite, but it is also an expensive material.

Cellulose is a promising bio-polymeric material due to its hydrophilicity, high porosity, cost-effectiveness, and environmentally friendly characteristics. The presence of hydroxyl groups makes it an excellent material for surface modification. The cellulose nanomaterials have been widely used in developing water treatment methods (Carpenter et al. 2015). Several studies have employed cellulose as the supporting matrix for iron hydroxides in the synthesis of arsenic composite adsorbents (Guo and Chen 2005, Yu et al. 2013, Zhao et al. 2009). However, drawbacks of these studies

include complicated loading process, small particle sizes and failure to elucidate the effects of iron contents on arsenic adsorption capacity. Therefore, more investigations are needed to elucidate the flexibility of application of cellulose in composition of arsenic removal materials.

1.2 Objectives of this study

Based on the factors discussed above, the overall objective of this study was to develop an effective adsorbent using cellulose and iron hydroxide through a simple modification process. Then the adsorbent was applied in batch and column experiments to investigate the adsorption removal of As(III) and As(V) from water.

Specifically, the objectives of the study were:

1) To determine adsorption kinetics and adsorption isotherms of As(III) and As(V) by the prepared adsorbents using batch experiments;

2) To investigate the effect of iron contents on adsorption capacity of the adsorbents for As(III) and As(V);

3) To investigate the influence of coexisting anions on the adsorption of As(III) and As(V);

4) To study the regeneration and reusability of the prepared adsorbent for arsenic adsorption;

5) To analyze the breakthrough behavior of As(III) and As(V) in pack bed columns;

6) To model the breakthrough curves of As(III) and As(V) using equilibrium and non-equilibrium models and estimate the key parameters controlling the breakthrough behavior.

CHAPTER 2
LITERATURE REVIEW

Contamination of groundwater by arsenic has posed great challenges to drinking water supply to millions of people all over the world. The occurrence of arsenic in groundwater is due to both natural processes and anthropogenic activities. Arsenic is present in groundwater in inorganic and organic forms. Inorganic forms of arsenic have caused the major health concerns. In groundwater, inorganic arsenic is mostly present in trivalent arsenite (As(III) as $HAsO_3^0$ and $H_2AsO_3^-$) and pentavalent arsenate (As(V) as $H_2AsO_4^-$, $HAsO_4^{2-}$ and AsO_4^{3-}) states.

Due to different states of arsenic and releasing mechanisms, the occurrence and transport behavior of arsenic in the environment vary largely in various countries and regions. However, the agreement has been achieved that the toxicity and mobility of As(III) is generally greater than As(V). Diseases and deaths caused by arsenic have been reported in many countries such as Bangladesh, China, Vietnam, India and United States (Astolfi et al. 1981, Das et al. 1996, Knobeloch et al. 2006, Mandal and Suzuki 2002). Due to the awareness of health threats caused by arsenic, the WHO has lowered the guideline maximum contaminant level for arsenic in drinking water to 10 µg/L. The US Environmental Protection Agency (USEPA) has adopted the standard for arsenic in drinking water at 10 µg/L, while in many developing countries the standard remains 50 µg/L. It is still common that arsenic concentrations in groundwater largely exceed this standard globally. Even higher concentrations ranging from 0.5-25 mg/L can be found in thermal water and contaminated groundwater (Sarkar and Paul 2016, Smedley and Kinniburgh 2002, Wang et al. 2015).

Therefore, to meet the drinking water standards, various arsenic removal

techniques have been developed and applied to many public drinking water systems. These techniques mainly include ion exchange, coagulation, precipitation, reverse osmosis and adsorption. Adsorption has become the most common techniques for arsenic removal from water because of its high efficiency, cost effectiveness and simplicity in operation (Ali and Gupta 2007, Mohan and Pittman 2007, Zhu et al. 2009). It can be easily applied in rural areas where people mostly rely on groundwater and most severe arsenic pollutions occur. In the past decades, numerous studies have developed a wide range of adsorbents for the removal of arsenic from water, such as activated carbons, carbon nanotubes, iron oxide and hydroxide, zerovalent iron, manganese oxide, titanium dioxide, activated alumina, binary metal oxide composites. Research has also focused on developing cheap and efficient iron-loading supporting materials such as activated carbon, biochar, sand, chitosan, and cellulose (Chen et al. 2007, Cundy et al. 2008b, Guan et al. 2012, Guo and Chen 2005, Hu et al. 2015, Lata and Samadder 2016, Li et al. 2012, Mohan and Pittman 2007, Muñoz et al. 2002, Qiu and Zheng 2007, Singh and Pant 2004, Xu et al. 2013, Yu et al. 2013, Zhang et al. 2007).

In this chapter, the occurrence, behavior and toxicity of arsenic in the environment have been reviewed. The current arsenic removal technologies have been listed and their advantages and disadvantages have been compared. The application of adsorption for arsenic removal and the most common adsorbents have been critically reviewed.

2.1 Occurrence of arsenic in groundwater

Arsenic is a metalloid element that is ubiquitously present in various

environmental components. Its abundance ranks the twentieth among all the elements in the earth's crust. Arsenic is mostly found associated with sulphides and oxides, both in inorganic and organic forms. It is mainly trapped in sulphide minerals such as iron sulphide, copper sulphide, lead sulphide and zinc sulphide by replacing sulphur and forming crystal structures. Pyrite has the most abundant of arsenic and is an important component in sedimentary environment under reductive conditions. These sulphides minerals are easily broken down by oxidation, with arsenic being released into environment. Arsenic is also immobilized through adsorption onto oxide minerals. Iron oxides have the largest capacity adsorbing arsenic and can be broken down under reductive environment such as groundwater. Hydrous aluminum and manganese oxides also provide considerable adsorption sites for arsenic. In addition to the sulphide minerals and oxide minerals, phosphate minerals and silicate minerals may also contain high contents of arsenic even though they are less abundant (Bostick and Fendorf 2003, Brannon and Patrick 1987, Cullen and Reimer 1989, Jain and Ali 2000, Pichler et al. 1999, Sankar et al. 2014). Arsenic can be mobilized from these components through naturally geochemical processes including redox condition change, mineral-water interactions, mineral dissolutions and some biological processes.

In addition, various anthropogenic activities such as disposal of industrial waste chemicals, use of pesticides, mining activities, combustion of fossil fuels and use of livestock additives can contribute arsenic occurrence in aquatic environment. Numerous research has suggested that the predominant source of arsenic in groundwater is from the dissolution of arsenic-rich sulphide minerals, desorption from iron oxides, and dissolution of arsenic-loaded iron oxides (Bissen and Frimmel 2003a, Labrenz et al. 2000, Mailloux et al. 2009, Molinari et al. 2013, Nordstrom 2002,

Polizzotto et al. 2008, Rittle et al. 1995, Smedley and Kinniburgh 2002). Besides, research has shown that the extraction of groundwater through deep wells would cause the compact of interbed of clays, which could expel the pore water containing mobilized arsenic to deep aquifers. This is an example of arsenic occurrence due to the combination of natural processes with anthropological processes.

2.1.1 Natural sources of arsenic in groundwater

Interactions between minerals and water can be a significant process controlling arsenic mobility, especially in groundwater and aquifers where mineral/water interface is present. Understanding the mechanisms and types of interactions is critical for predictions of arsenic occurrence in groundwater. However, it is difficult to investigate interactions directly in groundwater interface or in aquifers. Based on the basic understanding that oxides have played an important role in controlling arsenic concentrations in groundwater, most studies have treated the interactions using models of adsorption/desorption processes between arsenic and the key oxides in the minerals. Also, the dissolution of oxides in the minerals has also been regarded as an important mechanism that was responsible for arsenic release into groundwater. Because of the good correlation between the contents of arsenic and iron in environment, iron oxides are frequently employed to study the interactions controlling arsenic mobility (Bose and Sharma 2002, Guo et al. 2008, Johnston et al. 2011, Matisoff et al. 1982, Nickson et al. 2000, Smedley and Kinniburgh 2002, Welch et al. 2000).

The most important factor contributing to the desorption of arsenic from the minerals is the competitive anion exchange. Numerous studies have shown that the phosphate (PO_4^{3-}) posed the greatest potential in competing for adsorption sites on iron

hydroxides. So, the use of fertilizers containing phosphate and the natural present phosphate could displace arsenic into solutions (Acharyya et al. 1999, Bolan et al. 2013, Dixit and Hering 2006, van Geen et al. 2008). In addition to phosphate, the naturally coexisting anions including bicarbonate (HCO_3^-), sulphate (SO_4^{2-}) and silicate (SiO_4^{2-}) have been reported to be responsible for the mobilization of arsenic from minerals to groundwater (Ciardelli et al. 2008, Goh and Lim 2005, Holm 2002, Szramek et al. 2004). The massive dissolved natural organic matters (NOM) could also cause mobilization of arsenic from iron hydroxide surface by directly competing adsorption sites or being a redox driver causing iron hydroop0xide dissolution. The introduction of dissolved labile organic matters can stimulate microbial activities that have potential in leading to the change variations of arsenic speciation and enhancing dissolution of arsenic bearing minerals (Anawar et al. 2013, Bauer and Blodau 2006, Biswas et al. 2014, Buschmann et al. 2006, Copeland et al. 2007, Mladenov et al. 2010, Reza et al. 2010, Sharma et al. 2011, Sracek et al. 2004, Wang and Mulligan 2006). The adsorption of arsenic species onto iron hydroxides is pH dependent. The change of pH conditions in groundwater can lead to the mobilization of arsenic. Neutral and acidic pH conditions are favorable for the adsorption of arsenate onto hydrous iron hydroxide while the adsorption of arsenite is not sensitive to the change of pH conditions. At alkaline pH, the mineral surface is negatively charged, which posing repulsion to negatively charged arsenate species. The adsorption of arsenate onto hydrous iron oxide decreased dramatically with the increase of pH while the adsorption of arsenite was not largely affected by the change of pH (Fendorf and Kocar 2009b). Under neutral pH conditions, arsenite can be adsorbed to a greater extent onto iron hydroxides than arsenate. More retention can result in more desorption and higher aqueous concentrations (Dixit and

Hering 2003). The case studies of aquifers in states of Arizona and New England in the United States showed that the elevated arsenic concentrations were mainly derived from the pH-dependent desorption process (Robertson 1989, Robinson and Ayotte 2006).

Another mechanism for arsenic mobilization is the variations of environmental redox conditions. Experimental investigations and case survey have suggested that arsenic can be released via oxidation and reduction. Strong correlations between dissolved arsenic concentrations and iron in shallow wells have been reported and it can be attributed to the reductive dissolution of iron hydroxide and mobilization of arsenic (Ahmed et al. 2006, Amstaetter et al. 2010, Campbell et al. 2006, Jiang et al. 2009, Kirk et al. 2010, Leiva et al. 2014, Molinari et al. 2013, Nickson et al. 2000, Polizzotto et al. 2005, Van Geen et al. 2004). Transition of aerobic conditions to anaerobic conditions by limited oxygenation due to the introduction of organic matters has been reported to be responsible for dissolution iron hydroxide minerals that cause high level of dissolved arsenic (Datta et al. 2009a, O'Day et al. 2004, Rhine et al. 2008). Organic matters such as autochthonous peat and allochthonous organic matters from recharging waters can cause reduction of iron oxides containing arsenic (McArthur et al. 2001). Smedley et al. (Smedley and Edmunds 2002) has suggested that the most important source of arsenic in natural waters is the reduction dissolution of iron (oxy)(hydr)oxide under anoxic conditions. However, the reduction of arsenate to arsenite could lag behind the reduction of iron hydroxide (Islam et al. 2004). On the contrary, exposure to aerated water leads to the oxidation of arsenic loaded sulphide minerals, which also can release arsenic into groundwater. (Biswas et al. 2011, Fendorf and Kocar 2009a, Meng et al. 2003, Saunders et al. 2005, Zheng et al. 2004). Chowdhury et al. (Chowdhury et al. 1999) suggested that high concentrations of arsenic

found in shallow wells in Bangladesh were mainly due to the oxidation of arsenic containing pyrite. Role of microbial activities in the mobilization of arsenic from iron (hydr)oxides has been widely investigated (Vanbroekhoven et al. 2007). Experimental studies showed that the microbial activity enhanced the dissolution of iron hydroxides, with arsenic being released (Cummings et al. 1999, Jiang et al. 2009). Simultaneous reduction of both hydrous ferric oxide and arsenate species by two types of anaerobic bacterial incubations has been reported (Campbell et al. 2006). Case study of West Bengal also suggested that anaerobic metal reducing bacteria has played a critical role in arsenic mobilization from sediments (Islam et al. 2004). Redox transformations of arsenic species by microorganisms have been investigated in both laboratory and field studies. The respiratory pathway and detoxification pathway are the two known microbial pathways that transform arsenate to arsenite (Campbell et al. 2006, Oremland and Stolz 2003).

In summary, the four main geochemical processes contributing to arsenic mobilization into groundwater include competitive adsorption by coexisting anions and NOM, reductive dissolution of iron (oxy)(hydr)oxides, oxidation of arsenic containing pyrite and redox condition variations. It should be noticed that mechanisms causing arsenic in groundwater vary in different countries or under various environmental conditions. Field studies around the globe showed that arsenic occurrence in groundwater of Bangladesh, India, Northern China, Taiwan, Vietnam, Hungary and Romania were related to reducing conditions. Occurrence of arsenic in groundwater in South American countries such as Mexico, Chile and Argentina were due to oxidizing mechanisms. The case of arsenic pollution in South-western United States was attributed to mixed oxidizing and reducing conditions (Amini et al. 2008, Smedley and

Kinniburgh 2002).

2.1.2 Anthropogenic sources of arsenic in groundwater

Even though long before human activities had posed any effect on groundwater quality, arsenic was released into groundwater through natural geochemical processes, anthropogenic arsenic sources were realized nowadays. Firstly, arsenic has been widely used in industrial products such as pesticides, feed additives, wood preservation and drugs, the potential arsenic pollution related to the production, application and waste disposal of such products have attracted much attention. Secondly, human activities such as mining, combustion of fossil fuels and agriculture could cause arsenic release from where it has been immobilized (Mandal and Suzuki 2002). More than 50% of arsenic is used to produce pesticides in agriculture, such as monosodium methylarsenate, disodium methylarsenate, dimethylarsinic acid and arsenic acid. Another 30% of arsenic production is made for wood preservatives. The remaining arsenic is mainly used to produce glass, alloy, electronics and veterinary chemicals (Matschullat 2000). About 90% of the productions are in China, France, Mexico, Germany, Peru, Namibia, Sweden and the United States and 50% of the world production have been consumed in the United States (Mandal and Suzuki 2002, Nelson 1977). In addition to pesticides, many herbicides contain large amounts of inorganic arsenic such as sodium arsenite (Baker et al. 2017). Arsenic has also been widely used as a cotton desiccant and wood preservative in the United States (Mandal and Suzuki 2002). Therefore, the agricultural use of pesticides and herbicides has led to extensive contamination of surface and subsurface soils, which has caused arsenic concentrations in such soils ranging from 0.5 to 115 mg/kg, up to 30 times the background level (Smith et al. 2003). Due to the use of arsenic containing insecticides in sheep and cattle wastes,

arsenic in surface soil (10 cm) ranged from 37 to 3542 mg/kg and penetrated to a deeper level (40 cm), reaching 2282 mg/kg (McLaren et al. 1998). Positive correlations between the extensive application of arsenical pesticides and arsenic levels in sediments have been reported in New England by using a spatial statistics and isotopic tracer measurements. Arsenic concentrations ranged from 0.3 to 93 mg/kg in 1600 sediment samples (Robinson Jr and Ayuso 2004). Based on the estimation made by Murphy and Aucott (Murphy and Aucott 1998), in the United States, the use of arsenical pesticide products such as Paris Green began in the second half of the 19th century. More than 25 million kg of calcium arsenate and 9 million kg of lead arsenate were employed in soils of New Jersey from 1900 to 1980. Calcium arsenate was a broad-spectrum insecticide that was extensively used to protect cotton from boll weevil. Lead arsenate was used to control insects attacking of fruits and vegetables. Numerous studies on environmental behavior of arsenic have shown that arsenic could be transported to aquifers and groundwater after entering sediment and soils (Barringer et al. 2010, Brannon and Patrick 1987, Charlet et al. 2011, Fendorf and Kocar 2009b, Harvey et al. 2006, Kim et al. 2009, Leybourne and Cameron 2008, McArthur et al. 2010, Roberts et al. 2010, Xie et al. 2013, Zhang and Selim 2008). Due to the awareness of arsenic pollution caused by agricultural activities, the US Environmental Protection Agency has banned the use of several inorganic arsenic containing pesticides. Pesticides with organic arsenic such as monomethylarsenic acid and dimethylarsenic acid are still in use. However, further environmental risks are still of concern because it is possible for organic arsenic to be transformed to inorganic arsenic (Masuda et al. 2005, Su et al. 2011).

Another human activity that directly introduces arsenic in the environment is the wood preserving industry. Arsenic containing wood preserving compounds have

been widely applied in the United States to prevent decay of timbers caused by Crustacea, mollusks and fungi. The main component of such wood preservatives is chromated copper arsenate (CCA) (Hingston et al. 2001, Khan et al. 2006a, Khan et al. 2004, Khan et al. 2006b). Therefore, the contaminations of arsenic due to the treatment of wood, application of treated wood and disposal of waste have been reported. In addition, the effluent from the treatment has been regarded as an important source of arsenic in aquatic and terrestrial environment (Hopp et al. 2006, Rice et al. 2002). Even though the CCA and treated wood were not allowed to use from 2004, the disposal of such waste wood has caused severe leaching of arsenic into the field soils (Townsend et al. 2005).

The most important human activity that is causing arsenic mobilization from minerals is mining. Arsenic is naturally present in oxidized sulphide minerals including lead, zinc, copper and gold ores and can be mobilized through mining and smelting operations (Duker et al. 2005, Smedley and Kinniburgh 2002). Elevated concentrations of arsenic in soils, sediments and groundwater due to the smelting of sulphide minerals have been extensively reported (Madhavan and Subramanian 2000). Gold mining activities have cause groundwater arsenic contaminations in Austria and Brazil. In the vicinity of mining sites, arsenic concentrations could be as high as 300 µg/L in surface water and 4000 mg/kg in sediments.(Borba et al. 2003, Smith et al. 2003). The greatest environmental pollution accident in Spain was caused by the mine tailings (Grimalt et al. 1999). In the United States, groundwater arsenic contaminations in some areas have been reported to be related to the local mining sites such as the gold mining in Alaska, the lead-zinc-silver mining in Idaho, and Leviathan Mine in California (Mok and Wai 1990, Welch et al. 1988, Welch et al. 2000). Mining activities have also caused arsenic

occurrence in aquatic environment of Thailand. The poisoning of over 1000 people living was recognized near the Southeast Asian Tin belt, where arsenic in shallow groundwater with concentrations up to 5000 µg/L was reported (Williams et al. 1996). In addition to arsenic release directly from mining activities, mine tailings from historical mining industry also pose great arsenic risks to the environment (Morin and Calas 2006, Roussel et al. 2000).

2.1.3 Speciation of arsenic in groundwater

Arsenic is present in the environment in several oxidation states including -3, 0, +3 and +5. The predominant species of arsenic in the environment include arsenate [As(V) as $H_2AsO_4^-$, $HAsO_4^{2-}$ and AsO_4^{3-}], arsenite [As(III) as $HAsO_3^0$ and $H_2AsO_3^-$] and organic arsenic compounds such as monomethylarsonate (MMA) and dimethylarsinate (DMA). In natural aqueous environment, inorganic arsenic and organic arsenic can be coexisting. Techniques including chromatography and solid phase extraction have been applied to separate different arsenic species so that the dominant species can be determined. In groundwater, arsenic is mainly found as As(III) and As(V) while organic arsenic forms are less abundant. The speciation of arsenic is sensitive to the pH conditions, oxidizing and reducing conditions (Yan et al. 2000). As is shown in Fig. 2.1 and Fig. 2.2, under oxidizing conditions, $H_2AsO_4^-$ is the dominant species at pH values lower than 6.9, while at higher pH conditions, $HAsO_4^{2-}$ becomes dominant.

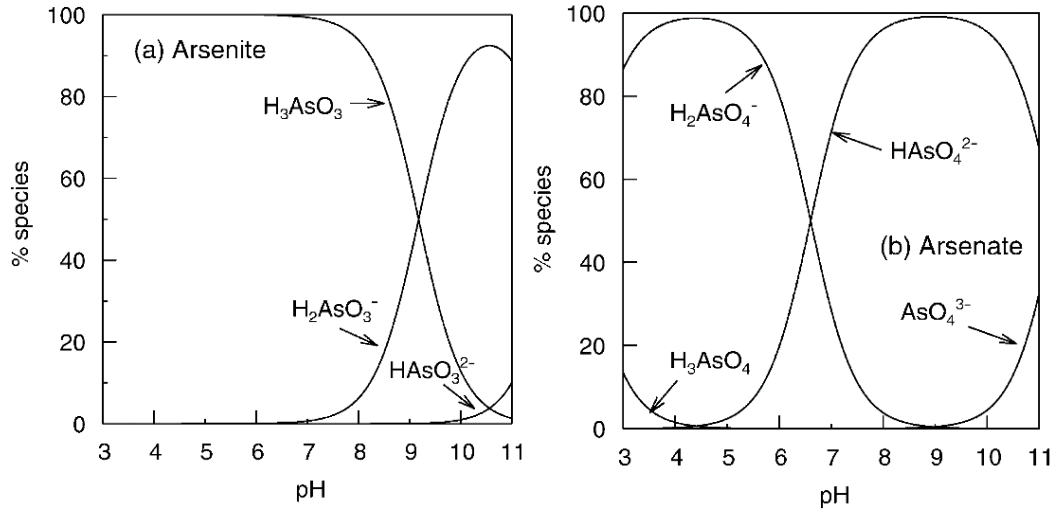

Fig. 2.1 Effects of pH on speciation of As(III) and As(V) under redox conditions (Smedley and Kinniburgh 2002).

Under reducing conditions and the pH values are lower than 9.2, the dominant arsenic species is the uncharged $H_3AsO_3^0$. The effects of pH on speciation of As(III) and As(V) can be expressed by the following equations (2.1)-(2.3) (Pierce and Moore 1982) and (2.4)-(2.6) (Goldberg and Johnston 2001, Sharma and Sohn 2009), respectively.

$$H_3AsO_3^{\ 0} \Leftrightarrow H_2AsO_3^{\ -} + H^+ \quad pK_{a1} = 9.2 \tag{2.1}$$

$$H_2AsO_3^{\ -} \Leftrightarrow HAsO_3^{\ 2-} + H^+ \quad pK_{a2} = 12.1 \tag{2.2}$$

$$HAsO_3^{\ 2-} \Leftrightarrow AsO_3^{3-} + H^+ \quad pK_{a3} = 12.7 \tag{2.3}$$

$$H_3AsO_4^{\ 0} \Leftrightarrow H_2AsO_4^{\ -} + H^+ \quad pK_{a1} = 2.3 \tag{2.4}$$

$$H_2AsO_4^{\ -} \Leftrightarrow HAsO_4^{\ 2-} + H^+ \quad pK_{a2} = 6.8 \tag{2.5}$$

$$HAsO_4^{\ 2-} \Leftrightarrow AsO_4^{\ 3-} + H^+ \quad pK_{a3} = 11.6 \tag{2.6}$$

The pH of groundwater is generally in the range of 6.5 to 8.5 (Pierce and Moore 1982) with both oxidizing and reducing conditions, under which the predominant arsenic species are $H_3AsO_3^0$ for As(III) and $HAsO_4^{2-}$ for As(V). The X-ray Absorption

Near Edge Structure (XANES) studies have demonstrated that arsenic speciation in the groundwater was usually associated with reducing conditions, and As(V) could be converted to As(III) in the sediments (Itai et al. 2010, Manning 2005).

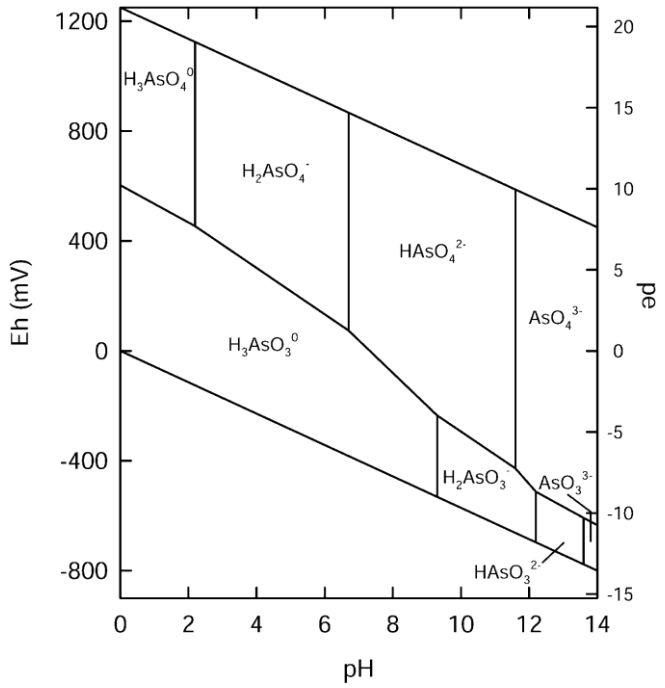

Fig. 2.2 Eh-pH diagram for aqueous arsenic species (Smedley and Kinniburgh 2002).

It has been well studied that at typical redox potentials of aerobic and oxygenated aquatic environment, As(V) species dominate As(III) species and at these redox potentials, a decrease in pH would cause an increase in the amount of As(III) over As(V). It is also predicted by the equilibrium thermodynamic calculation that As(V) should dominate over As(III) in oxidizing environment while As(III) can only be present in strongly reducing conditions. However, the ratio between concentrations of As(V) and As(III) in natural waters may not necessarily follow the theoretical prediction when different redox couples indicating different redox potentials. It has been reported that in reducing groundwaters, the concentration of As(III) can account for 75% of the total dissolved arsenic (Aurillo et al. 1994, Bhattacharya et al. 2009,

Datta et al. 2009b, Guo et al. 2008, He et al. 2010, Meng et al. 2001). As(III) has also been found in oxidizing conditions with a As(V)/As(III) ratio ranging from 0.1 to 250 (Cullen and Reimer 1989). Another example of the effect of redox potential on inorganic arsenic speciation was that in well oxidizing water, As(III) was predominant over As(III) with the concentration ratio As(III)/As(V) ranging from 0.07 to 0.12. However, in the depth where dissolved oxygen was depleted, the presence of hydrogen sulfide and low pH was favor for the dominance of As(III) with the concentration ratio As(III)/As(V) ranging from 0.51 to 0.9. The research also suggested that As(III) was detected in well highly oxygenated surface water with the concentration ratio As(III)/As(V) close to 1(Seyler and Martin 1989). The oxidation of As(III) to As(V) by dissolved oxygen is proved to be slow in kinetics that half-lives could range from several months to a year. This was also supported by the stability of As(V) ratios over weeks with no particular operation to prevent oxidation (Johnson and Pilson 1975, Yan et al. 2000). In contrast to other cationic heavy metals such as copper, zinc, chromium and lead, arsenic in molecular and oxyanion forms has posed great challenges to the development of removal technology because of its high mobility under a wide range of reducing and oxidizing conditions. In addition, the coexistence of different arsenic species under the complex pH and redox conditions has raised new requirements for the proposal of remediation technologies.

2.2 Toxicity of arsenic

Environmental hazards caused by the pollution of arsenic have been posing acute and chronic health effects to millions of people who are consuming arsenic contaminated water. Illness associated with inorganic arsenic intake is most likely to occur through the consumption of arsenic contaminated drinking water via oral route,

while the exposure to arsenic through diet is much lower (Das et al. 2012, Smith et al. 2000). Acute poisoning symptoms caused by intake of arsenic include gastrointestinal effects such as nausea, vomiting, abdominal pain and diarrhea, decreased production of red and white blood cells, and abnormal heart rhythms. However, arsenic levels in drinking water can rarely be high enough to cause acute poisoning. The chronic ingestion of low levels of arsenic is the main concern that can cause serious health consequences such as bladder cancer, lung cancer, liver cancer and skin pigmentation or lesions (Anawar et al. 2002, Bates et al. 1992, Brammer and Ravenscroft 2009, Hunt et al. 2014, Mazumder and Dasgupta 2011, Mazumder 2007, Rahman et al. 2001, Sarkar and Paul 2016, Sharma et al. 2014, Sharma and Sohn 2009). Many of these health effects have been reported in populations in Bangladesh, Argentina, India and Taiwan (Choong et al. 2007a, Duker et al. 2005). The recommended maximum contaminant (MCL) for arsenic in drinking water of 10 µg/L given by the WHO is usually taken for reference to determine if the arsenic level is excessive. One estimation in Bangladesh reported that consumption of water containing arsenic with concentrations higher than 50 µg/L has resulted in 9,136 deaths and 174,174 disability-adjusted life years (DALYs) lost per year (Amini et al. 2008, Lokuge et al. 2004). Among all the arsenic species, sodium arsenite and arsenic trioxide are regarded as the most toxic. As(III) is 60 times more toxic than As(V) (Jain and Ali 2000). The lethal dose 50 (LD_{50}) was used to assess the acute toxicity of arsenic and it ranged from 15-40 mg/kg for sodium arsenite and 34 mg/kg for arsenic trioxide, respectively, with regard to different human body weights (Petrusevski et al. 2007). Based on the investigations of molecular mechanisms of carcinogenesis, arsenic does not react with DNA directly. However, it can cause gene amplification, chromosomal damage and

enhance mutagenesis at lower doses. In addition, As(III) can derange the spindle apparatus by accelerating microtubule polymerization (Abernathy et al. 1999). Generally, there are four stages for arsenic to cause chronic poisoning: preclinical stage, clinical stage, complication stage and malignancy stage. No symptoms occur in the preclinical stage but arsenic can be detected in urine and body tissue samples. In the clinical stage which may occur after 5-10 years of exposure to arsenic, symptoms start showing on the skin such as darkening on the palms, dark spots on chest and more seriously hardening of skin into nodules. In the complication stage, symptoms on the skin are more pronounced and pathological effects such as enlargement start showing on internal organ including liver, kidneys and spleen. In the malignancy stage, skin, lung or bladder cancer may occur (Choong et al. 2007a). Both of As(III) and As(V) can inhibit the energy-linked functions of the cell mitochondria but the action mechanisms are different and As(III) can be adsorbed faster in biological systems than As(V) (Bissen and Frimmel 2003a). The mechanism of toxicity caused by As(III) is mainly the reaction in vitro with thiol-containing molecules. Due to its higher affinity to dithiol than monothiols, As(III) can bind to critical thiol groups, which may inhibit essential biochemical events for human health (Hughes 2002). As(III) can also be transported into cells through aquaglycerolporins due to its similar structure to glycerol (Liu et al. 2002). For As(V), the mechanism is the reaction in vitro with glucose and gluconate to form glucose-6-arsenate and 6-arsenogluconate, which can inhibit hexokinase. Arsenate has similar molecular structure with phosphate. So, it can use phosphate transporters to enter the cells. In addition, toxicity caused by arsenic has been divided into three categories: epidemiological, cytotoxicity and genotoxicity. For these three types of toxicity, reactive oxygen species have played an important role by reducing

DNA methylation and specific protein expression (Sun et al. 2014).

2.3 Arsenic removal technologies

For the past decades, various methods have been developed and employed to remove arsenic from water. Generally, the most studied technologies include oxidation, coagulation and precipitation, lime softening, ion exchange, membrane filtration and adsorption (Mondal et al. 2006, Sarkar and Paul 2016, Singh et al. 2015). To meet the requirements of safe drinking water supply, any developed technology to be used in arsenic polluted areas, especially in rural areas of developing countries, should consider the factors such as simplicity in operation, cost-effectiveness, versatility and use environmentally friendly resources. It is important to consider the accessibility of such technologies to local communities and if these technologies can fit well with the rural circumstances (Chwirka et al. 2000, Hsiao-Wen et al. 1999). So, this section is to make an overview of these treatment processes for arsenic removal from water and to compare advantage and disadvantage for each technology.

2.3.1 Oxidation

Under the near neutral pH and slightly reducing conditions in groundwater, arsenic is mainly present as As(III), which is in the form of uncharged molecules. However, many techniques are effective to remove the negatively charged As(V). Thus, oxidation has been applied as a pre-treatment process to transform As(III) to As(V) before the treatment such as filtration, coagulation and adsorption (Baig et al. 2013, Bissen and Frimmel 2003b). The general redox transformation between As(III) and As(V) can be described as:

$$H_3AsO_4 + 2H^+ + 2e^- \rightarrow H_3AsO_3 + H_2O \quad E_0 = +0.56\,V \tag{2.7}$$

Common oxidants for As(III) include oxygen, hypochlorous acid and permanganate. The reactions are described by the following equations (Whitacre et al. 2012).

$$H_3AsO_3 + \frac{1}{2}O_2 \rightarrow H_2AsO_4^- + 2H^+ \quad (2.8)$$

$$H_3AsO_3 + HClO \rightarrow HAsO_4^- + Cl^- + 3H^+ \quad (2.9)$$

$$H_3AsO_3 + 2KMnO_4 \rightarrow 3HAsO_4^- + 2MnO_2^+ + 2K^+ + 4H^+ + H_2O \quad (2.10)$$

Even though aeration is the simplest method for arsenic oxidation, the reaction rate is low, which may require several weeks for complete oxidation (Pierce and Moore 1982). It took 5 days to oxidize 25% of 200 µg/L As(III) by purging air and it took 60 min to oxide 8% of As(III) by pure oxygen (Clifford et al. 1983, Frank and Clifford 1986). So, other strong oxidants such as hydrogen peroxide, ozone and manganese oxide are also used to accelerate the oxidation process (Bordoloi et al. 2013). As(III) of 40 µg/L could be totally oxidized in 20 min in the presence of ozone (Kim and Nriagu 2000). The oxidation of As(III) by means of four conventional oxidants (chlorine dioxide, sodium hypochlorite, potassium permanganate and monochloramine) under various pH conditions and water compositions were investigated. The results showed that the oxidation efficiency of potassium permanganate was highest and the oxidation was slow by monochloramine (Sorlini and Gialdini 2010). In addition, photochemical oxidation of As(III) has been investigated. In the presence of oxygen, the oxidation rate was largely increased by UV irradiation (Mondal et al. 2013). Although oxidation is a simple process and can be easily applied to the treatment of large volumes of water, it can produce unwanted toxic by-products which need further treatments.

2.3.2 Coagulation and flocculation

The coagulation reaction between arsenic and coagulants can transform soluble arsenic into floc which is easier to be separated from water by sedimentation or filtration. Floc or large aggregates are formed due to the reduction of negative charge of arsenic colloids by the positively charged coagulants (Choong et al. 2007b). Then the removal of arsenic from water by coagulation and flocculation can be attributed to three mechanisms: 1) direct precipitation reactions between arsenic and coagulants; 2) the coprecipitation of arsenic during the growing insoluble flocs; and 3) adsorption of arsenic species onto the surface of the formed solid aggregates through electrostatic attractions. Coagulation is generally followed by filtration to remove the flocs, which is an effective combination and widely used for arsenic removal. Because As(III) is uncharged, it needs to be oxidized to As(V) for better removal by coagulation. Among all the coagulants, iron and aluminum based coagulants such as alum ($Al_2(SO_4)_3 \cdot 18H_2O$), ferric chloride ($FeCl_3$) and ferric sulfate ($Fe_2(SO_4)_3 \cdot 7H_2O$) are most commonly used (Hering Janet et al. 1997). Besides, flocculants are used to promote the formation of aggregates, which are better to be separated from water. For example, the process of alum coagulation can be divided into dissolution, precipitation and coprecipitation, using the following equations, respectively (Mondal et al. 2013, Whitacre et al. 2012).

$$Al_2(SO_4)_3 \cdot 18H_2O \rightarrow 2Al^{3+} + 3SO_4^{2-} + 18H_2O \quad (2.11)$$

$$2Al^{3+} + 6H_2O \rightarrow 2Al(OH)_3 + 6H^+ \quad (2.12)$$

$$H_2AsO_4^- + Al(OH)_3 \rightarrow Al - As(complex) \quad (2.13)$$

The Al-As complex may include precipitate $Al(AsO_4)$ or adsorbed arsenic onto

the aluminum hydroxide. Similarly, iron species are known to form such complex with arsenic, which can be removed by sedimentation or filtration. The coagulation of arsenic using iron oxide can be described using the equations below (Hering et al. 1996).

$$Fe(OH)_3 + H_3AsO_4 \rightarrow FeAsO_4 \bullet 2H_2O + H_2O \quad (2.14)$$

$$\equiv FeOH^0 + AsO_4^{3-} + 3H^+ \rightarrow \equiv FeH_2AsO_4 + H_2O \quad (2.15)$$

$$\equiv FeOH^0 + AsO_4^{3-} + 2H^+ \rightarrow \equiv FeHAsO_4^- + H_2O \quad (2.16)$$

The formation of hydrous ferric oxide and hydrous aluminum oxide provides adsorption sites for arsenic, which can result in an adsorption capacity of 46 mg As(V)/g ferric chloride and 23 mg As(V)/g alum, respectively. It is reported that the iron based coagulants are more effective than aluminum based coagulants. Besides, the iron based coagulants are stable in a wider range of pH conditions (Gadd and Ravenscroft 2009, Hering Janet et al. 1997). The main influencing factors for arsenic coagulation are pH, dosage of coagulants and coexisting anions. The adsorption of arsenic to the oxide surface is favored at a low pH which is below the zero charge points of the oxides. With regard to the coagulant dosage, an iron/arsenic mass ratio over 40 is required to reduce arsenic concentration to lower than 50 ppb. The presence of anions such as PO_4^{3-}, SiO_4^{2-}, and SO_4^{2-} can compete with arsenic for adsorption sites and lower the removal rate. The affinity between PO_4^{3-} and oxide surface is the highest among the anions. This is consistent with results from the investigation of arsenic adsorption (Whitacre et al. 2012). Coagulation combined with precipitation and filtration is an efficient method to remove arsenic from water. However, the problems such as low removal efficiency for As(III) and disposal of produced coagulation sludge have limited the applicability of this technology.

2.3.3 Ion exchange

Ion exchange method has been widely used for arsenic removal from water. It utilizes a physicochemical process in which arsenic exchange with ions on the solid phases, which are in most cases the synthetic resins. The surface of synthetic resins can be modified using charged functional groups including strongly and weakly acidic groups or strong and weakly basic groups by covalent bonds (Clifford 1999). For arsenic removal, the resin is usually modified using chloride ions. So, water containing arsenic passing through the resin columns is lower in arsenic but higher in chloride till the ion-exchange capacity of the resin is depleted when most the exchange sites of the resin are loaded with arsenic (Choong et al. 2007b). The ion exchange resins can be regenerated by exchanging the loaded arsenic using NaCl solutions. Arsenic removal and regeneration of resin can be described by equation (2.17) and (2.18), respectively.

$$2R-Cl+HAsO_4^- \rightarrow R_2HAsO_4+2Cl^- \quad (2.17)$$

$$R_2HAsO_4+2Na^++2Cl^- \rightarrow 2R-Cl+HAsO_4^-+2Na^+ \quad (2.18)$$

Where R is the ion exchange resin.

The concept of ion-exchange capacity for arsenic is usually expressed using milliequivalents (mEq)/mL. The exchange capacities for arsenic using strong base anionic exchange resins are from 1 to 1.4 mEq/mL. Besides, ion exchange is also affected by other coexisting anions such as phosphate, sulphate and nitrate by competing for exchange sites with arsenic. Generally, these anions have higher affinity to the resins than arsenic does. The ion exchange is less sensitive to the pH conditions. However, it requires the uncharged As(III) to be oxidized to As(V) before passing through the resin column and the oxidant should be removed in case the chemicals

cause damage to the resins (Whitacre et al. 2012).

2.3.4 Membrane filtration

Arsenic species can be separated from water by passing through a semi permeable membrane under the pressure as driving force. Membrane has been regarded as one of the most promising technologies for deep treatment of water. There are four types of membrane filtration processes that are most widely studied for arsenic removal. They are microfiltration (MF), ultrafiltration (UF), nanofiltration (NF), and reverse osmosis (RO), of which MF is the low-pressure membrane process while the other three need high pressure to provide driving force (Mondal et al. 2013). The property that decides if arsenic can be separated from water is the pore size of the membranes. Among the four membranes, RO and NF are able to separate arsenic by capillary flow or solution diffusion due to the pore sizes smaller than 2 nm in diameter. Pore sizes of MF and UF are not small enough to remove soluble arsenic. But they can be used to removal particulate arsenic after coagulation and flocculation (Chwirka et al. 2004, Ghurye et al. 2004). Research has shown that the combination of coagulation and microfiltration is more efficient than that of coagulation and sedimentation (Han et al. 2002). The advantage of membrane filtration processes for arsenic removal is independence of pH. In addition, there is no toxic by-product generated from the process. But the processes can be affected by the presence of specific colloids which foul the back wash. So, pretreatment is need for water containing high level of colloids. Another disadvantage for membrane method is the high cost and high energy consumption, which may not be acceptable for people in rural areas in developing countries (Mondal et al. 2013).

2.3.5 Adsorption

Adsorption for arsenic removal is the process of accumulating arsenic species onto the solid surface by physical as well as chemical forces. Numerous adsorbents have been developed and applied for arsenic removal in the past decades. To better under the development of ideas for the design of arsenic adsorbents, Mohan and Pittman critically evaluated the performances of numerous adsorbents including the conventional activated carbon, natural constituents, industrial by-products, metal oxides, and composite materials (Mohan and Pittman Jr 2007). In this section, a brief review is made based on some of the most commonly used adsorbents.

The most well-known adsorbent is activated carbon due to its high specific surface area, which could be up to 2000 m^2/g based on different activation methods. It has been reported that the adsorption capacity of activated carbon for arsenic was only a few milligrams arsenic per gram activated carbon. For example, arsenic adsorption by a set of 28 activated carbons with the surface areas ranging from 388 to 1747 m^2/g was studied. It showed that the largest adsorption capacity was 2.0 mg/g. Sometimes the adsorption rate is not sufficient to reach drinking water quality. However, a huge adsorption capacity (2860 mg/g) was reported with a coal-derived commercial activated carbon (Mohan and Pittman Jr 2007). The adsorption of arsenic using activated carbon is dependent on the pH of the water. The carbon-based nanomaterials such as graphene and carbon nanotubes are also used for arsenic removal with the surface being functionalized by hydroxyl (-OH) or carboxyl (-COOH) (Kuila et al. 2012). The granular activated carbon has been modified using impregnation of metallic silver and copper to improve the adsorption capacity (Rajaković 1992). Extensive reviews have been conducted on the metal based materials, the most extensively studied are activated

alumina, granular ferric hydroxide, iron oxide coated carbon materials, and metal - metal composites (Adeleye et al. 2016, Lata and Samadder 2016, Mehta et al. 2015, Ray and Shipley 2015). Adsorption of As(III) onto activated aluminum has was investigated in terms of kinetics and isotherms. The adsorption equilibrium was achieved within 6 hours and was dependent on initial concentrations. The Langmuir isotherm showed the highest adsorption capacity was 2.29 mg/g. The intraparticle modeling showed that the mechanisms for arsenic to be adsorbed included surface adsorption and intraparticle diffusion (Singh and Pant 2004). For As(V), the adsorption removal using activated aluminum showed a Langmuir behavior and the adsorption capacity reached 36.6 mg/g (Han et al. 2013). This suggests that activated aluminum is more effective for adsorption of As(V) than As(III). Various adsorption models have been used to fit the adsorption data of As(III) and As(V) by activated aluminum grains. The adsorption can be described using both Freundlich and Langmuir adsorption model (Lin and Wu 2001). A mesoporous alumina was used for arsenic adsorption and the adsorption capacity reached 121 mg/g for As(V) and 47 mg/g for As(III) (Kim et al. 2004).

Iron based adsorbents have been most widely studied and applied for arsenic adsorption in recent years. Due to the high affinity to arsenic species, iron oxides and hydroxides have attracted great attention. The adsorption capacity of iron oxides for arsenic was reviewed to be higher than 100 mg/g. Studies have shown that the high affinity was attributed to the formation of surface complex between iron hydroxide and arsenic species. (Appelo et al. 2002, Farquhar et al. 2002, Sherman and Randall 2003) This indicated that iron oxides are ideal materials for selective adsorption of arsenic from water. However, if the iron hydroxides are applied alone, disadvantages of iron

oxides for arsenic removal include slow adsorption kinetics, narrow applicable pH range and difficulty in disposal after adsorption. Also, because of its small particle size, iron oxide nanoparticle cannot be used in continuous flow system. To overcome these difficulties, novel materials were developed by combining iron oxides with other traditional adsorbents. In the modification process, the traditional adsorbents serve as supporting matrix while iron oxides selectively remove arsenic from water (Adeleye et al. 2016, Lata and Samadder 2016, Mehta et al. 2015, Mohan and Pittman 2007). The most frequently used method is the modification of activated carbon by impregnating iron oxides on the activated carbon surface. This kind of materials could take advantages of both activated carbon as an ideal supporting media and iron oxides offering high affinity with arsenic species (Chen et al. 2007). Studies have shown that in the adsorption process, arsenate oxyanions could exchange with hydroxyl groups from iron hydroxides and form inner-sphere monodentate or bidentate surface complex, represented as Fe-O-AsO(OH)-O-Fe. Comparative studies showed that the impregnation of iron oxides with activated carbon increased the adsorption capacity by more than ten times. Javier et al. studied the influencing factors affecting arsenic adsorption by iron modified activated carbon. It was proposed that the most important factor was the pH_{pzc} value, followed by iron content of the iron doped activated carbon. An iron content of about 1 wt.% was most favorable for arsenic adsorption. Mechanism study demonstrated that arsenic was removed by both ligand exchange with hydroxyl groups and electrostatic attraction with surface groups (Arcibar-Orozco et al. 2014). Muniz et al. compared arsenic adsorption performance by activated carbon impregnated with Fe(III) and Fe(II). The impregnation of iron could obviously improve arsenic removal efficiency and the increase of iron content in iron impregnated activated carbon

always increased arsenic uptake. Iron contents higher than 2 wt.% could contribute to the removal of 100% arsenic with an initial concentration of $311\,\mu g\,L^{-1}$. However, Arsenic adsorption performance was highly dependent on the impregnation methods, which could result in different degree of dispersion of the iron impregnated activated carbon. Specifically, small and highly dispersed particles were favorable to higher arsenic removal efficiency. Besides, the use of Fe(II) was more favorable to obtain good iron-impregnated activated carbon particles for arsenic removal (Muniz et al. 2009).

Nanoscale zero-valent iron (NZVI) has been reported as an ideal material in remediation of arsenic contaminated groundwater. Because of its large active surface area, it has high adsorption capacity for arsenic (Cundy et al. 2008a, Daus et al. 2004). A comparative study has shown the adsorption capacity of NZVI for arsenate was larger than activated carbon, but smaller than iron hydroxide and zirconium loaded activated carbon. For the adsorption of arsenite, the adsorption capacity of activated carbon was larger than zirconium loaded activated carbon, iron hydroxide and NZVI, which could be due to the enhanced oxidation of arsenite to arsenate by activated carbon. However, direct application of NZVI in water treatment may cause fast loss of NZVI and iron pollution because it usually appears as fine powders (Daus et al. 2004). Therefore, studies have attempted to load NZVI onto supporting adsorbents for arsenic adsorption from polluted water. Zhu et al. developed a novel material by loading NZVI on activated carbon. At pH 6.5, the adsorption capacity of this novel adsorbent for arsenite and arsenate was 18.2 and 12.0 mg/g, respectively, which was higher than arsenic adsorption performance of most available adsorbents at near neutral pH conditions (Zhu et al. 2009). Apart from the adsorbents mentioned above, the requirement of arsenic removal has triggered numerous research on the development of other adsorptive

materials including multiple oxide nanoparticles, binary metal adsorbents, zirconium based adsorbents, titanium based adsorbents copper based adsorbents and manganese based adsorbents (Adeleye et al. 2016, Lata and Samadder 2016, Mehta et al. 2015, Mohan and Pittman 2007, Smith and Rodrigues 2015).

Cellulose has been employed in arsenic removal because of its advantage in hydrophilicity, cost effectiveness, high porosity and environmentally friendly properties (Carpenter et al. 2015, Hokkanen et al. 2015, Muñoz et al. 2002, Tian et al. 2011). Guo et al. developed a β-FeOOH loaded cellulose adsorbent through a seven-step impregnation process. The iron content of the obtained adsorbent was 50% and the diameter of the bead was around 0.2 mm. The adsorption capacity for arsenite and arsenate reached 99.6 and 33.2 mg/g due to the high content of $\beta-\mathrm{FeOOH}$. For the aspects of kinetics, the adsorption equilibrium was achieved in 10 h and the adsorption rate of arsenite is faster than that of arsenate, with a second order adsorption coefficient being 0.66 and 0.09 $\mathrm{mL\cdot mg^{-1}\cdot h^{-1}}$, respectively (Guo and Chen 2005). Another $\mathrm{Fe_2O_3}$ nanoparticle modified cellulose adsorbent was synthesized using an easier method of one-step co-precipitation. The adsorption capacity for arsenite and arsenate was 23.16 and 32.11 mg/g, respectively, which was inconsistent with most research reporting that the adsorption capacities of iron oxide modified materials for arsenite were larger than that of arsenate (Yu et al. 2013).

However, most adsorbents obtained so far are not adaptive to packed bed filters due to their nanometer level particle sizes. This is a major limitation for these adsorbents to be applied in practical water purification projects. Also, for the iron based composite adsorbents, the iron loading is a key factor affecting arsenic adsorption

behavior. It can be concluded that, to increase the adsorption capacity and adsorption rate of iron-based adsorbents for arsenic, it is generally necessary to increase the loading contents of iron and at the same time make the effective adsorption sites more accessible to arsenic species (Yang et al. 2014). However, there is a lack of sufficient study on the relations of iron loading contents and the adsorption capacity and kinetics for arsenic. Therefore, in the present study, an iron hydroxide loaded cellulose bead adsorbent was synthesized using a simple hydrolysis loading process. The potential of the obtained adsorbent in application of arsenic adsorption was investigated through batch and column study. The effects of iron hydroxide loading amount on arsenic adsorption capacity and kinetics were studied.

CHAPTER 3
ADSORPTION KINETICS AND ISOTHERMS

Adsorption kinetics and isotherms are the two most important parameters to understand the adsorption rate and the capacity of the adsorbent. Generally, the adsorption kinetics and isotherms are determined in batch experiments. Adsorption kinetics is the relationship between arsenic concentration or adsorbed amount with time and the adsorption isotherm represents the relationship between the equilibrium adsorption capacity and equilibrium concentration. The experimental data can be fitted using some classic adsorption models such as pseudo-first order, pseudo-second order kinetics and intra-particle diffusion models for kinetics, and Langmuir and Freundlich equation for isotherms to better understand the adsorption properties of the adsorbent. In the present research, the adsorption kinetics of As(III) and As(V) with concentrations ranging from 5 mg/L to 800 mg/L onto five iron hydroxides loaded cellulose beads (FeCB) were determined in batch experiments. The kinetic data was fitted using pseudo-second kinetic equation and the equilibrium concentration and capacity were estimated and used for building the adsorption isotherms. The isotherms were fitted using Langmuir and Freundlich equations and the adsorption capacities were compared under the different iron loadings on FeCB. So, the effects on iron hydroxide loading on the adsorption capacities of As(III) and As(V) were determined. In addition, the effects of coexisting anions including phosphate and sulphate were studied using adsorption kinetics. Desorption of arsenic from the adsorbents was conducted using different regeneration agents and the best agent was used for further regeneration experiments.

The potential of the newly prepared adsorbents for arsenic removal was fully examined in this chapter. This would provide important information for the application

of these adsorbents in column experiments.

3.1 Experimental section

3.1.1 Materials

Sodium (meta)arsenite ($NaAsO_2$, Sigma Aldrich) and sodium arsenate dibasic heptahydrate ($Na_2HAsO_4 \cdot 7H_2O$, Sigma Aldrich) were used for the source of As(III) and As(V), respectively. The stock solution of 1000 mg/L was prepared by dissolving 0.866 g $NaAsO_2$ and 2.080 g $Na_2HAsO_4 \cdot 7H_2O$ into 500 mL ultrapure water (resistivity $\geq$18.0 MΩ). The stock solutions were diluted for adsorption experiments. All water used for As(III) solutions was purged using ultrapure nitrogen for 30 min till the concentration of dissolved oxygen was 0, measured by a dissolved oxygen meter (Microsensor multimeter, Unisense, USA). The cellulose powder, urea, ferric chloride, and sodium hydroxide were of reagent grade and obtained from Sigma Aldlich. The nitric acid and hydrochloric acid were obtained from Fisher Chemical and of trace metal grade.

3.1.2 Synthesis of FeCB

The mixture of NaOH/urea/H_2O of 7:12:81 by weight was cooled to -12 ℃, and then 8 g cellulose was dispersed in to 200 mL of the prepared mixture under vigorous stirring for 3 min to obtain a transparent cellulose solution. The resulting suspension was added drop wise into 500 mL of 2 M HNO_3 solution at a rate of 3 mL/min using a syringe pump. Height of the tip was manually adjusted in situ 1-2 cm above the surface to gain spherical beads. Coagulated beads were left in acid for 12 h. All the beads were washed in deionized water for 30 min and stored in deionized water for iron hydroxide loading.

The cellulose hydrogel beads were immersed in 200 mL of 0.1, 0.2, 0.5, 0.75 and 1.0 M $FeCl_3$ solution with shaking for 60 min. Then the cellulose hydrogel beads were collected by filtration. Then the beads were immersed in 2 M NaOH solution for 20 min. Finally, the beads were filtrated out and washed thoroughly using deionized water and finally stored in deionized water at room temperature for further use. In this thesis, the prepared iron hydroxide loaded cellulose beads are denoted as FeCB1, FeCB2, FeCB3, FeCB4 and FeCB5, indicating the five different iron contents.

3.1.3 Arsenic adsorption kinetics

In a batch of 50 mL centrifuge tubes, 40 mL arsenic solution of concentration ranging from 5 mg/L to 800 mg/L was added. The initial pH of each solution was adjusted to 7.0 ± 0.2 using 0.1 and 1.0 M HCl solutions. To each solution, 10 wet each FeCB were added. Then the batch was shaken on a rotating plate to ensure the complete mixing. At prescribed time intervals, 0.1 mL solution was taken from each tube and diluted to 10 mL using 2% nitric acid solution. The diluted solutions were used for arsenic concentration analysis. After the adsorption experiments, the FeCBs were collected and dried and the dry mass were recorded for calculation of adsorption capacities.

3.1.4 Arsenic adsorption isotherms

The adsorption isotherms by each FeCB were obtained using the equilibrium concentrations and capacities estimated from the kinetics experiments. This method was different from the generally applied single time point measurement which only measured the initial concentration and the final concentration at another time point when the equilibrium was assumed to have occurred. This could cause errors in

measurements and fitting because whether the adsorption equilibrium for each concentration has actually occurred was unknown.

3.1.5 Effects of coexisting anions

The effects of PO_4^{3-} and SO_4^{2-} on the adsorption of As(III) onto FeCB5 were investigated using kinetic experimental method. To a batch of 50 mL centrifuge tubes, 40 mL As(III) solution in the absence and presence of PO_4^{3-} or SO_4^{2-} were added. The initial pH of the solution was adjusted to 7.0 ± 0.2. The concentration of As(III) was 5 mg/L. The concentrations of PO_4^{3-} were 1 mg P/L and 5 mg P/L and the concentrations of SO_4^{2-} were 200 mg/L and 500 mg/L. Ten beads of FeCB5 were added to each solution. The batch was shaken on a rotating plate to ensure the complete mixing. At prescribed time intervals, 0.1 mL solution was taken from each tube and diluted to 10 mL using 2% nitric acid solution. The diluted solutions were used for arsenic concentration analysis.

3.1.6 Regeneration

A 40 mL 2.0 M NaOH solution was applied for the regeneration of As(III) loaded FeCB5, which was collected from the adsorption kinetic experiment with As(III) concentration of 5 mg/L. The batch was shaken using the rotating plate. At prescribed time intervals, 0.1 mL solution was taken from each tube and diluted to 10 mL using 2% nitric acid solution. The diluted solutions were used for arsenic concentration analysis. After the first desorption experiment, the residual solution was removed, and the beads were collected and washed using ultrapure water till the pH was 7. Then the beads were used for adsorption of 5 mg/L As(III) following the kinetics experiment procedure. Two cycles of desorption and adsorption were conducted and then the beads

were dried, and the dry mass was used for calculations.

3.1.7 Analytical procedures

The iron contents of the synthesized FeCBs were measured using thermogravimetric analyzer (TGA, SDTA851e, Mettler, Switzerland). The beads were freeze dried for 48 hours and about 25 mg of each dried sample was used for the measurements. The measurements were processed under air and the heating process was set from room temperature to 800 ºC at a rate of 10 ºC/min. During this process, cellulose was totally burned, and the loaded iron hydroxide was completely oxidized to Fe_2O_3. The change of sample weight from the initial to the final state was recorded during the heating process. By calculating the weight difference, the amount and percentage of Fe_2O_3 and Fe was obtained. Concentrations of As(III) and As(V) were analyzed using Inductively Coupled Plasma Mass Spectrometry (ICP-MS, ELAN DRC-e, PerkinElmer, USA). The method detection limit (MDL) of ICP-MS for arsenic was 0.04 µg/L, which was measured by 7 duplicates of standard solutions of 1 µg/L and calculated using student t value with 99% confidence. For each measurement, 10 mL of solution including arsenic sample, 2% HNO_3 and 1% internal standard of In was prepared.

3.2 Results and Discussions

3.2.1 Iron contents of FeCBs

The results of TGA measurements are shown in Fig. 3.1. The TGA measurements represented the decreasing of bead weight during the heating procedure. Because the heating procedure was conducted in air atmosphere, the decreasing of bead weight during 200 ℃ to 400 ℃ was due to the combustion of cellulose. During the

heating process, the iron hydroxide species were oxidized to Fe_2O_3. When the temperature reached 400 ℃, the weights of all the beads kept stable, suggesting that cellulose was totally combusted and only Fe_2O_3 remained. Therefore, the iron content of FeCB1, FeCB2, FeCB3, FeCB4 and FeCB5 was calculated to be 3.8%, 9.5%, 17.7%, 20.5% and 21.7%, respectively. The five beads were prepared using ferric chloride solutions with concentrations of 0.1, 0.2, 0.5, 0.75 and 1.0 mole/L. The effect of the used ferric chloride concentrations on the bead iron contents is shown in Fig. 3.2.

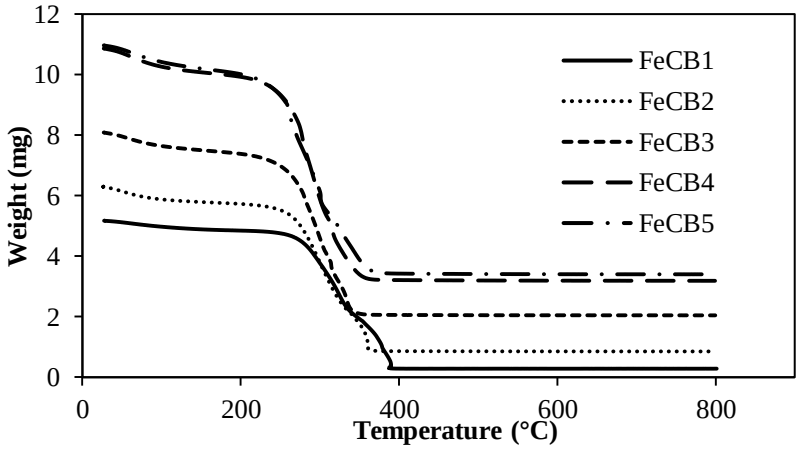

Fig. 3.1 TGA curves of the iron hydroxide load cellulose beads with a heating procedure from temperature to 800 ℃ at a rate of 10 °C/min.

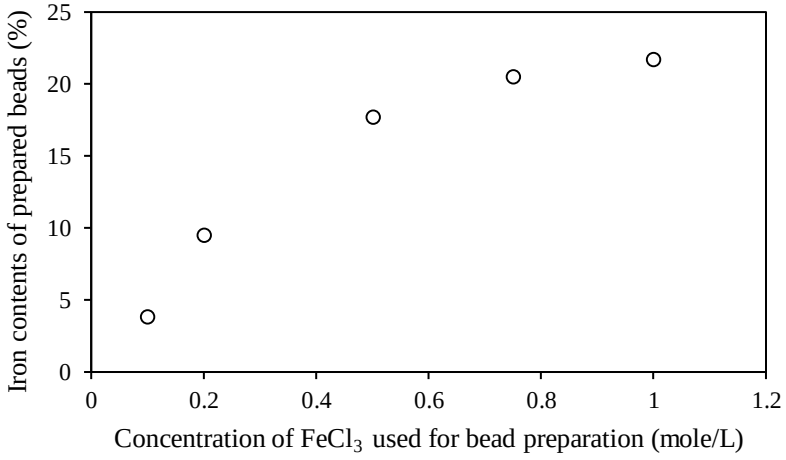

Fig. 3.2 Effect of $FeCl_3$ concentration used for bead preparation on the iron contents of the prepared beads.

It shows that the iron contents of the obtained beads are linearly correlated with the concentrations of $FeCl_3$ when the concentrations were lower than 0.5 mole/L. But when the concentration continued increasing to 0.75 and 1.0 mole/L, the increase of iron contents on the beads would reach a stable level.

3.2.2 Adsorption kinetics

Adsorption kinetics is one of the important properties assessing the efficiency of adsorption. Hence, in the present study, the adsorption kinetics of the prepared five FeCBs for As(III) and As(V) were determined in batch experiments The pseudo-second-order kinetic equation was used to fit the experimental kinetic data and estimate the equilibrium adsorption capacity and kinetic coefficient. The equation can be derived based on Azizian's method (Azizian 2004). The general form of kinetic equation can be written as

$$\frac{d\theta}{dt} = k_a(C_0 - \beta\theta)(1-\theta) - k_d\theta \tag{3-1}$$

Where, $\theta(0 \le \theta \le 1)$ is the coverage fraction; k_a and k_d are the adsorption and desorption rate constants; C_0 is the initial concentration; $\beta = \frac{C_0 - C_e}{\theta_e}$ where C_e and θ_e is the equilibrium concentration and coverage fraction, respectively. Then equation (3-1) can be written as

$$\frac{d\theta}{dt} = k_a\beta\theta^2 - (\beta + C_0 + \frac{1}{K})k_a\theta + k_aC_0 \tag{3-2}$$

Where, $K = \frac{k_a}{k_d}$. Let $a = k_a\beta$, $b = -(\beta + C_0 + \frac{1}{K})k_a$ and $f = k_aC_0$, equation (3-2) can be written as

$$\frac{d\theta}{dt} = a\theta^2 + b\theta + f \tag{3-3}$$

By integration, the analytical solution can be obtained as

$$\theta = \frac{\xi e^{\lambda t+\tau} - \gamma}{2a(1-e^{\lambda t+\tau})} = \frac{\xi e^{\lambda t} e^{\tau} - \gamma}{2a(1-e^{\lambda t} e^{\tau})} \tag{3-4}$$

Where, $\lambda = \sqrt{b^2 - 4af}$; $\xi = b + \lambda$; $\gamma = b - \lambda$ and $\tau = \ln\frac{\gamma}{\xi}$. So, at equilibrium when $t \to \infty$, equation (3-4) turns out to be

$$\theta_e = -\frac{\xi}{2a} \tag{3-5}$$

Or

$$\theta_e = \frac{KC_e}{1+KC_e} \tag{3-6}$$

Which is the Langmuir adsorption isotherm equation. Assume the value of λt is small such that the equation (3-4) can be reduced to

$$\theta \approx \frac{\xi\gamma\lambda t}{2a(2\lambda - \gamma\lambda t)} = -\frac{\theta_e\gamma\lambda t}{(2\lambda - \gamma\lambda t)} \tag{3-7}$$

This expressed as

$$\frac{t}{\theta} = -\frac{2}{\gamma\theta_e} + \frac{t}{\theta_e} \tag{3-8}$$

Because $\theta = \frac{q_t}{q_m}$ and $\theta_e = \frac{q_e}{q_m}$, the equation can be written as

$$\frac{t}{q_t} = -\frac{2}{\gamma q_e} + \frac{t}{q_e} \tag{3-9}$$

By defining k_2 as $k_2 = -\frac{\gamma}{2q_e}$, equation (3-9) can be rewritten as

$$\frac{t}{q_t} = \frac{1}{k_2 q_e^{\,2}} + \frac{1}{q_e} t \tag{3-10}$$

This is the linear form of the pseudo-second-order kinetic model, which is expressed as

$$\frac{dq_t}{dt} = k_2 (q_e - q_t)^2 \tag{3-11}$$

Where q_e and q_t (mg/g) represents the adsorption capacity at equilibrium and the surface loading of arsenic at time t. The surface loading q_t can be expressed as

$$q_t = \frac{C_0 - C_t}{m} V \tag{3-12}$$

Where C_0 and $C_t\,(mg/L)$ is the initial concentration and concentration measured at time t. m is the dosage of adsorbent dry mass and V is the volume of the batch.

The constant $k_2 (g/mg\,h)$ is the pseudo-second-order kinetic constant. The expression $V_0 = k_2 q_e^{\,2}$ ($mg/g\,h$) when q_t / t approaches 0 is defined as the initial adsorption rate. The parameter $k_2^{'} = q_e k_2\,(h^{-1})$ has been regarded as the true (Azizian 2004, Coleman et al. 1956, Ho 2006, Ho and McKay 1999, Ho et al. 2000, Liu 2008). So, in this study, the three kinetic constants were applied to discuss the adsorption kinetics of arsenic onto the five FeCBs.

The By plotting t/qt versus t, q_e can be determined using the slope and k_2 can be calculated using the intercept. In the present study, the modeled q_t was then calculated using equation (3-4) and plotted versus t.

$$q_t = \frac{t}{1/k_2 q_e^{\,2} + t/q_e} \tag{3-13}$$

The equilibrium concentration can be calculated using the equation

$$C_e = C_0 - \frac{q_e m}{V} \tag{3-14}$$

3.2.2.1 Adsorption kinetics of As(III) on FeCBs

The adsorption kinetic data of As(III) with different concentrations onto FeCB1 are shown in Fig. 3.3 and the fitting results are listed in Table 3-1. The results show that the adsorption kinetics of As(III) onto FeCB1 was time dependent and affected by concentrations. When the initial concentrations were lower than 100 mg/L, the adsorption equilibrium generally occurred at 48 hours. It has been reported that the adsorption of arsenic on iron coated cellulose beads could be divided into two steps: 1) the saturation of exterior surface and 2) the diffusion in intraparticle pores. The diffusion rate decreased with the decrease of bulk solution concentration, which led to equilibrium when the diffusion rate became constantly lower.

Thus, the initial rate of adsorption could be used to represent the kinetics (Guo and Chen 2005). The V_0 increased with the increase of initial concentrations from 1.67 to 86.64 $mg \cdot g^{-1}h^{-1}$. The fitting results showed that the pseudo-second-order kinetic model fitted the experimental data well, suggested by all the determination coefficients greater than or equal to 0.99. This also indicated that the equilibrium concentrations and capacities were accurately estimated to be applied for adsorption isotherms.

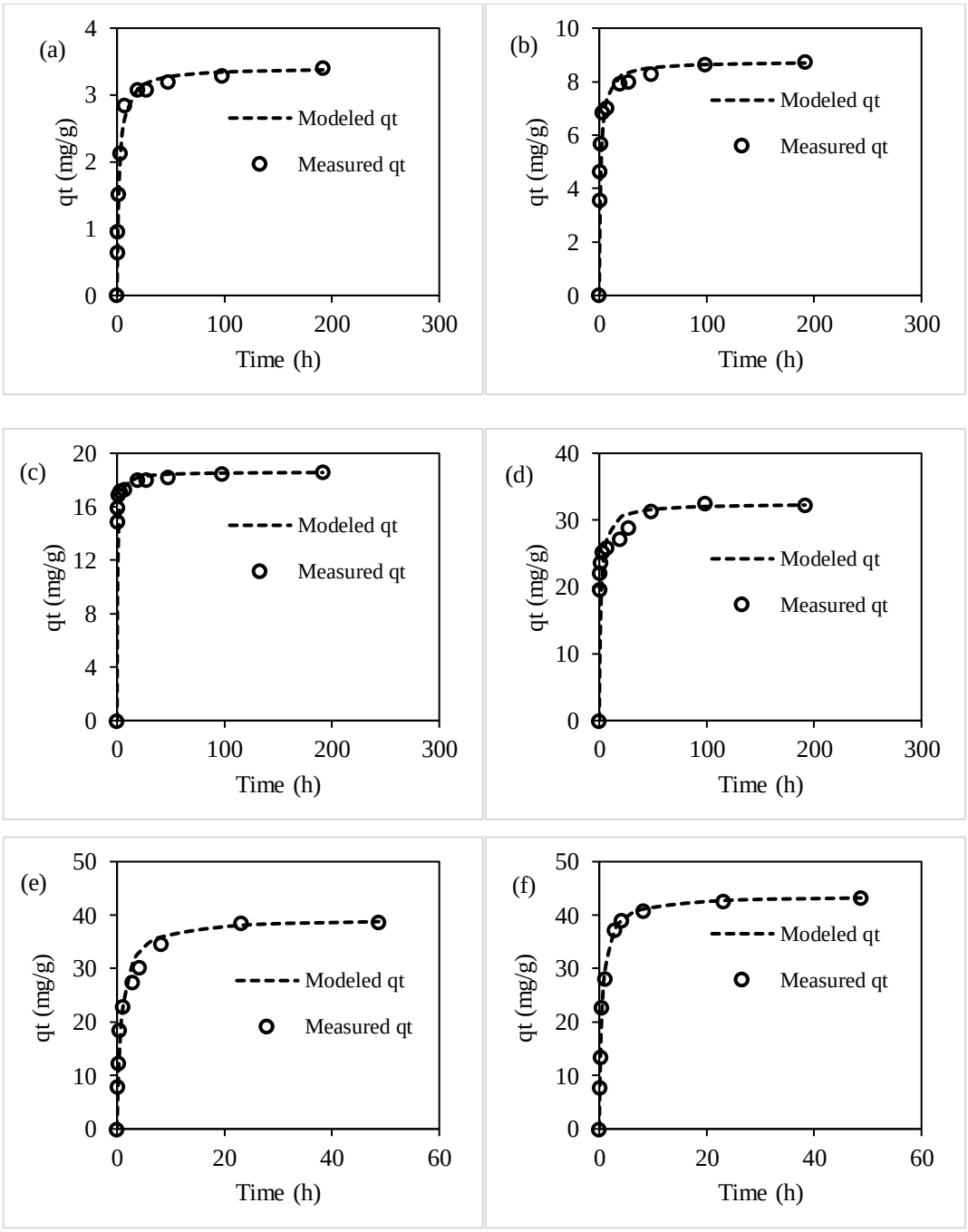

Fig. 3.3 Adsorption kinetic and pseudo-second-order modeling of As(III) on FeCB1. Initial concentration of As(III) in (a) to (f) was 5.19, 19.93, 51.36, 101.80, 293.20 and 486.01 mg/L. The concentration of dry mass FeCB1 in (a) to (f) was 0.25, 0.25, 0.25, 0.26, 0.26 and 0.26 g/L. Iron content of FeCB1 was 3.8%.

Adsorption kinetics of As(III) with different concentrations by FeCB2 are shown in Fig. 3.4 and the fitting results are listed in Table 3-2. Based on the fitting results, the pseudo-second-order fitted the data well with all the determination

coefficients greater than 0.99.

Table 3-1 Pseudo-second-order fitting of kinetic data of As(III) adsorption on FeCB1.

$C_0\,(mg/L)$	$C_e\,(mg/L)$	$q_e\,(mg/g)$	$k_2\,(g/mg\,h)$	$V_0\,(mg/g\,h)$	$k_2^{'}\,(h^{-1})$	R^2
5.19	4.34	3.41	0.14	1.67	0.49	0.99
19.93	17.74	8.76	0.08	6.37	0.73	0.99
51.36	46.71	18.60	0.12	41.43	2.23	1.00
101.80	93.35	32.48	0.02	23.13	0.71	0.99
293.20	282.95	39.42	0.03	49.22	1.25	0.99
486.01	474.658	43.66	0.04	86.64	1.98	1.00

Adsorption of As(III) onto FeCB2 approached equilibrium in about 70 hours when the concentrations were lower than 100 mg/L. When the concentrations increased to greater than 100 mg/L, the adsorption equilibrium could be achieved in 24 hours. However, the initial adsorption rates showed variations during the increase of concentrations.

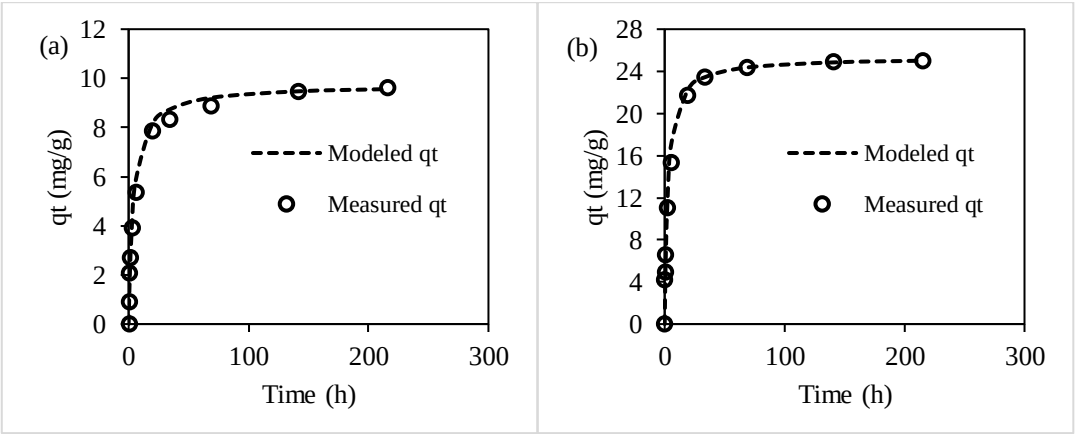

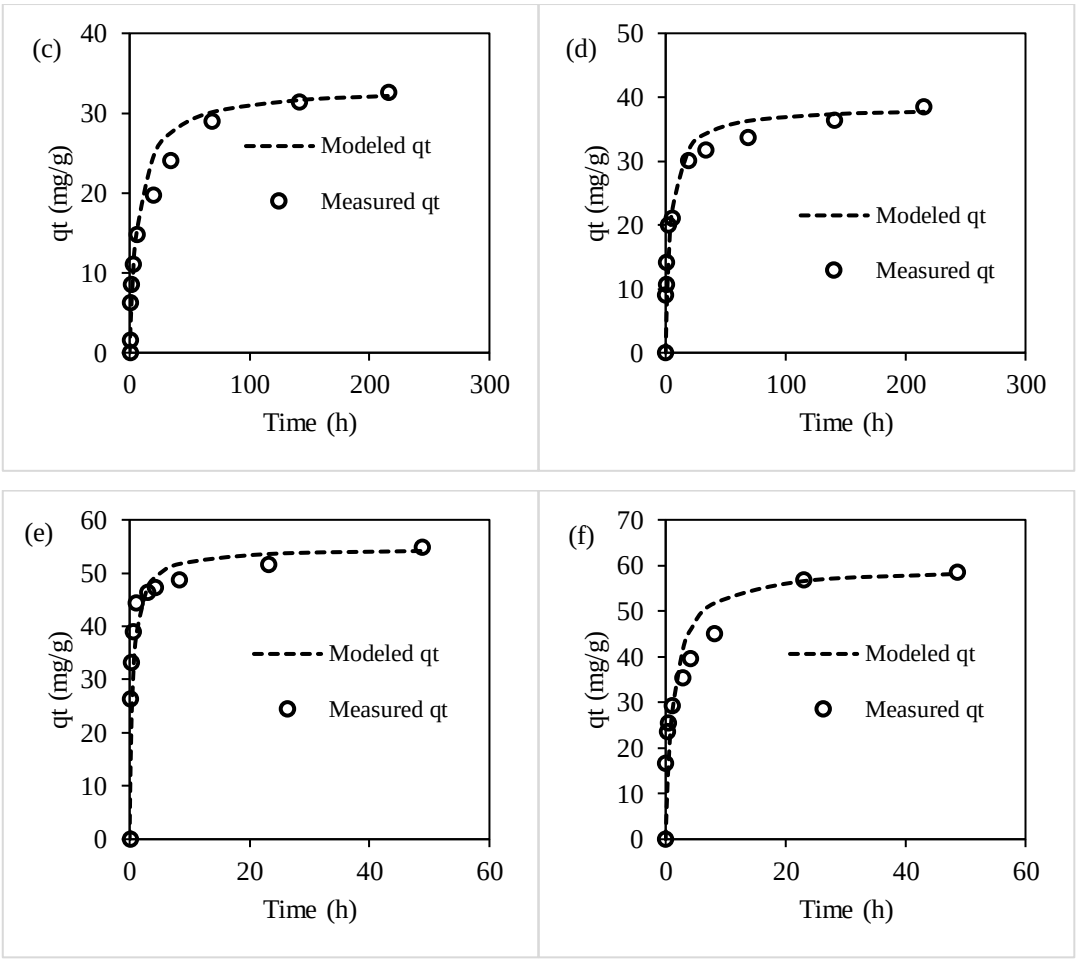

Fig. 3.4 Adsorption kinetic and pseudo-second-order modeling of As(III) on FeCB2. Initial concentration of As(III) in (a) to (f) was 5.29, 20.73, 50.42, 100.87, 296.20 and 486.01 mg/L. The concentration of dry mass FeCB2 in (a) to (f) was 0.26, 0.29, 0.29, 0.28, 0.26 and 0.27 g/L. Iron content of FeCB2 was 9.5%.

This could indicate that there could be several steps during the process of adsorption being rate limiting. Another reason could be the pH, agitation rate and adsorbent dosage in each batch were somewhat different even though the conditions were set to be identical.

Table 3-2 Pseudo-second-order fitting of kinetic data of As(III) adsorption on FeCB2.

$C_0\,(mg/L)$	$C_e\,(mg/L)$	$q_e\,(mg/g)$	$k_2\,(g/mg\,h)$	$V_0\,(mg/g\,h)$	$k_2^{'}\,(h^{-1})$	R^2
5.29	2.76	9.73	0.03	2.49	0.26	0.99

20.73	13.39	25.32	0.01	9.40	0.37	0.99
50.42	40.79	33.20	0.004	4.72	0.14	0.99
100.87	90.15	38.42	0.006	9.49	0.25	0.99
296.20	281.98	54.67	0.009	115.71	2.12	0.99
486.01	469.91	59.63	0.02	47.87	0.80	0.99

The adsorption kinetics of As(III) on FeCB3 is shown in Fig. 3.5 and the fitting results are listed in Table 3-3. The fitting results show that all the determinant coefficients are greater than or equal to 0.99, which suggests that the estimation of equilibrium concentrations and capacities are accurate to be applied for adsorption isotherms. The initial rates increased continuously from 4.57 to 240.42 mg/gh with the increase of initial concentrations.

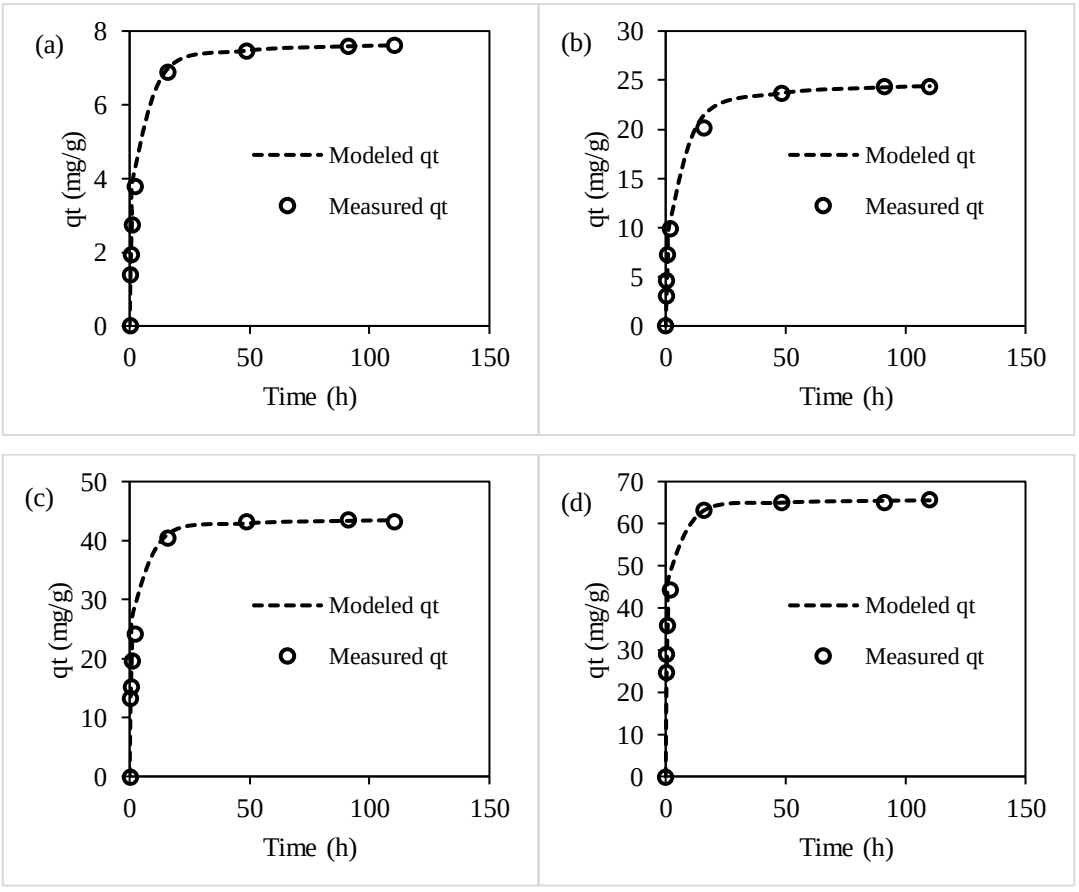

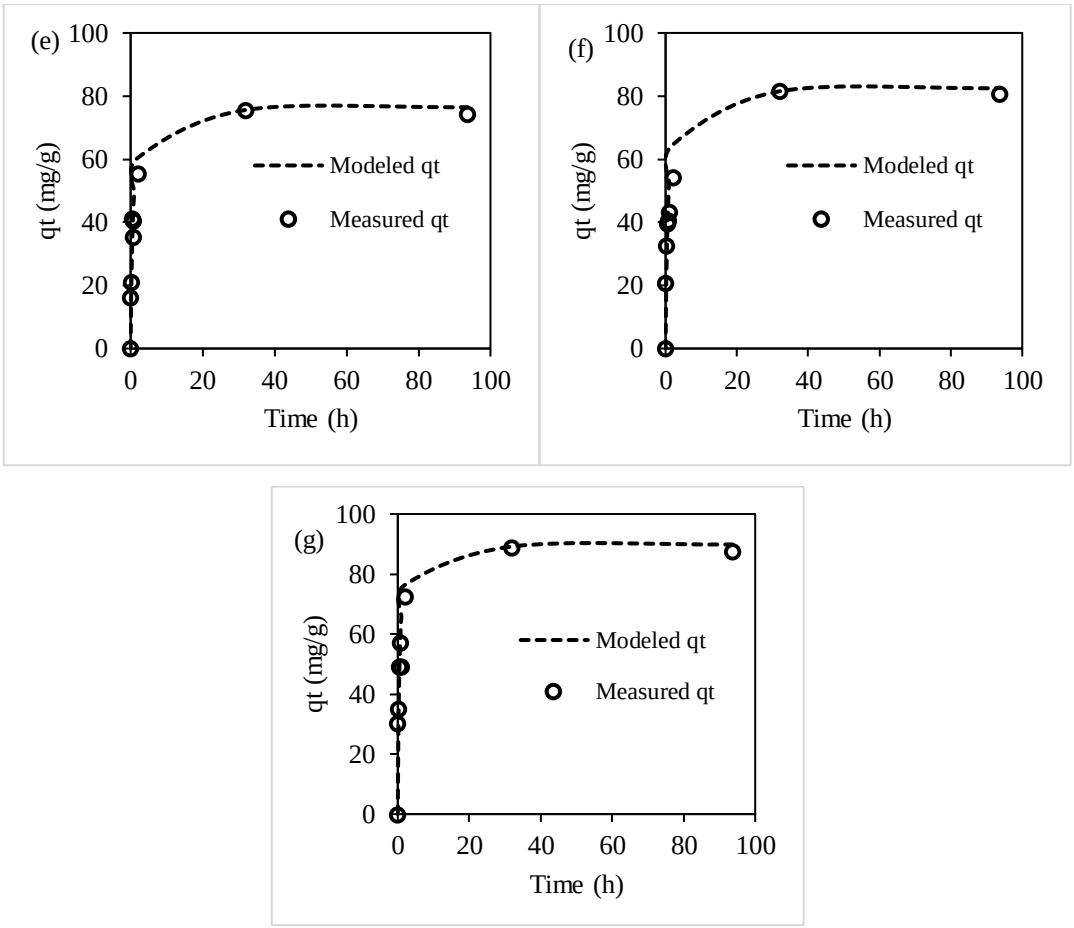

Fig. 3.5 Adsorption kinetic and pseudo-second-order modeling of As(III) on FeCB3. Initial concentration of As(III) in (a) to (g) was 5.01, 19.61, 49.08, 96.54, 198.44, 296.35 and 489.38 mg/L, respectively. The concentration of dry mass FeCB3 in (a) to (f) was 0.60, 0.62, 0.61, 0.58, 0.61, 0.65 and 0.72 g/L, respectively. Iron content of FeCB3 was 17.7%.

Table 3-3 Pseudo-second-order fitting of kinetic data of As(III) adsorption on FeCB3

$C_0(mg/L)$	$C_e(mg/L)$	$q_e(mg/g)$	$k_2(g/mg\,h)$	$V_0(mg/gh)$	$k_2^{'}(h^{-1})$	R^2
5.01	0.36	7.73	0.08	4.57	0.59	1.00
19.61	4.13	24.97	0.02	9.51	0.38	0.99
49.08	22.44	43.85	0.02	41.06	0.94	0.99

96.54	58.11	65.95	0.02	92.70	1.40	0.99
198.44	151.90	76.94	0.02	136.03	1.46	1.00
296.35	242.38	83.04	0.02	140.22	1.48	0.99
489.38	424.41	90.23	0.02	240.42	2.14	0.99

For the FeCB4, adsorption kinetics of As(III) with 7 initial concentrations are shown in Fig. 3.6. The pseudo-second-order equation fitting results are listed in Table 3-4. From the experimental data, the adsorption equilibrium could be achieved in 48 hours with the concentrations lower than 100 mg/L. If the concentrations were increased to over 100 mg/L, the adsorption equilibrium were reached in 6 hours.

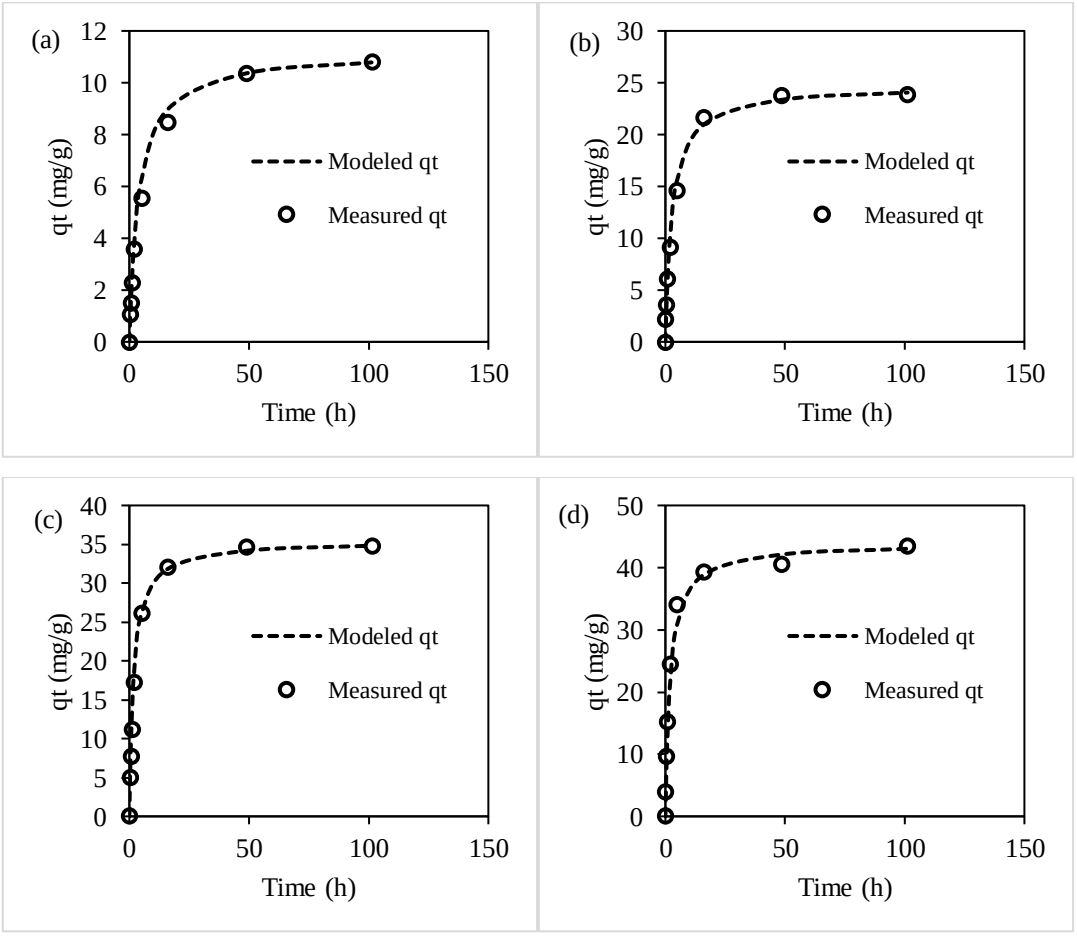

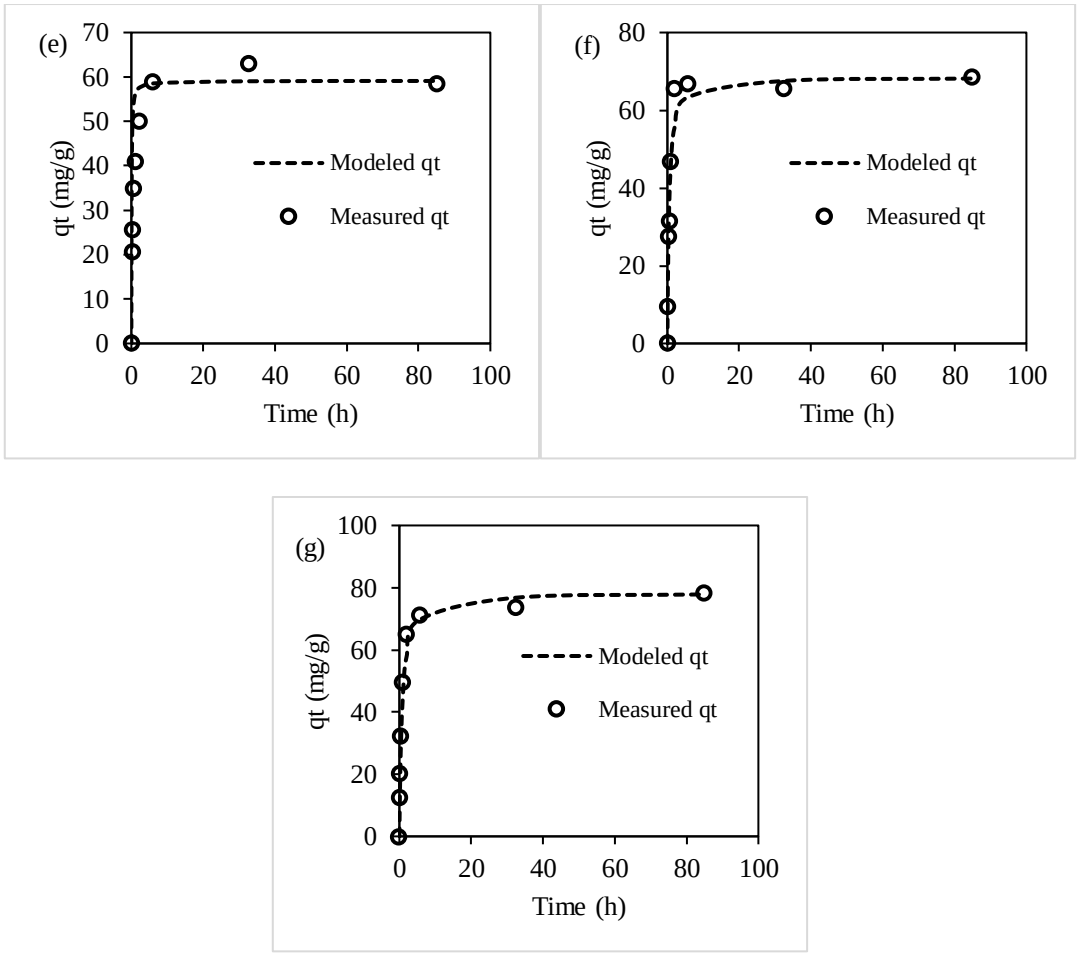

Fig. 3.6 Adsorption kinetic and pseudo-second-order modeling of As(III) on FeCB4. Initial concentration of As(III) in (a) to (g) was 5.01, 19.61, 49.08, 96.54, 198.44, 291.26 and 489.38 mg/L, respectively. The concentration of dry mass FeCB4 in (a) to (f) was 0.40, 0.40, 0.40, 0.42, 0.43 and 0.44 g/L, respectively. Iron content of FeCB4 was 20.5%.

Table 3-4 Pseudo-second-order fitting of kinetic data of As(III) adsorption on FeCB4

$C_0(mg/L)$	$C_e(mg/L)$	$q_e(mg/g)$	$k_2(g/mg\,h)$	$V_0(mg/gh)$	$k_2^{'}(h^{-1})$	R^2
5.01	0.56	11.21	0.02	2.81	0.25	0.99
19.61	9.65	24.74	0.01	8.59	0.35	0.99
49.08	34.73	35.44	0.02	19.49	0.55	0.99
96.54	78.20	43.92	0.01	21.04	0.48	0.99

198.44	173.01	59.13	0.29	1007.43	17.04	0.99
291.26	261.45	68.53	0.03	146.48	2.14	0.99
485.19	460.268	78.47	0.02	109.29	1.39	0.99

Adsorption kinetics of As(III) on FeCB5 are shown in Fig. 3.7. The experimental data were described using pseudo-second-order equation and the results are listed in Table 3-5. The adsorption of As(III) on FeCB5 was also time dependent and affected by initial concentrations. When the concentrations were lower than 50 mg/L, the adsorption equilibrium could be achieved in 50 hours. When the initial concentrations increased to over 50 mg/L, the time needed to reach equilibrium was less than 10 hours. Generally, in our present study, the time needed to achieve adsorption equilibrium decreased with the increase of concentrations. The increase of adsorption rate can also be expressed in terms of the initial rates V_0. With the increase of initial concentrations, the initial rates increased from 2.52 to 99.75 mg/gh. To better understand the effects of initial concentrations of As(III) on the adsorption rates, the initial rates were plotted versus initial concentrations, as shown in Fig. 3.8. For the FeCB2, the initial adsorption rates were linearly correlated to the initial concentrations. The fast adsorption kinetics can be attributed to the cellulose properties including high hydrophilicity, porosity and surface area. In addition, the uniform in situ formation of iron hydroxide on cellulose beads can improve the adsorption kinetics (Guo and Chen 2005).

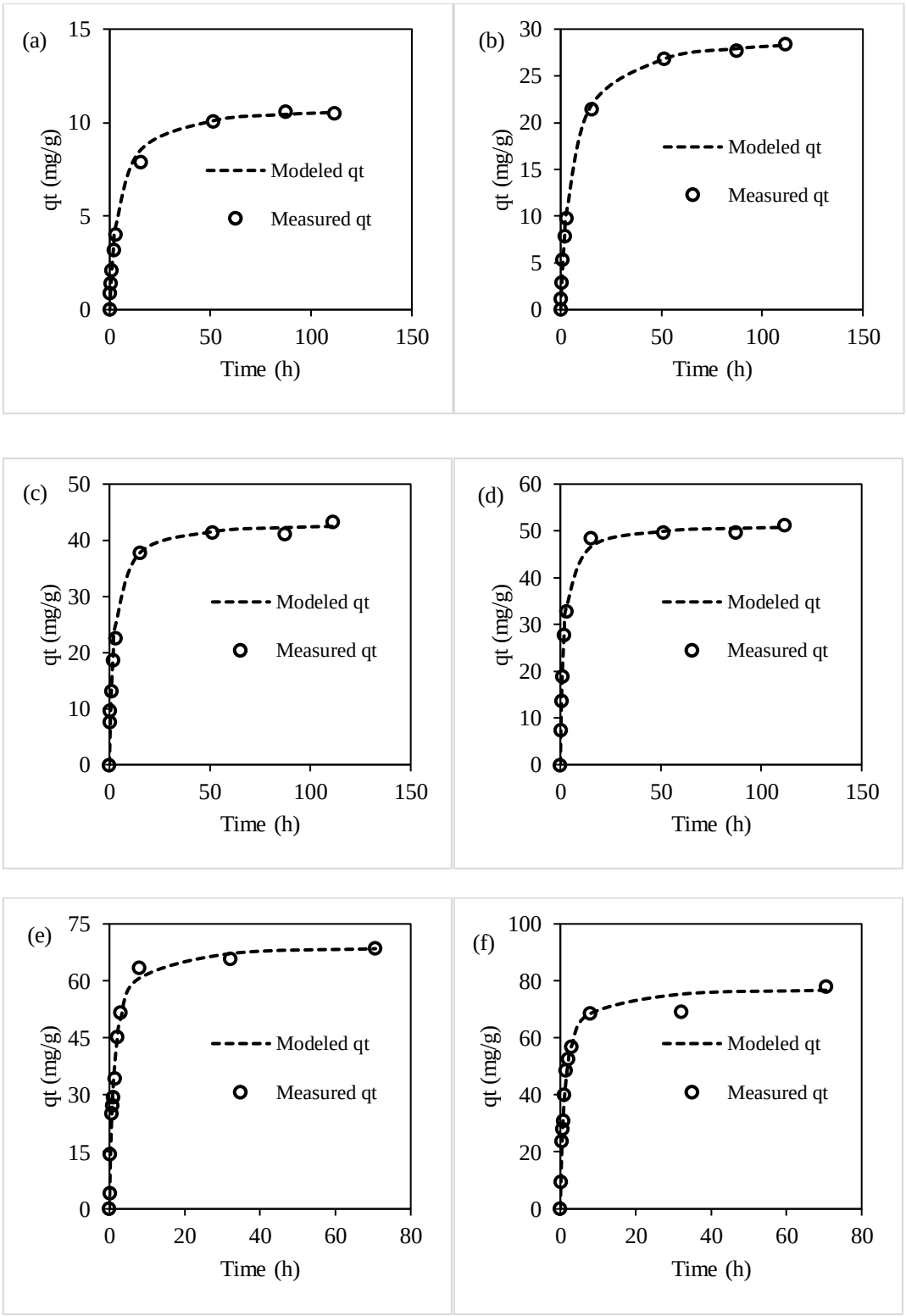
(a)
qt (mg/g)
Time (h)
Modeled qt
Measured qt
(b)
qt (mg/g)
Time (h)
Modeled qt
Measured qt
(c)
qt (mg/g)
Time (h)
Modeled qt
Measured qt
(d)
qt (mg/g)
Time (h)
Modeled qt
Measured qt
(e)
qt (mg/g)
Time (h)
Modeled qt
Measured qt
(f)
qt (mg/g)
Time (h)
Modeled qt
Measured qt

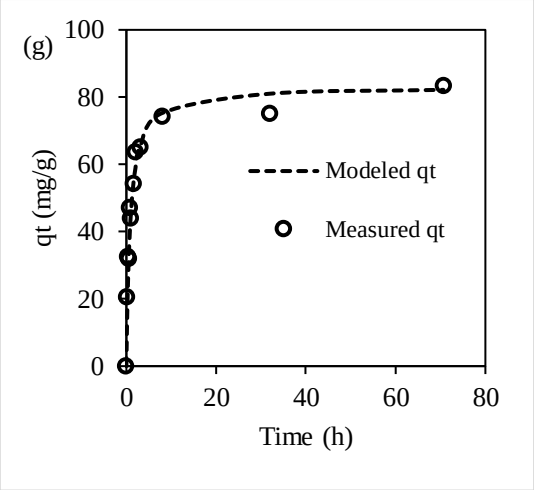

Fig. 3.7 Adsorption kinetic and pseudo-second-order modeling of As(III) on FeCB5. Initial concentration of As(III) in (a) to (g) was 5.01, 19.61, 49.08, 96.54, 198.44, 296.35 and 489.38 mg/L, respectively. The concentration of dry mass FeCB5 in (a) to (f) was 0.41, 0.41, 0.42, 0.46 0.47, 0.47 and 0.49 g/L, respectively. Iron content of FeCB5 was 21.7%.

Table 3-5 Pseudo-second-order fitting of kinetic data of As(III) adsorption on FeCB5

$C_0(mg/L)$	$C_e(mg/L)$	$q_e(mg/g)$	$k_2(g/mg\,h)$	$V_0(mg/gh)$	$k_2^{'}(h^{-1})$	R^2
5.01	0.49	10.96	0.02	2.52	0.23	0.99
19.61	7.38	29.65	0.006	5.45	0.18	0.99
49.08	30.99	43.32	0.01	19.39	0.45	0.99
96.54	74.66	51.46	0.01	32.40	0.63	0.99
194.67	162.64	69.62	0.01	59.61	0.86	0.99
295.85	259.04	77.90	0.01	71.67	0.92	0.99
477.27	436.74	83.13	0.01	99.75	1.20	0.99

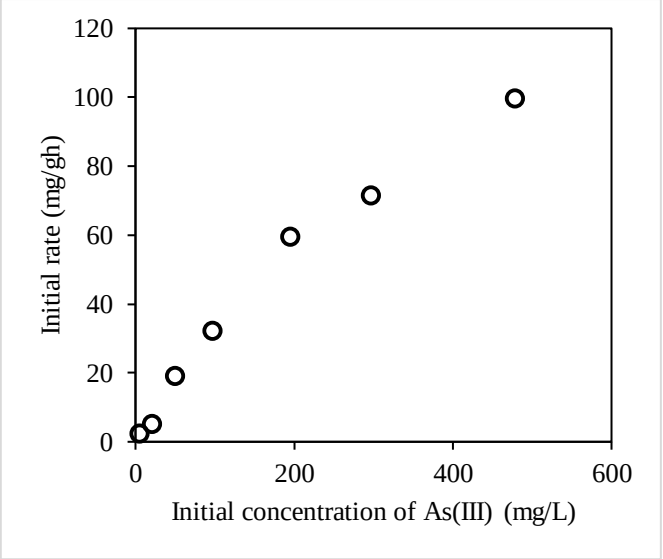

Fig. 3.8 Effects of initial concentrations on adsorption rate of As(III) onto FeCB5.

3.2.2.2 Adsorption kinetics of As(V) on FeCBs

For FeCB1, the adsorption kinetics for As(V) was determined in a concentration range of 1.06 to 52.56 mg/L. The experimental data and pseudo-second-order fitting are shown in Fig. 3.9. The fitting results are listed in Table 3-6. Based on the fitting results, the initial rates increased with the increase of initial concentration, which is similar to the adsorption behavior of As(III). The initial rate for the adsorption of 5.33 mg/L As(V) on FeCB1 was 1.11 mg/gh, which was close to that for As(III) adsorption on FeCB1.

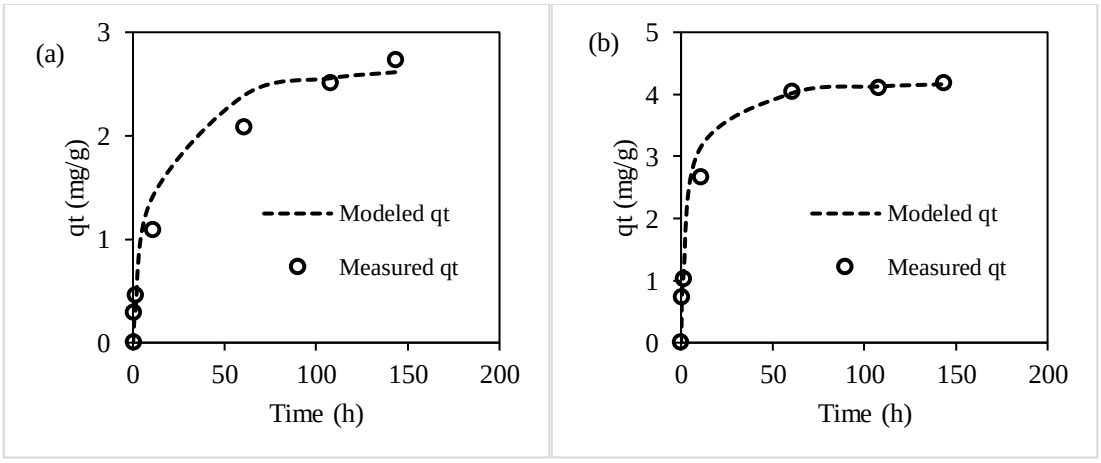

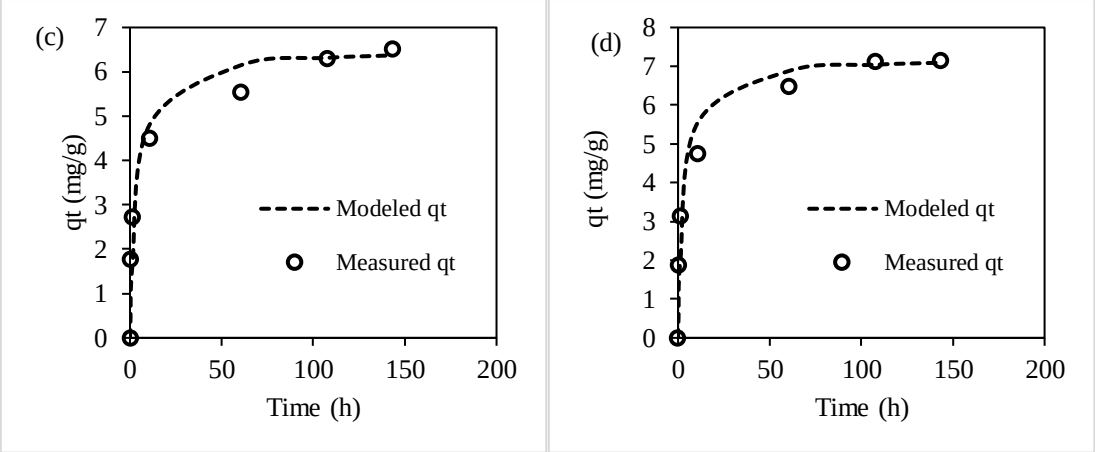

Fig. 3.9 Adsorption kinetics data and pseudo-second-order fitting of As(V) on FeCB1. Initial concentration of As(V) in (a) to (d) was 1.06, 5.33, 20.92, and 52.56 mg/L. The concentration of dry mass FeCB1 in (a) to (d) was 0.25, 0.26, 0.25, and 0.26 g/L. Iron content of FeCB1 was 3.8%.

Table 3-6 Pseudo-second-order fitting of kinetic data of As(V) adsorption on FeCB1

$C_0(mg/L)$	$C_e(mg/L)$	$q_e(mg/g)$	$k_2(g/mg\,h)$	$V_0(mg/gh)$	$k_2^{'}(h^{-1})$	R^2
1.06	0.36	2.81	0.03	0.26	0.09	0.99
5.33	4.23	4.27	0.06	1.11	0.26	0.99
20.92	19.30	6.54	0.04	1.69	0.26	0.99
52.56	50.66	7.26	0.04	2.20	0.30	0.99

However, with the increase of concentration, the increase of initial rates for As(III) increased dramatically while the increase of adsorption rate for As(V) showed slight increase. For example, when the concentration of As(III) increased to 51.36 mg/L, the estimated initial rate was 41.43, which was 18.8 times of the initial rate for As(V) when the concentration was 52.56 mg/L. This indicated that for FeCB1, the adsorption of As(III) was much faster than that of As(V), especially with high concentrations, suggesting the higher affinity of FeCB1 to As(III). The experimental pH was 7 ± 0.2, under which the As(V) was negatively charged $H_2AsO_4^-$ and $HAsO_4^{2-}$. The adsorption could be due to the electrostatic attraction between the surface iron species and arsenic

species. In addition, it has been reported that arsenic especially As(V) species could form inner-sphere surface complexes through ligand exchange with the surface hydroxyl groups (Farquhar et al. 2002, Sherman and Randall 2003). So, the rate limiting steps of adsorption may include surface diffusion, intraparticle diffusion and surface reactions.

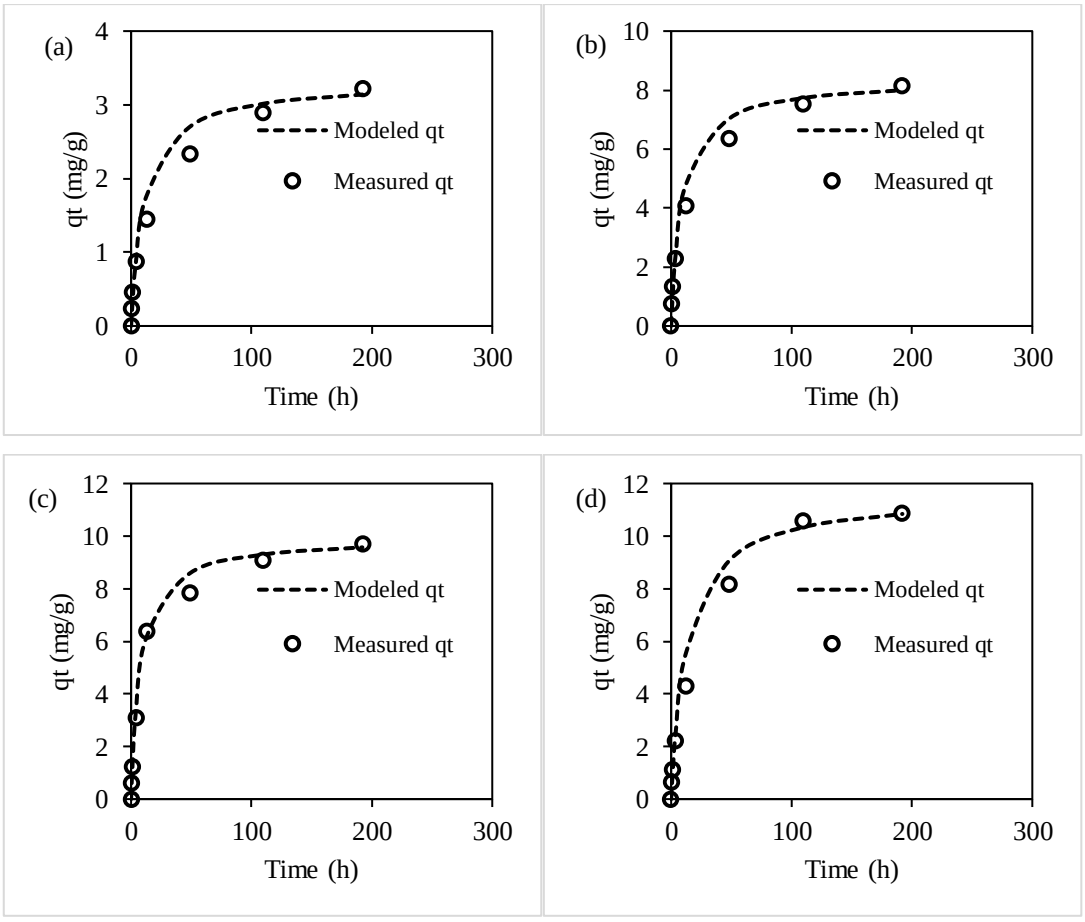

Fig. 3.10 Adsorption kinetics of As(V) on FeCB2 and the pseudo-second-order fittings. Initial concentration of As(V) in (a) to (d) was 1.03, 5.20, 20.27, and 51.51 mg/L. The concentration of dry mass FeCB2 in (a) to (d) was 0.29, 0.28, 0.27 and 0.30 g/L. Iron content of FeCB2 was 9.5%.

The adsorption kinetics of As(V) on FeCB2 and the pseudo-second-order fitting are shown in Fig. 3.10. The estimated parameters from the fitting are listed in Table 3-7. The adsorption behavior of As(V) onto FeCB2 was similar to that on FeCB1. With the increase of iron content on FeCB, the uptake of As(V) at equilibrium state increased

due to the availability of more adsorption sites. With regard to the kinetics, the adsorption of As(V) with all four concentrations was approaching adsorption equilibrium after 109 hours.

Table 3-7 Pseudo-second-order fitting of kinetic data of As(V) adsorption on FeCB2

$C_0(mg/L)$	$C_e(mg/L)$	$q_e(mg/g)$	$k_2(g/mg\,h)$	$V_0(mg/gh)$	$k_2^{'}(h^{-1})$	R^2
1.03	0.06	3.32	0.03	0.30	0.09	0.99
5.20	2.89	8.38	0.01	0.91	0.11	0.99
20.27	17.58	9.96	0.01	01.27	0.13	0.99
51.51	48.08	11.60	0.006	0.86	0.07	0.99

For FeCB3, the adsorption kinetics for As(V) was determined with concentrations ranging from 5.82 to 348.76 mg/L. The adsorption kinetics and pseudo-second-order kinetic fitting are shown in Fig. 3.11. The fitting results are listed in Table 3-8. The adsorption equilibrium for As(V) achieved equilibrium in 48 hours when the initial concentrations were lower than 100 mg/L. It took 10 hours for the adsorption to approach equilibrium for As(V) with concentrations above 100 mg/L. In addition, the initial rates of adsorption of As(V) with concentrations higher than 5 mg/L were linearly correlated with the initial concentrations.

The adsorption kinetics of As(V) by FeCB4 was investigated in a concentration ranging from 5.82 to 340.99 mg/L. The results and pseudo-second-order kinetic fitting are shown in Fig. 3.12. The fitting results of the parameters are listed in Table 3-9.

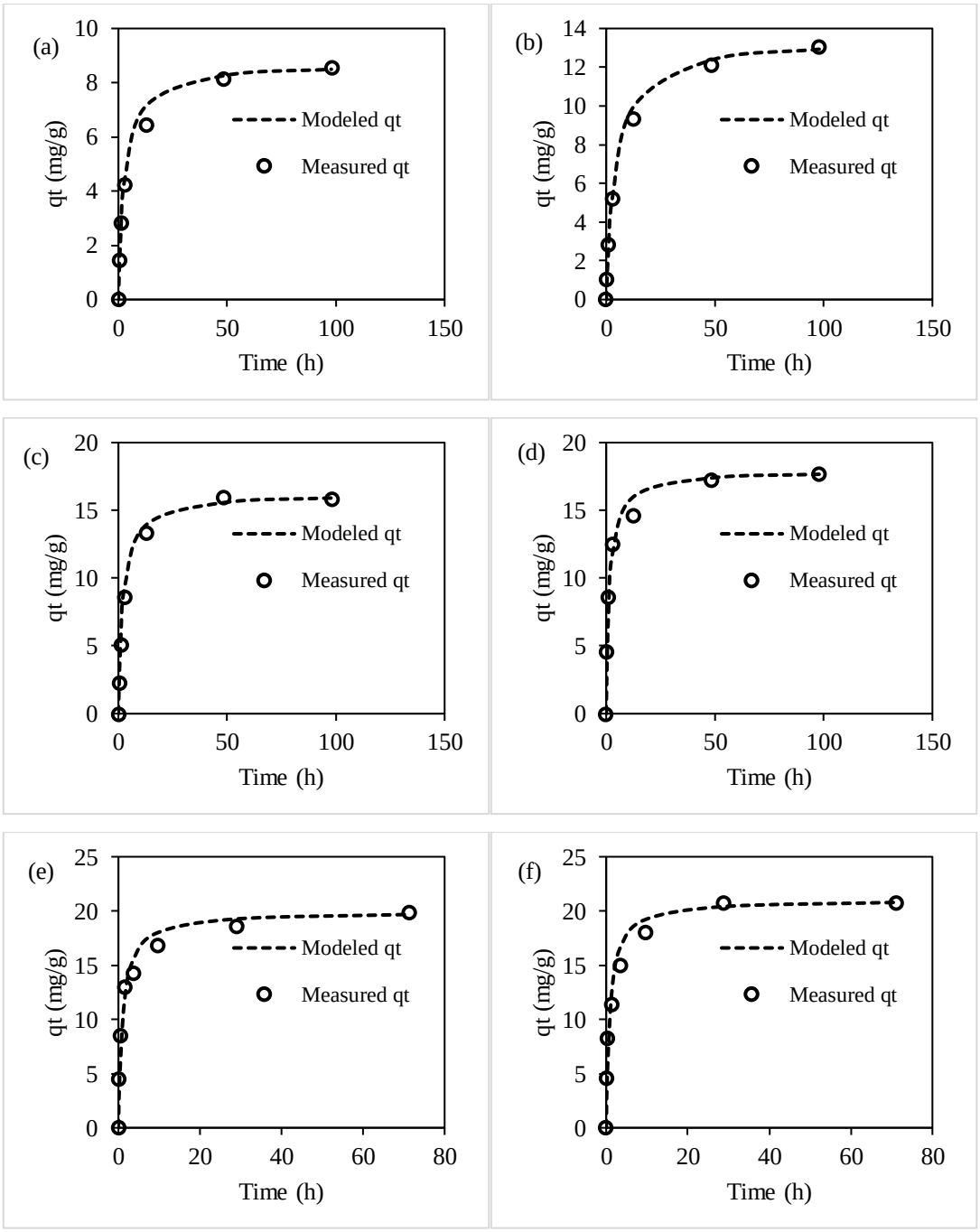

Fig. 3.11 Adsorption kinetics of As(V) on FeCB3 and the pseudo-second-order fittings. Initial concentration of As(V) in (a) to (f) was 5.82, 23.81, 59.87, 120.52, 228.88 and 348.76 mg/L. The concentration of dry mass FeCB3 in (a) to (f) was 0.62, 0.58, 0.62, 0.62, 0.60 and 0.66 g/L. Iron content of FeCB3 was 17.7%.

Table 3-8 Pseudo-second-order fitting of kinetic data of As(V) adsorption on FeCB3

$C_0(mg/L)$	$C_e(mg/L)$	$q_e(mg/g)$	$k_2(g/mg\,h)$	$V_0(mg/gh)$	$k_2^{'}(h^{-1})$	R^2
5.82	0.44	8.74	0.04	3.08	0.35	0.99
23.81	15.93	13.52	0.02	2.99	0.22	0.99
59.87	49.78	16.26	0.03	7.62	0.47	0.99
120.52	109.40	17.93	0.04	11.85	0.66	0.99
228.88	216.90	19.97	0.05	18.96	0.95	0.99
348.76	334.86	21.06	0.05	22.72	1.08	0.99

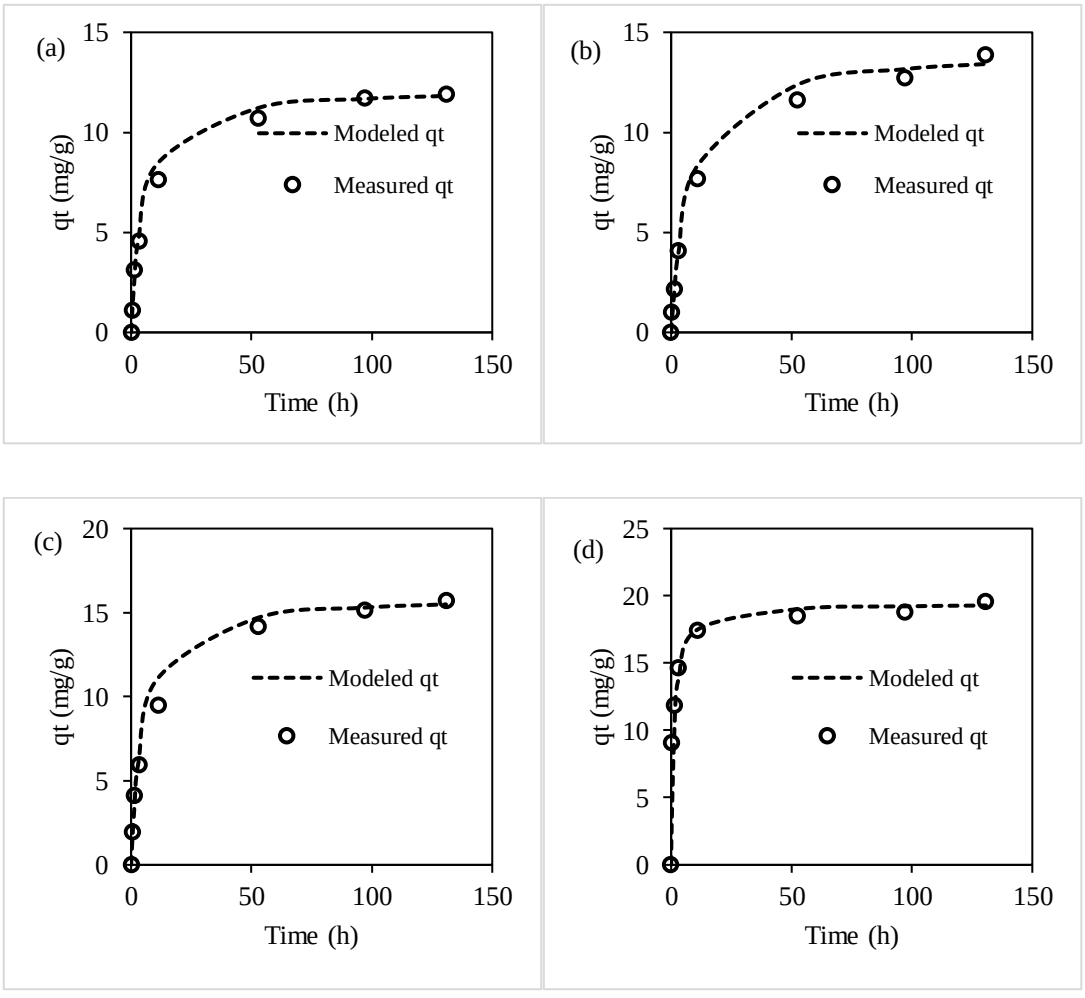

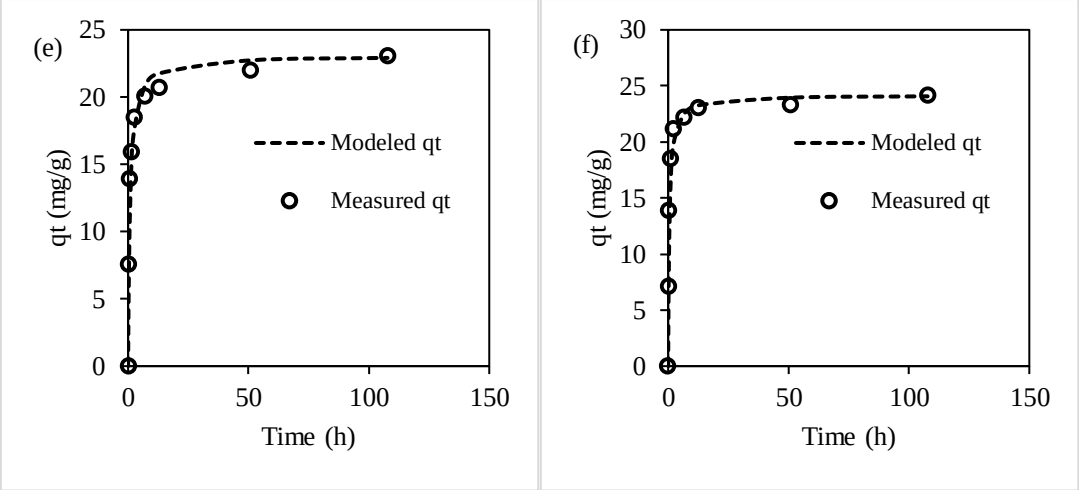

Fig. 3.12 Adsorption kinetics of As(V) on FeCB4 and the pseudo-second-order fittings. Initial concentration of As(V) in (a) to (f) was 5.82, 23.88, 57.02, 116.07, 228.88 and 340.99 mg/L. The concentration of dry mass FeCB4 in (a) to (f) was 0.42, 0.42, 0.42, 0.42, 0.41 and 0.44 g/L. Iron content of FeCB4 was 20.5%.

Adsorption of As(V) on FeCB4 could achieve equilibrium at 50 hours when the concentrations were lower than 100 mg/L. When the concentration increased to above 100 mg/L, the equilibrium occurred at 10 hours. With regard to the initial rates, adsorption of arsenic with higher concentrations had greater initial adsorption rates, which was consistent with the adsorption of As(III). The initial rates derived from the adsorption of As(V) with concentrations higher than 20 mg/L showed a linear correlation with the initial concentrations.

The adsorption kinetics of As(V) by FeCB5 was investigated in a concentration ranging from 5.82 to 48.76 mg/L. The results and pseudo-second-order kinetic fitting are shown in Fig. 3.13. The fitting results of the parameters are listed in Table 3-9. With regard to the kinetics, the kinetic behavior of adsorption of As(V) on FeCB5 was similar to that on the other FeCBs. When the concentrations were lower than 50 mg/L, the adsorption equilibrium was approached after 54 hours. With the increase of As(V) concentrations, the adsorption equilibrium could be achieved in 20 hours.

Table 3-9 Pseudo-second-order fitting of kinetic data of As(V) adsorption on FeCB4

$C_0(mg/L)$	$C_e(mg/L)$	$q_e(mg/g)$	$k_2(g/mg\,h)$	$V_0(mg/gh)$	$k_2^{'}(h^{-1})$	R^2
5.82	0.66	12.27	0.02	2.46	0.20	0.99
23.87	17.83	14.21	0.01	1.83	0.13	0.99
57.02	50.18	16.08	0.01	3.22	0.20	0.99
116.07	107.90	19.46	0.04	15.70	0.81	0.99
228.88	219.42	23.08	0.06	29.79	1.29	0.99
340.99	330.47	24.18	0.08	49.26	2.04	0.99

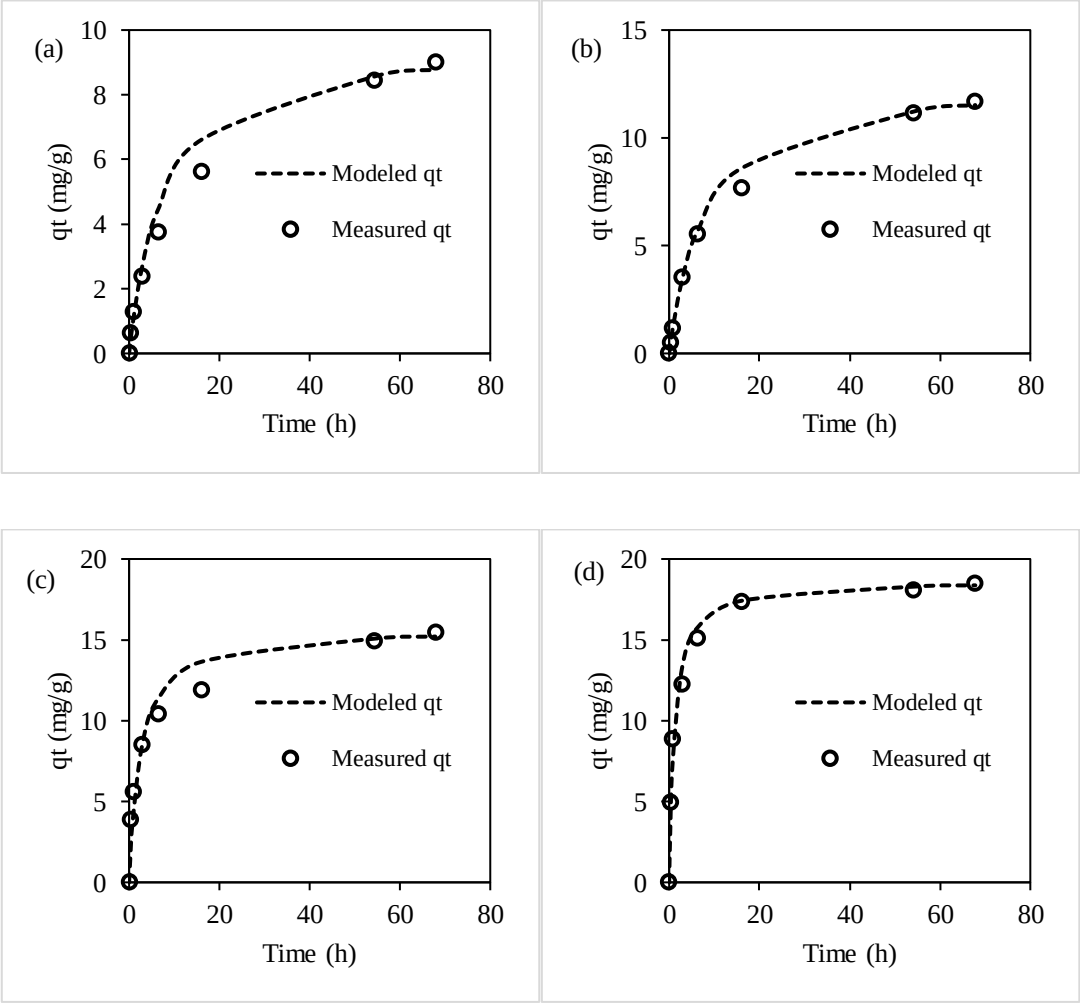

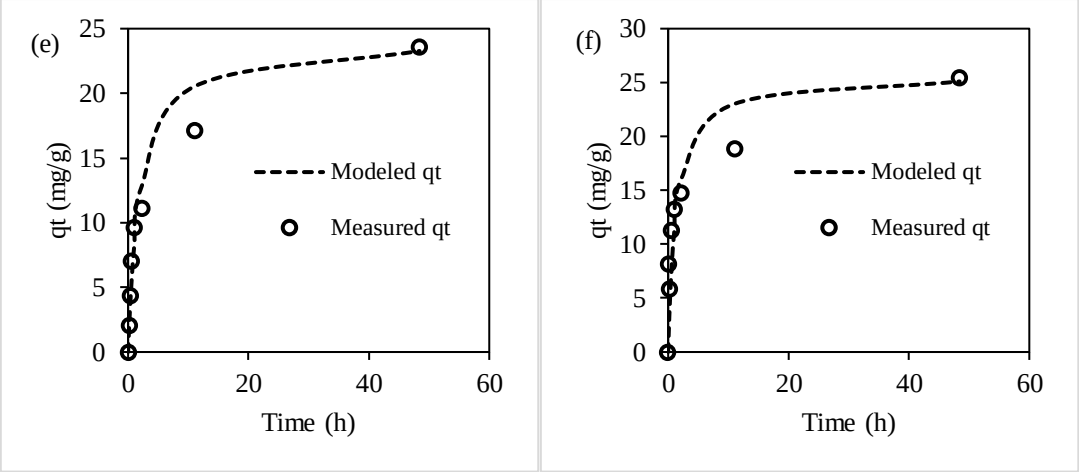

Fig. 3.13 Adsorption kinetics of As(V) on FeCB5 and the pseudo-second-order fittings. Initial concentration of As(V) in (a) to (f) was 5.82, 23.17, 56.74, 116.07, 228.88 and 348.76 mg/L. The concentration of dry mass FeCB4 in (a) to (f) was 0.43, 0.43, 0.44, 0.41, 0.43 and 0.42 g/L. Iron content of FeCB4 was 20.5%.

Table 3-10 Pseudo-second-order fitting of kinetic data of As(V) adsorption on FeCB5

$C_0(mg/L)$	$C_e(mg/L)$	$q_e(mg/g)$	$k_2(g/mg\,h)$	$V_0(mg/gh)$	$k_2^{'}(h^{-1})$	R^2
5.82	1.62	9.77	0.01	1.28	0.13	0.99
23.17	17.60	12.88	0.01	1.61	0.12	0.99
56.74	49.88	15.76	0.02	6.34	0.40	0.99
116.07	108.46	18.69	0.04	15.98	0.85	0.99
228.88	218.47	24.23	0.02	12.19	0.50	0.99
348.76	337.80	25.79	0.05	19.47	0.75	0.99

The initial rates of the adsorption of As(V) increased when the initial concentrations increased to 116.07 mg/L. Research has been conducted to compare the adsorption kinetics of As(III) and As(V) onto iron or aluminum based adsorbents. In our present study, by the estimation of initial adsorption rates, the adsorption rate of As(III) on FeCBs was greater than that of As(V). This is consistent with the results reported by Wilkie et al. (Wilkie and Hering 1996). Kim et al. reported that adsorption

kinetics of As(V) on alumina was greater than that of As(III) (Kim et al. 2004). Therefore, adsorption kinetic behavior is one of the most important factors for designing arsenic adsorbents for specific application scenarios, especially for waters with different predominant arsenic species.

3.2.3 Adsorption isotherms

The adsorption isotherms of As(III) and As(V) by each FeCB were determined using the estimated equilibrium concentrations and equilibrium capacities from the kinetic study. The data were fitted using Langmuir and Freundlich isotherm models. The Langmuir isotherm is expressed as

$$q_e = \frac{k_L q_{\max} C_e}{1 + k_L C_e} \tag{3-13}$$

Where $q_{\max}\,(mg/g)$ is the maximum adsorption capacity of the FeCBs for arsenic; $q_e\,(mg/g)$ is the equilibrium adsorption capacity; $C_e\,(mg/L)$ is the equilibrium concentration, and $k_L\,(L/mg)$ is the equilibrium constant (Langmuir 1918). The linear form of the equation can be written as

$$\frac{C_e}{q_e} = \frac{1}{k_L q_{\max}} + \frac{C_e}{q_{\max}} \tag{3-14}$$

By plotting $\frac{C_e}{q_e}$ versus C_e, $q_{\max}$ and k_L can be obtained through the slope and intercept, respectively. Then the modeled q_e can be calculated by the equation written as

$$q_e = \frac{C_e}{1/k_L q_{\max} + C_e / q_{\max}} \tag{3-15}$$

So, the modeled q_e was plotted versus C_e.

The Freundlich equation is expressed as

$$q_e = k_F C_e^{1/n} \tag{3-16}$$

Where, k_F and n are empirical constants, representing the adsorption capacity. The linear form of the equation can be written as

$$\lg q_e = \lg k_F + \frac{1}{n} \lg C_e \tag{3-17}$$

By plotting $\lg q_e$ with $\lg C_e$, the k_F can be obtained from the intercept and n can be obtained from the slope.

3.2.3.1 Adsorption isotherms of As(III) on FeCBs

To investigate the adsorption capacities of As(III) on the five FeCBs, adsorption equilibrium concentrations and capacities were compiled from kinetic experiments and modeling. The adsorption isotherms of As(III) on the five FeCBs and the Langmuir adsorption equation fittings are shown in Fig. 3.14. The fitting of isotherm data using linear form of Freundlich equation is shown in Fig. 3.15. Parameters estimated using Langmuir and Freundlich equation are listed in Table 3-1. The equilibrium data fitted the Langmuir and Freundlich equations well with the $R^2 \geq 0.94$. The high correlation coefficients suggested that both Langmuir and Freundlich models were suitable to describe the adsorption of As(III) onto FeCBs at equilibrium state. The Langmuir model represents the monolayer saturated loading of arsenic species on the surface of FeCBs at equilibrium. The saturation adsorption capacity $q_{\max}$ of FeCBs for As(III) increased from 49.88 mg/g to 92.03 mg/g when the iron content of FeCB increased to 17.7%.

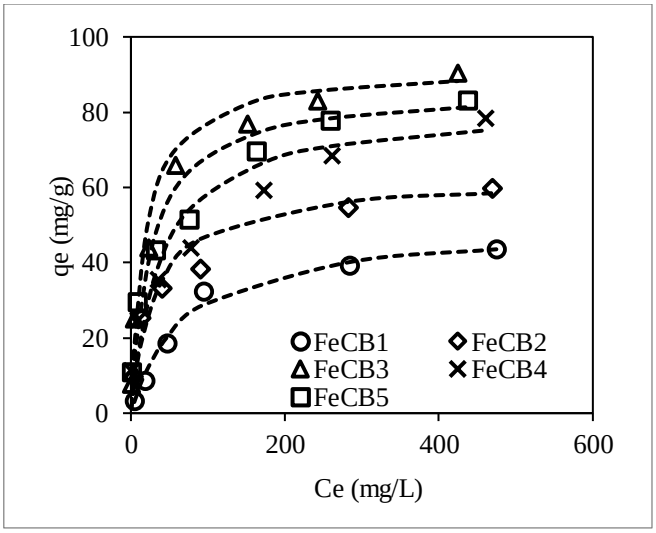

Fig. 3.14 Adsorption isotherms of As(III) on FeCBs and the Langmuir equation fitting. The equilibrium concentrations and capacities were estimated by the pseudo-second-order equation based on the kinetic data.

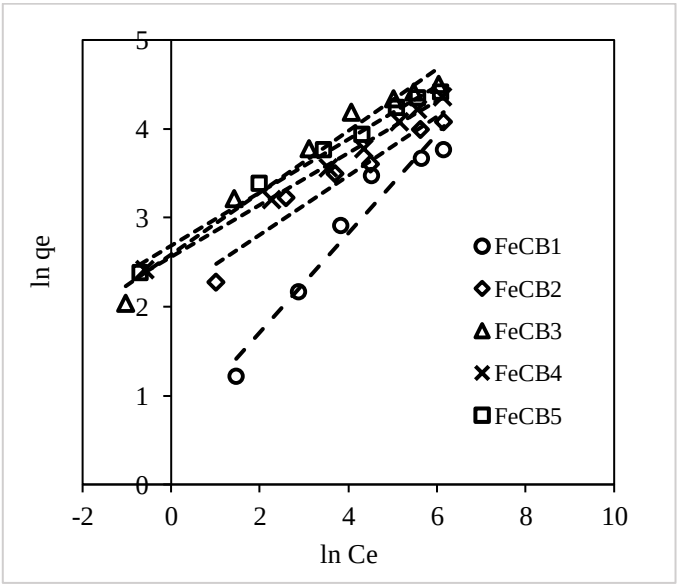

Fig. 3.15 Fitting of adsorption isotherms of As(III) on FeCBs using Freundlich equation. The equilibrium concentrations and capacities were determined using pseudo-second-order equation based on the kinetic data.

This could be attributed to the more available adsorption sites provided by the iron species. When the iron content continued to increase, the adsorption capacity decreased slightly, which could be due to the decreased porosity of FeCB surface caused by more iron hydroxide loading. The Freundlich equation is not used for

describing the equilibrium adsorption behavior. The constant k_F indicates the adsorption capacity of FeCB for As(III) and n is an indication of adsorption intensity which represents the effect of concentration on the adsorption capacity. Based on the fitting results, the values of k_F also show a peak at iron content of 17.7%, which could be regarded as the optimum iron loading on cellulose for As(III) adsorption. This is inconsistent with preliminary conclusion that the highest adsorption capacity is from the largest iron loading (Guo and Chen 2005).

Table 3-11 Isotherm fittings for the adsorption of As(III) on FeCBs

FeCB	Langmuir Equation			Freundlich Equation		
	$k_L\ (L/mg)$	q_{max}	R^2	$1/n$	k_F	R^2
FeCB1	0.01	49.88	0.99	0.56	1.81	0.95
FeCB2	0.03	62.37	0.99	0.33	8.54	0.94
FeCB3	0.06	92.03	0.99	0.35	13.29	0.97
FeCB4	0.02	81.43	0.98	0.29	12.94	0.99
FeCB5	0.04	86.10	0.99	0.30	14.67	0.99

3.2.3.2 Adsorption isotherms of As(V) on FeCBs

The adsorption capacity of the newly developed FeCB for As(III) was investigated in adsorption isotherms. The adsorption isotherms were built using equilibrium adsorption concentrations and capacities estimated by the pseudo-second-order kinetics based on the kinetics data. In addition, these equilibrium data were also described using Langmuir and Freundlich adsorption models. The adsorption isotherms

and Langmuir fitting are shown in Fig. 3.16. The Freundlich equation fitting is shown in Fig. 3.17. The fitting results from Langmuir and Freundlich equations are listed in Table 3-12.

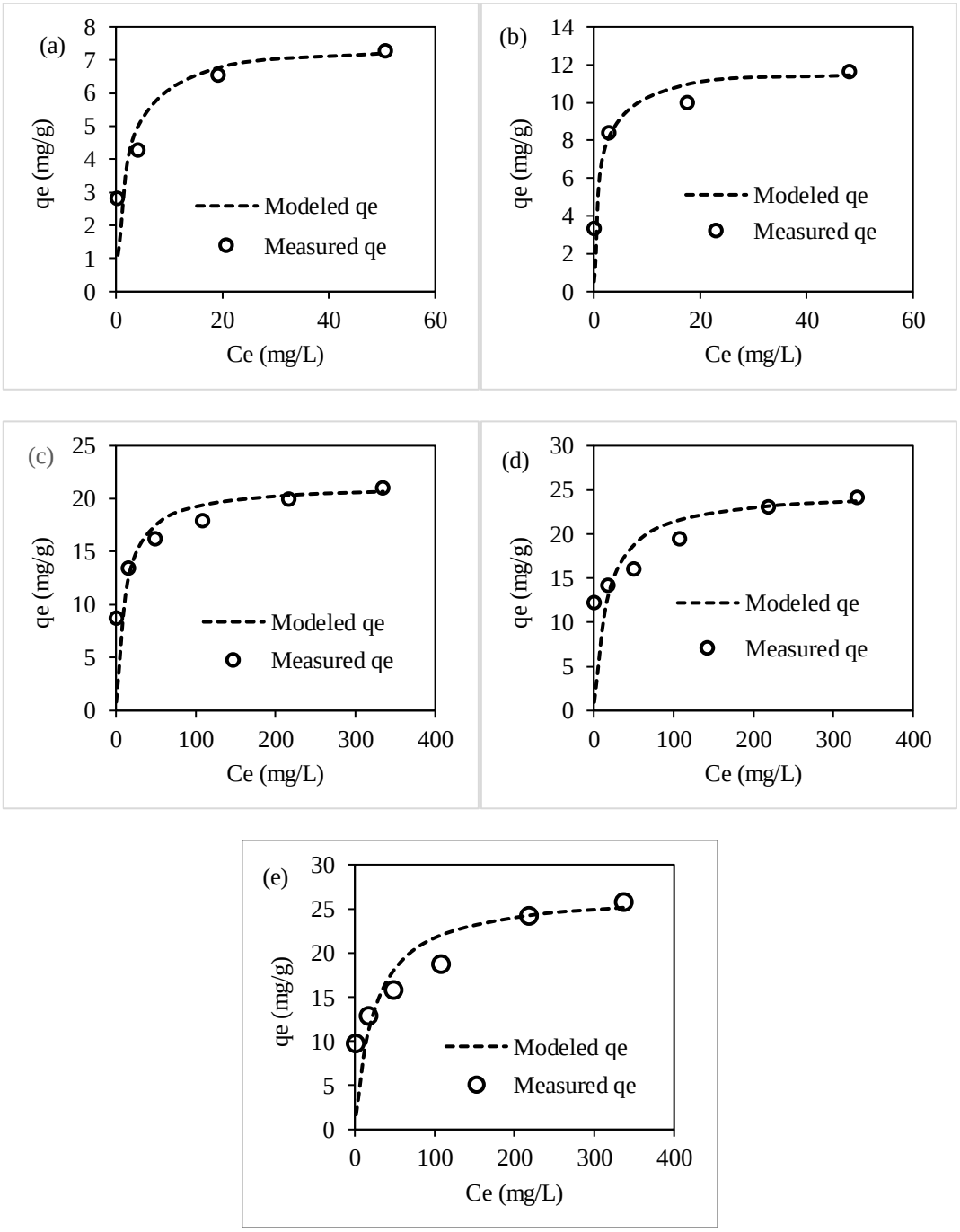

Fig. 3.16 Adsorption isotherms of As(V) on FeCB1 to FeCB5, represented by (a) to (e), respectively. The equilibrium concentrations and capacities were estimated using the pseudo-second-order equation based on the kinetic data.

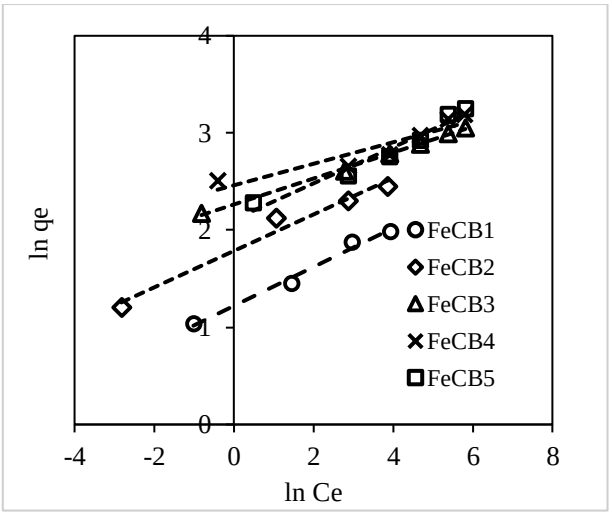

Fig. 3.17 Fitting of adsorption isotherms of As(V) on FeCBs by the linear form of Freundlich equation.

Table 3-12 Fittings of adsorption isotherms of As(V) on FeCBs

FeCB	Langmuir Equation			Freundlich Equation		
	$k_L\ (L/mg)$	q_{max}	R^2	$1/n$	k_F	R^2
FeCB1	0.48	7.50	0.99	0.20	3.39	0.98
FeCB2	0.80	11.74	0.99	0.19	5.96	0.97
FeCB3	0.09	21.35	0.99	0.13	9.62	0.99
FeCB4	0.06	24.92	0.99	0.11	11.72	0.86
FeCB5	0.04	26.93	0.98	0.18	8.24	0.95

For As(V), the Langmuir could be better used to describe the isotherms with all the fitting determination coefficients greater than 0.98. With the increase of iron content, the highest adsorption capacity was achieved on FeCB5. This is inconsistent with As(III) for which the highest adsorption capacity occurred on FeCB3. Compared to that of As(III), the adsorption capacities of As(V) were much lower. For example,

the Langmuir adsorption capacity for As(V) on FeCB3 was 21.35 mg/g, which was 23.20% of the capacity for As(III), which was 92.03 mg/g. This is consistent with a reported iron hydroxide loaded cellulose bead adsorbent on which the adsorption capacity of As(III) is three times larger than that of As(V) (Guo and Chen 2005). However, it is also reported that the adsorption capacity of As(V) on another iron cellulose composite adsorbent were higher than that for As(III) (Yu et al. 2013). The higher capacity for As(III) reported in this study suggests that the adsorbents are potential in application of arsenic removal from groundwater where As(III) is predominantly present. From the equation (3-9), the adsorption capacity can be obtained from the intercepts. Therefore, the fitting suggested that with the increase of iron content in FeCB, the adsorption capacity increased exponentially. This was because the adsorbent surface has not been saturated. So, more iron loading could provide more adsorption sites.

3.2.3.3 Effect of iron content on adsorption capacity

Generally, a large iron content is preferred when designing an arsenic adsorbent. For example, Guo et al. employed a seven-loading-step to prepare an iron hydroxide loaded cellulose bead with maximum iron loading, which reached 50% in terms of the mass of iron. However, there is a lack of study on the effects of iron content of an iron based adsorbent on its adsorption for arsenic. One of the objectives of this present study was to elucidate the relationship between the adsorption capacity and the iron contents. In this study, the adsorption kinetics and isotherms of As(III) and As(V) on iron hydroxide loaded cellulose beads with five iron loading amounts were investigated. For As(III), the effects of iron loading on the adsorption capacity are shown in Fig. 3.18. It is indicated that the adsorption capacity of As(III) increased linearly with the increase

of iron content when the iron content was below 17.7%. The slight decrease and following increase of adsorption capacity when the iron content was higher than 17.7% can be regarded as a stable level. This suggests that the continuous loading of iron hydroxide on cellulose beads would not result in a continuous increase of adsorption capacity for As(III).

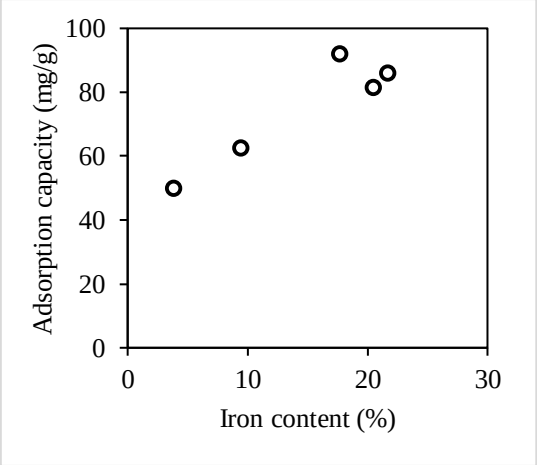

Fig. 3.18 Effects of iron content on the adsorption capacity of FeCBs for As(III).

The effects of iron contents of FeCBs on the adsorption capacity for As(V) is shown in Fig. 3.19. It shows that the Langmuir estimated adsorption capacity of FeCBs for As(V) is linearly related to the iron content.

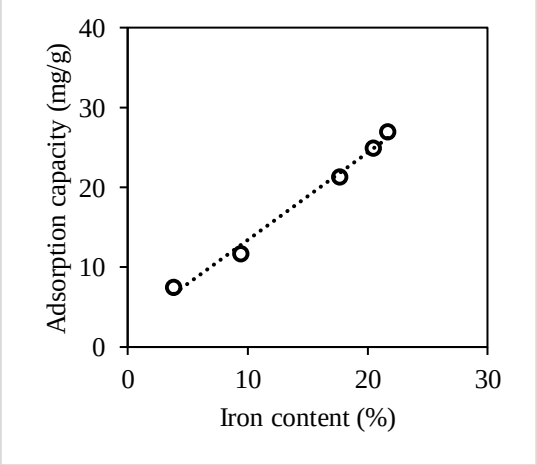

Fig. 3.19 Effects of iron contents of FeCBs on the adsorption capacity for As(V).

3.2.4 Effects of coexisting anions

In natural groundwater, many coexisting anions are present with arsenic species. The most studied coexisting anions are phosphate and sulphate because these anions can interfere the adsorption removal of arsenic by competing with arsenic for adsorption sites. In this study, kinetic method was applied to investigate the effects of phosphate with concentrations of 1 mg P/L and 5 mg P/L and sulphate with concentrations of 200 mg/L and 500 mg/L on the adsorption of As(III) on FeCB3. The kinetic data were fitted using the pseudo-second-order equation and the estimated equilibrium adsorption capacities and initial rates were compared. The kinetics and pseudo-second-order equation fitting are shown in Fig. 3.20. The fitting results are listed in Table 3-13. Most reported studies only compared the equilibrium adsorption capacities in the presence of competing anions while the effects on kinetics were less studied. In the present study, both equilibrium capacity and kinetics were compared to fully investigate the effects of coexisting anions.

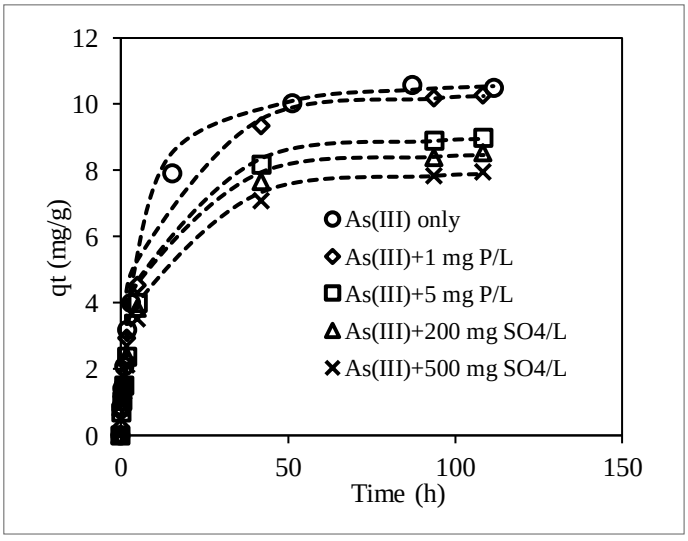

Fig. 3.20 Effects of coexisting phosphate and sulphate on the adsorption kinetics of As(III) on FeCB5.

The coexisting 1 mg/L P had no significant effect on the equilibrium adsorption capacity but reduced the initial rate by 17.9%. The presence of 5 mg/L P reduced the equilibrium adsorption capacity and initial rate by 15.5% and 26.8%, respectively. Due to the similar molecular structure with arsenic, phosphate has been regarded as the most important competing anion for arsenic. It has been reported that phosphate has the greatest potential for competing adsorption sites compared to other anions such as nitrate and sulphate (Yu et al. 2013). However, this conclusion should be restricted to specific concentrations of the anions. In this study, the equilibrium adsorption capacity and initial rate of As(III) in the presence of 200 mg/L SO_4^{2-} was 19.4% and 24.9 % lower than that of As(III) without the presence of SO_4^{2-}. The presence of 500 mg/L SO_4^{2-} reduced the adsorption capacity and initial rate by 24.4% and 39.3, respectively. This suggests that the presence of sulphate with high concentrations can pose greater effects on arsenic adsorption than lower concentration of phosphate.

Table 3-13 Fitting of adsorption kinetics of As(III) on FeCB5 with or without the presence of phosphate or sulphate

Adsorption system	$q_e(mg/g)$	$V_0(mg/gh)$	R^2
5 mg As(III)/L	10.96	2.52	0.99
5 mg As(III)/L +1 mg P/L	10.74	2.07	0.93
5 mg As(III)/L+5 mg P/L	9.37	1.84	0.93
5 mg As(III)/L+ 200 mg SO_4^{2-}/L	8.83	1.89	0.92
5 mg As(III)/L+ 500 mg SO_4^{2-}/L	8.29	1.53	0.92

3.2.5 Regeneration

To investigate the reusability of FeCBs, two cycles of desorption and adsorption

were conducted using 2 M NaOH as a regeneration reagent. In each cycle, the As(III) loaded FeCB5 contained one desorption and one adsorption experiment. The adsorption kinetics were fitting using the pseudo-second-order kinetic equations and the adsorption capacity and initial rate were compared. The results are shown in Fig. 3.21 and the fitting results are listed in Table 3-14. The desorption rate in regeneration cycle 1 and cycle 2 by 2 M NaOH was 85.95% and 79.46%, respectively.

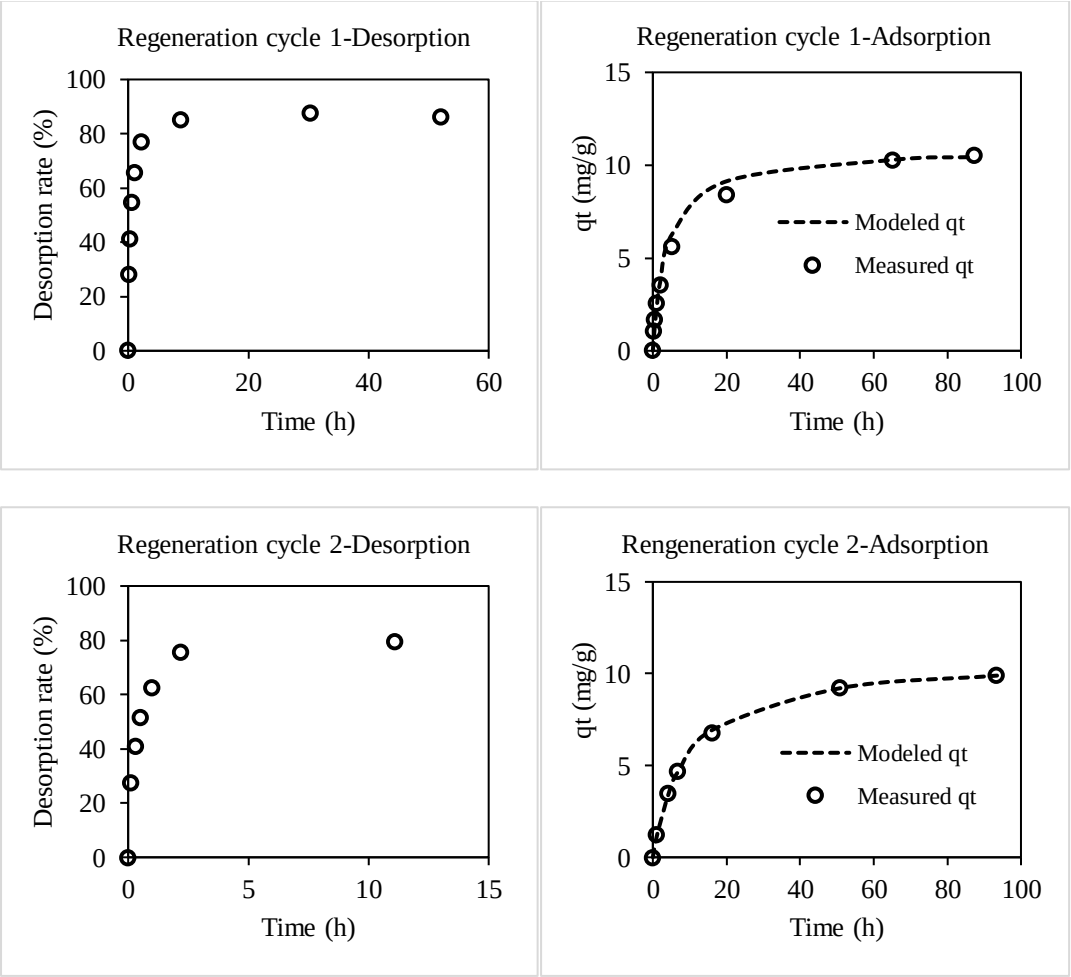

Fig. 3.21 Two cycles of regeneration performance of As(III) loaded FeCB5 by 2 M NaOH solution. The As(III) loaded FeCB5 was collected from the adsorption kinetics of 5.01 mg/L As(III) and washed using ultrapure water.

The adsorption capacities of the two cycles were 99.5% and 99.1% of the original capacity. There was no decrease for the initial rate in the first cycle. However,

the initial rate for the second cycle was 47.2% of the original initial rate. This means even though two cycles of regeneration did not significantly reduce the equilibrium capacity, the initial rate for adsorption was dramatically reduced. So the adsorption rate is an important to be consider for regeneration.

Table 3-14 Fitting of adsorption of As(III) on the first and second regenerated FeCB5.

Regeneration adsorption	$q_e(mg/g)$	$V_0(mg/gh)$	R^2
Cycle 1-Adsorption	10.90	2.52	0.99
Cycle 2-Adsorption	10.86	1.19	0.99

3.3 Conclusions

Iron hydroxide loaded cellulose beads with were successfully developed using five iron contents. The adsorption kinetics and isotherms of the newly developed FeCBs for As(III) and As(V) were investigated in batch experiments. Generally, the initial rates of adsorption increased with the increase of arsenic concentrations. Adsorption isotherms showed that the adsorption capacity for As(III) reached maximum (92.03 mg/g) when the iron content was 17.7%. The adsorption capacity for As(V) increased exponentially with iron contents. Effects of coexisting phosphate and sulphate on the adsorption of As(III) was dependent on concentrations of the anions. The presence of 1 mg/L P posed little effect on As(III) adsorption while the 500 mg/L SO_4^{2-} largely interfered the adsorption by reducing both adsorption capacity and kinetics. The equilibrium adsorption capacity did not change in two cycles of regeneration. However, the adsorption rate was dramatically reduced in the second cycle.

CHAPTER 4
BREAKTHROUGH OF ARSENIC IN COLUMNS

Practical application of adsorption is in many cases associated with adsorption in packed bed columns to achieve a continuous operation. The adsorbents are packed in a column and fluid containing adsorbate flows through the bed. Adsorption happens from the influent position to the effluent position. The transport behavior of the target adsorbate is described in terms of breakthrough curves, which is usually expressed as the effluent concentration versus time or volume of the effluent. During this process, the breakthrough behavior or the shape of breakthrough curve is controlled by several parameters including convection, dispersion, and adsorption kinetics. A laboratory scale column experiment is important to understand the mass transfer process in the column and to provide insights to a practical scale column. The dimensionless mathematical parameters can be used to scale down a pilot scale column (Ali and Gupta 2007). The most important solute transport model is the convection-dispersion equation (CDE) with or without equilibrium adsorption. For one-dimensional transport, the CDE is written as

$$\frac{\partial C}{\partial t} = \frac{\partial}{\partial x}(D_H \frac{\partial C}{\partial x}) - u\frac{\partial C}{\partial x} \tag{4-1}$$

Where $C(ML^{-3})$ is the concentration of the solute; $D_H(L^2T^{-1})$ is the hydrodynamic dispersion coefficient; $u(LT^{-1})$ is the pore water velocity; $x(L)$ is the distance and $t(T)$ is time. The dispersion coefficient D_H is defined as

$$D_H = D_0 / \tau + \alpha u \tag{4-2}$$

Where $D_0(L^2T^{-1})$ is the molecular diffusion coefficient; $\alpha(L)$ is the

dispersivity. Generally, the diffusion term is negligible. So, the dispersion term is reduced to

$$D_H = \alpha u \tag{4-3}$$

The estimation of parameters is an inverse problem, which can be done by fitting the experimental date to the solution of the equation. For the breakthrough behavior of arsenic in a column packed with adsorbents, the adsorption is taken into consideration in the CDE, which is turned out to be a convection-dispersion -adsorption equation. The adsorption can occur at equilibrium state and nonequilibrium state. In this study, breakthrough behavior of As(III) and As(V) were determined and described using equilibrium and nonequilibrium models.

4.1 Experimental section

4.1.1 Materials

The column experiments were conducted using glass columns of 14.0 cm in length and 1.0 or 2.5 cm in diameter. The FeCB3 was used for the packed bed column experiments. Influent As(III) and As(V) solutions of 50 µg/L were prepared by diluting the stock solutions. The average particle size of FeCB3 was 3.3 mm determined by a particle size distribution analysis.

4.1.2 Tracer experiment

To determine the dispersion coefficients, a tracer breakthrough curve was obtained using methylene blue and bare cellulose beads that was uniformly packed in a column of 14.0 cm in length and 2.5 cm in diameter. The empty bed contact time (EBCT) was 26.1 min. The porosity of the packed bed was 0.42. The influent concentration of methylene blue was 1 mg/L. The influent solution was pumped

through the packed column using a peristaltic pump (BT100-2J, Longer, China) at a rate of 2.63 mL/min. The pore velocity was determined to be 77.00 cm/h. At prescribed time intervals, 3.0 mL of effluent was collected for analysis. The concentration of methylene blue was analyzed using a UV-Visible spectrophotometer (Aqualog, Horiba, France) with a wave length of 660 nm. The obtained breakthrough was fitted to the CDE with equilibrium adsorption using Stanmod modeling package.to determine the dispersion coefficient

4.1.3 Breakthrough of arsenic

Columns used in the arsenic breakthrough experiments were of 14.0 cm in length and 1.0 cm in diameter. The columns were uniformly packed with wet FeCB3 beads. The bulk density of the column was 0.055 g/mL. The porosity of the packed column was 0.30. The influent concentration of As(III) and As(V) were 50 µg/L. The influent solutions were pumped upward through the column at a rate of 1.43 mL/min for As(III) and 2.22 mL/min for As(V). At prescribed time intervals, 5.0 mL of effluents were collected and passed through a 0.45-µm membrane filter. Then 1.0 mL of the filtrate was taken and diluted to 10 mL using 2% nitric acid. The concentration was analyzed using ICP-MS. The obtained breakthrough data was fitted to the two-sties nonequilibrium CDE model using Stanmod modeling package to estimate the key parameters.

4.2 Modeling discussion

4.2.1 The equilibrium CDE for breakthrough behavior

The governing equation is written as (Shi et al. 2016)

$$R\frac{\partial C}{\partial t}+u\frac{\partial C}{\partial x}=D\frac{\partial^2 C}{\partial x^2} \tag{4-4}$$

Where R is the retardation factor, which is defined as

$$R=1+\frac{\rho_b K_d}{\theta} \tag{4-5}$$

Where $\rho_b\,(g/mL)$ is the bulk density; $K_d\,(L/kg)$ is the partition coefficient; θ is the porosity. To make the equation dimensionless, let $\theta=\frac{C}{C_0}, \tau=\frac{ut}{L}, X=\frac{x}{L}$, the dimensionless form of the equation can be expressed as

$$\frac{\partial\theta}{\partial\tau}+\frac{1}{R}\frac{\partial\theta}{\partial X}=\frac{1}{R}\frac{1}{Pe}\frac{\partial^2\theta}{\partial X^2} \tag{4-6}$$

Where $\frac{1}{Pe}=\frac{D}{Lu}$, Pe is called Peclet number.

The analytical solution for the dimensional equation is

$$C(x,t)=C_0\{\frac{1}{2}erfc[\frac{Rx-ut}{2(DRt)^{1/2}}]+\frac{1}{2}\exp(\frac{ux}{D})erfc[\frac{Rx+ut}{2(DRt)^{1/2}}]\} \tag{4-7}$$

4.2.2 Nonequilibrium models of breakthrough behavior

The nonequilibrium transport behavior of arsenic in the column can be attributed to two factors: adsorption kinetics on different sites and heterogeneous flow regions (Toride et al. 1993). For the kinetic controlled transport process, adsorption of arsenic on some sites is equilibrium and instantaneous, while adsorption on other sites is governed by first-order kinetics. Based on this assumption, a two-site nonequilibrium model can be derived. The equations are written as:

$$(1+\frac{f\rho_b K_d}{\theta})\frac{\partial C}{\partial t}=D\frac{\partial^2 C}{\partial x^2}-v\frac{\partial C}{\partial x}-\frac{\alpha\rho_b}{\theta}[(1-f)K_d C-s_k] \tag{4-8}$$

$$\frac{\partial s_k}{\partial t} = \alpha[(1-f)K_d C - s_k] \tag{4-9}$$

Where, f is the fraction of sites at equilibrium adsorption; ρ_b is the bulk density; K_d is the partition coefficient; s_k is the adsorbed concentration on kinetic adsorption sites; α is the first-order adsorption coefficient;

To make the equations dimensionless, let $C_1 = \frac{C}{C_0}$, $T = \frac{vt}{L}$, $X = \frac{x}{L}$,

$$C_2 = \frac{s_k}{(1-f)K_d C_0} \tag{4-10}$$

Therefore, the dimensionless form of equations can be obtained and written as

$$(\frac{\theta + f\rho_b K_d}{\theta})\frac{\partial C_1}{\partial T} = \frac{D}{vL}\frac{\partial^2 C_1}{\partial X^2} - \frac{\partial C_1}{\partial X} - \frac{\alpha\rho_b L}{\theta v}(1-f)K_d(C_1 - C_2) \tag{4-11}$$

It can be reduced to

$$\beta R\frac{\partial C_1}{\partial T} = \frac{1}{Pe}\frac{\partial^2 C_1}{\partial X^2} - \frac{\partial C_1}{\partial X} - \omega(C_1 - C_2) \tag{4-12}$$

The dimensionless form of equation (4-9) is

$$\frac{v(1-f)K_d}{L}\frac{\partial C_2}{\partial T} = \alpha(1-f)K_d(C_1 - C_2) \tag{4-13}$$

It can be reduced to

$$(1-\beta)R\frac{\partial C_2}{\partial T} = \omega(C_1 - C_2) \tag{4-14}$$

Where, $\beta = \frac{(\theta + f\rho_b K_d)}{(\theta + \rho_b K_d)}$ is a partition coefficient; $R = 1 + \frac{\rho_b K_d}{\theta}$ is the retardation factor; $\omega = \frac{\alpha(1-\beta)RL}{v}$ is the dimensionless mass transfer coefficient;

$Pe = \frac{vL}{D}$ is the Peclet number.

For the heterogeneous flow controlled nonequilibrium transport, the flow in the column can be divided to mobile and immobile liquid regions. The exchange of arsenic between the two regions is a first-order mass transfer process. Therefore, a two-region nonequilibrium transport model can be derived.

$$(\theta_m + f\rho_b K_d)\frac{\partial C_m}{\partial t} = \theta_m D_m \frac{\partial^2 C_m}{\partial x^2} - u\frac{\partial C_m}{\partial x} - \alpha(C_m - C_{im}) \tag{4-15}$$

$$[\theta_{im} + (1-f)\rho_b K_d]\frac{\partial C_{im}}{\partial t} = \alpha(C_m - C_{im}) \tag{4-16}$$

Where, C_m and C_{im} is the concentration in the mobile and immobile liquid regions, respectively; $\theta = \theta_m + \theta_{im}$; $v = \frac{u}{\theta}$; $v_m = \frac{u}{\theta_m}$; f is the fraction of adsorption sites for equilibrium adsorption in the mobile liquid region; α is the first-order mass transfer coefficient between the mobile and immobile region.

Similarly, to make the equations dimensionless, let $C_1 = \frac{C_m}{C_0}$, $C_2 = \frac{C_{im}}{C_0}$, $T = \frac{vt}{L}$, and $X = \frac{x}{L}$. The dimensionless form of equations (4-15) is

$$(\frac{\theta_m + f\rho_b K_d}{\theta})\frac{\partial C_1}{\partial T} = (\frac{\theta_m D_m}{Lv\theta})\frac{\partial^2 C_1}{\partial X^2} - \frac{\partial C_1}{\partial X} - \frac{\alpha L}{v\theta}(C_1 - C_2) \tag{4-17}$$

$$\beta R\frac{\partial C_1}{\partial T} = \frac{1}{Pe}\frac{\partial^2 C_1}{\partial X^2} - \frac{\partial C_1}{\partial X} - \omega(C_1 - C_2) \tag{4-18}$$

The dimensionless form of equation (4-16) is

$$(\frac{\theta_{im} + (1-f)\rho_b K_d}{\theta})\frac{\partial C_2}{\partial T} = \frac{\alpha L}{v\theta}(C_1 - C_2) \tag{4-19}$$

It can be reduced to

$$(1-\beta)R\frac{\partial C_2}{\partial T}=\omega(C_1-C_2) \tag{4-20}$$

Where, $\beta=\frac{\theta_m+f\rho_b K_d}{\theta+\rho_b K_d}$, $Pe=\frac{v_m L}{D_m}$, $R=1+\frac{\rho_b K_d}{\theta}$, and $\omega=\frac{\alpha L}{\theta v}$.

This suggests that the dimensionless equations of two-site nonequilibrium transport model and two-region transport model are identical.

The initial condition is: $C_1(X,0)=C_2(X,0)=0$.

The boundary conditions are: $C_1(0,T)=C_0$ and $\frac{\partial C_1}{\partial X}(\infty,T)=0$.

The analytical solution for this equation is

$$C_1(Z,T)=C_0\int_0^T \Gamma_1(Z,\tau)J(a,b)d\tau \tag{4-21}$$

$$C_2(Z,T)=C_0\int_0^T \Gamma_1(Z,\tau)[1-J(b,a)]d\tau \tag{4-22}$$

Where, $\Gamma_1(Z,T)=\frac{Z}{\tau}\sqrt{\frac{\beta RPe}{4\pi\tau}}\exp\left(-\frac{Pe(\beta RZ-\tau)^2}{4\beta R\tau}\right)$

$$J(a,b)=1-\exp(-b)\int_0^a \exp(-\lambda)I_0[2(\mathrm{b}\lambda)^{1/2}]d\lambda$$

$J(b,a)=1+\exp(-a-b)I_0[2(ab)^{1/2}]-J(a,b)$; I_0 is the modified Bessel function of order zero; $a=\frac{\omega^2\tau}{\omega\beta R}$; $b=\frac{\omega(T-\tau)}{(1-\beta)R}$.

The two-site and two-region nonequilibrium transport models are implemented in the CXTFIT modeling package which is written in the Stanmod software. Transport parameters can be estimated by the inverse problem solver based on the experimental

data.

4.3 Results and discussions

4.3.1 Breakthrough curve of methylene blue

The breakthrough curve of methylene and equilibrium CDE fitting are shown in Fig. 4.1. The effluent concentration was plotted versus number of pore volumes, which was calculated by $PV = t \times u / 14$. Based on the breakthrough curve, the dispersion coefficient D is small. So, the second term of the analytical solution (4-7) is equal to 0. Thus, the concentration profile can be described using the equation

$$C(x,t) = \frac{1}{2} C_0 erfc[\frac{Rx - ut}{2(DRt)^{1/2}}] \tag{4-23}$$

then $Modeled\ \theta = C/C_0 = \frac{1}{2} erfc[\frac{Rx - ut}{2(DRt)^{1/2}}]$, $x = 14cm$,When $C/C_0 = 0.5$, then

$erfc[\frac{Rx - ut}{2(DRt)^{1/2}}] = 1$,which means $Rx - ut = 0 \Rightarrow R = \frac{ut_{c/c_0=0.5}}{x} = 208.6$, which was obtained from the breakthrough curve. By least square fitting method, the dispersion coefficient D can be determined to be $0.4 cm^2 / h$ with R^2 being 0.99 and SSE being 0.03. The modeled breakthrough curve was obtained by plotting the analytical solution versus number of pore volumes.

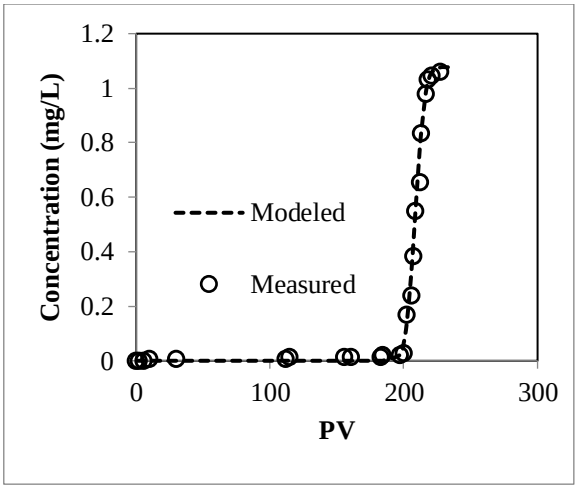

Fig. 4.1 Breakthrough curve of methylene and the equilibrium CDE fitting. The influent concentration was 1 mg/L. The flow rate was 2.63 mL/min. EBCT=15.2 min.

4.3.2 Breakthrough of As(III)

The breakthrough of As(III) in the column packed with FeCB3 is shown in Fig. 4.3. The equilibrium CDE was firstly used to fit the breakthrough data, as shown in Fig. 4.2. It shows that the equilibrium adsorption cannot describe the breakthrough behavior well. So, the experimental data was fitted to the two-site-nonequilibrium CDE. Based on equation (4-8), four parameters need to be estimated using the inverse problem solver. In dimensional form, the four parameters are dispersion coefficient D, fraction of adsorption at equilibrium sites f, the partition coefficient K_d, and the first order kinetic constant α. In dimensionless form, the parameters to be estimated are D, $\beta = \frac{\theta_m + f\rho_b K_d}{\theta + \rho_b K_d}$, $R = 1 + \frac{\rho_b K_d}{\theta}$ and $\omega = \frac{\alpha L}{\theta v}$. If these four parameters are estimated, then the dimensional forms of parameters can be calculated.

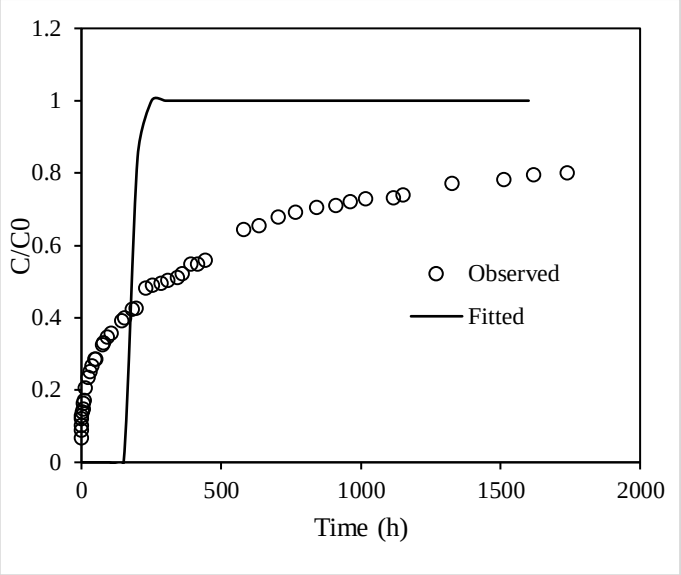

Fig. 4.2 Equilibrium CDE fitting of breakthrough of As(III)

However, it's difficult to estimate four parameters directly. The dispersion coefficient can be estimated by the tracer experiment. Based on equation (4-3), the dispersion coefficient is linearly dependent on the pore velocity. From the tracer experiment, the dispersion coefficient is estimated to be 0.4 cm^2/h at 77 cm/h. For As(III), the pore water velocity is 361.4 cm/h. So, the dispersion coefficient for As(III) is 1.88 cm^2/h. The initial values and estimated values are listed in Table 4-1. Then the dimensional parameters can be calculated as $f = 0.04$, $K_d = 99812.7\,L/kg$, and the first order kinetic constant α=0.0017h^{-1}. This suggests that all the adsorption sites are at nonequilibrium state. The large value of K_d indicates the potential of the prepared adsorbent for As(III) using columns.

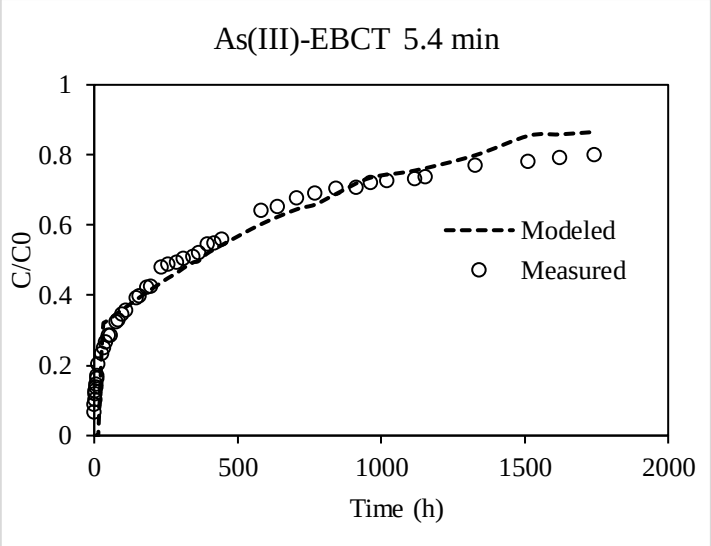

Fig. 4.3 Breakthrough curve of As(III) and the fitting using two-site-nonequilibrium model. The influent concentration was 50 μg/L. The flow rate was 1.43 mL/min. The EBCT was 5.4 min.

Table 4-1 Parameter estimation by two-site-nonequilibrium model for As(III)

Parameter	v	D	R	β	ω
Initial value	361.44	1.88	10000	0.1	1
Estimated value	361.44	1.88	18300	0.0355	1.15

4.3.3 Breakthrough of As(V)

For As(V), the breakthrough data was also firstly fitted using the equilibrium CDE, shown in Fig. 4.4. It shows that the equilibrium model cannot fit the data well. Thus, the breakthrough curve was modeled using the two-sites nonequilibrium model. The pore water velocity is 561.12 cm/h, so the estimated dispersion coefficient is $D = 2.91 cm^2/h$. The breakthrough curve and two-site-nonequilibrium fitting are shown in Fig. 4.5. The fitting results show that the nonequilibrium can better describe the breakthrough of As(V). The initial values and estimated values of the key parameters are listed in Table 4-2. The dimensional parameters can be calculated as

$f = 0.004$, $K_d = 200721.8\,L/kg$ and the kinetic constant α=0.0018h^{-1}.

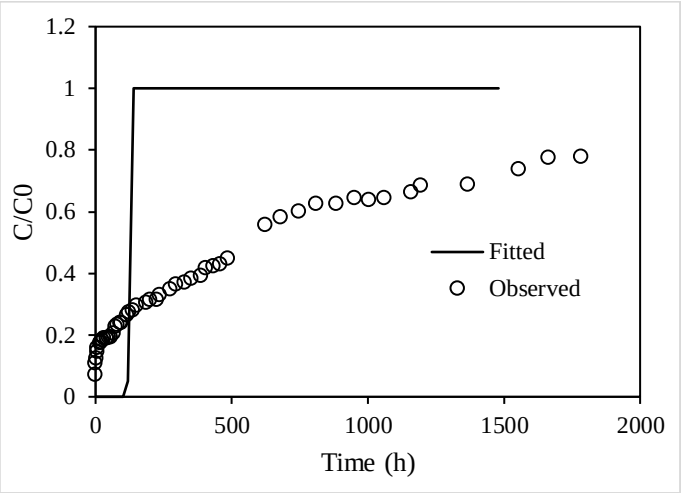

Fig. 4.4 Equilibrium CDE fitting of breakthrough of As(V)

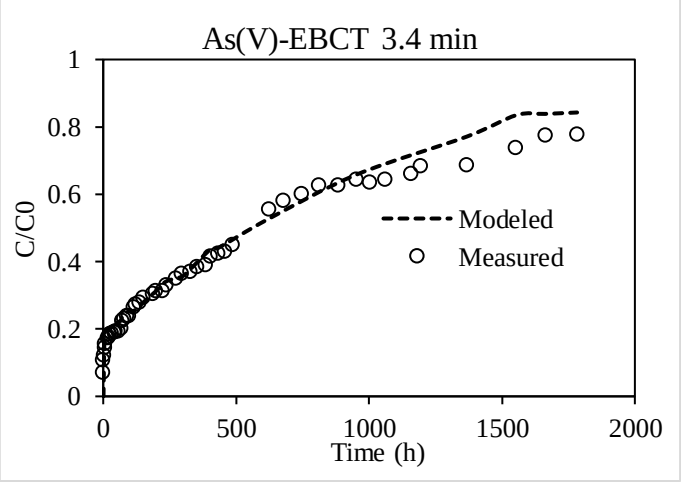

Fig. 4.5 Breakthrough curve of As(V) and the fitting using two-site-nonequilibrium model. The influent concentration was 50 µg/L. The flow rate was 2.22 mL/min. The EBCT was 3.4 min.

Table 4-2 Parameter estimation by two-site-nonequilibrium model for As(V)

Parameter	v	D	R	β	ω
Initial value	561.12	2.91	10000	0.1	1
Estimated value	561.12	2.91	36800	0.0044	1.65

4.4 Conclusions

The breakthrough behavior of As(III) and As(V) in pack bed columns have been determined. To determine the dispersion coefficients for As(III) and As(V), breakthrough of methylene blue as a tracer was conducted and the dispersion coefficient was estimated by equilibrium CDE. Then the parameters controlling breakthrough of As(III) and As(V) were estimated. The two-site-nonequilibrium model fitted the breakthrough data of As(III) and As(V) well. The results suggest that almost all the adsorption sites are at nonequilibrium state for both As(III) and As(V). In addition, the adsorption of arsenic in the column is controlled by first order kinetics. The high partition coefficients indicate the develop iron hydroxide loaded cellulose beads have great potential for arsenic removal from water in column filters.

CHAPTER 5
CONCLUSIONS AND RECOMMENDATIONS

5.1 Conclusions

In this study, iron hydroxide loaded cellulose beads (FeCBs) have been successfully developed with five iron loadings. The potential of the adsorbents for adsorption removal of arsenic from water was investigated in both batch and column experiments. Kinetic equation, isothermal models and transport models were applied to fully elucidate the adsorption behavior of arsenic on the adsorbents. The main conclusion are as follows:

1) Adsorption kinetics was dependent on arsenic initial concentrations and iron content of the adsorbents. Generally, the adsorption initial rates increased with the increase of arsenic concentrations.

2) For As(III), the adsorption capacity was linearly correlated with iron content when the iron loading reached 17.7%, then decreased slightly with continuous increase of iron content. For As(V), the adsorption capacity increased exponentially with the increase of iron contents.

3) The adsorption capacities of the five adsorbents for As(III) were higher than those for As(V).

4) The presence of 5 mg/L P reduced the equilibrium adsorption capacity and initial rate by 15.5% and 26.8%, respectively. The coexisting 500 mg/L SO_4^{2-} reduced the adsorption capacity and initial rate by 24.4% and 39.3, respectively.

5) Two cycles of regeneration did not significantly reduce the adsorption capacity but the initial rate for the second cycle was 47.2% of the original initial rate.

6) The two-state-nonequilibrium models fitted the breakthrough data

well. The adsorption of As(V) and As(III) in the column were at nonequilibrium state. Adsorption in the column was controlled by first order kinetics. The large values of partition coefficients indicated the potential of the prepared FeCBs for arsenic removal from water in columns.

5.2 Recommendations

1) To better understand the adsorption mechanisms of arsenic onto FeCBs, the surface properties of FeCB particles should be should be characterized.

2) The relationship between breakthrough behavior and equilibrium parameters obtained from batch modes may be investigated.

REFERENCE

Abernathy, C.O., Liu, Y.P., Longfellow, D., Aposhian, H.V., Beck, B., Fowler, B., Goyer, R., Menzer, R., Rossman, T., Thompson, C. and Waalkes, M. (1999) Arsenic: health effects, mechanisms of actions, and research issues. *Environmental Health Perspectives* **107**(7), 593-597.

Acharyya, S.K., Chakraborty, P., Lahiri, S., Raymahashay, B.C., Guha, S. and Bhowmik, A. (1999) Arsenic poisoning in the Ganges delta. *Nature* **401**(6753), 545-545.

Adeleye, A.S., Conway, J.R., Garner, K., Huang, Y., Su, Y. and Keller, A.A. (2016) Engineered nanomaterials for water treatment and remediation: Costs, benefits, and applicability. *Chemical Engineering Journal* **286**, 640-662.

Ahmed, M.F., Ahuja, S., Alauddin, M., Hug, S.J., Lloyd, J.R., Pfaff, A., Pichler, T., Saltikov, C., Stute, M. and van Geen, A. (2006) Ensuring Safe Drinking Water in Bangladesh. *Science* **314**(5806), 1687.

Ali, I. (2012) New Generation Adsorbents for Water Treatment. *Chemical Reviews* **112**(10), 5073-5091.

Ali, I. and Gupta, V.K. (2007) Advances in water treatment by adsorption technology. *Nat. Protocols* **1**(6), 2661-2667.

Amini, M., Abbaspour, K.C., Berg, M., Winkel, L., Hug, S.J., Hoehn, E., Yang, H. and Johnson, C.A. (2008) Statistical Modeling of Global Geogenic Arsenic Contamination in Groundwater. *Environmental Science & Technology* **42**(10), 3669-3675.

Amstaetter, K., Borch, T., Larese-Casanova, P. and Kappler, A. (2010) Redox Transformation of Arsenic by Fe(II)-Activated Goethite (alpha-FeOOH). *Environmental Science & Technology* **44**(1), 102-108.

Anawar, H.M., Akai, J., Mostofa, K.M.G., Safiullah, S. and Tareq, S.M. (2002) Arsenic poisoning in groundwater - Health risk and geochemical sources in Bangladesh. *Environment International* **27**(7), 597-604.

Anawar, H.M., Tareq, S.M. and Ahmed, G. (2013) Is organic matter a source or redox driver or both for arsenic release in groundwater? *Physics and Chemistry of the Earth* **58-60**, 49-56.

Appelo, C.A.J., Van Der Weiden, M.J.J., Tournassat, C. and Charlet, L. (2002) Surface Complexation of Ferrous Iron and Carbonate on Ferrihydrite and the Mobilization of Arsenic. *Environmental Science & Technology* **36**(14), 3096-3103.

Arcibar-Orozco, J.A., Josue, D.-B., Rios-Hurtado, J.C. and Rangel-Mendez, J.R. (2014) Influence of iron content, surface area and charge distribution in the arsenic removal by activated carbons. *Chemical Engineering Journal* **249**, 201-209.

Astolfi, E., Maccagno, A., García Fernández, J.C., Vaccaro, R. and Stímola, R. (1981) Relation between arsenic in drinking water and skin cancer. *Biological Trace*

Element Research **3**(2), 133-143.

Aurillo, A.C., Mason, R.P. and Hemond, H.F. (1994) SPECIATION AND FATE OF ARSENIC IN 3 LAKES OF THE ABERJONA WATERSHED. *Environmental Science & Technology* **28**(4), 577-585.

Ayotte, J.D., Nolan, B.T., Nucklos, J.R., Cantor, K.P., Robinson, G.R., Baris, D., Hayes, L., Kargas, M., Bress, W., Silverman, D.T. and Lubin, J.H. (2006) Modeling the probability of arsenic in groundwater in New England as a tool for exposure assessment. *Environmental Science & Technology* **40**(11), 3578-3585.

Azizian, S. (2004) Kinetic models of sorption: a theoretical analysis. *Journal of Colloid and Interface Science* **276**(1), 47-52.

Baig, S.A., Sheng, T., Hu, Y., Lv, X. and Xu, X. (2013) Adsorptive removal of arsenic in saturated sand filter containing amended adsorbents. *Ecological Engineering* **60**, 345-353.

Baker, R.S., Arle, H.F., Miller, J.H. and Holstun, J.T. (2017) Effects of Organic Arsenical Herbicides on Cotton Response and Chemical Residues. *Weed Science* **17**(1), 37-40.

Barringer, J.L., Mumford, A., Young, L.Y., Reilly, P.A., Bonin, J.L. and Rosman, R. (2010) Pathways for arsenic from sediments to groundwater to streams: Biogeochemical processes in the Inner Coastal Plain, New Jersey, USA. *Water Research* **44**(19), 5532-5544.

Bates, M.N., Smith, A.H. and Hopenhayn-Rich, C. (1992) Arsenic Ingestion and Internal Cancers: A Review. *American Journal of Epidemiology* **135**(5), 462-476.

Bauer, M. and Blodau, C. (2006) Mobilization of arsenic by dissolved organic matter from iron oxides, soils and sediments. *Science of The Total Environment* **354**(2-3), 179-190.

Berg, M., Tran, H.C., Nguyen, T.C., Pham, H.V., Schertenleib, R. and Giger, W. (2001) Arsenic Contamination of Groundwater and Drinking Water in Vietnam: A Human Health Threat. *Environmental Science & Technology* **35**(13), 2621-2626.

Bhattacharya, P., Hasan, M.A., Sracek, O., Smith, E., Ahmed, K.M., von Bromssen, M., Huq, S.M.I. and Naidu, R. (2009) Groundwater chemistry and arsenic mobilization in the Holocene flood plains in south-central Bangladesh. *Environmental Geochemistry and Health* **31**, 23-43.

Bissen, M. and Frimmel, F.H. (2003a) Arsenic - a review. - Part 1: Occurrence, toxicity, speciation, mobility. *Acta hydrochimica et hydrobiologica* **31**(1), 9-18.

Bissen, M. and Frimmel, F.H. (2003b) Arsenic — a Review. Part II: Oxidation of Arsenic and its Removal in Water Treatment. *Acta hydrochimica et hydrobiologica* **31**(2), 97-107.

Biswas, A., Gustafsson, J.P., Neidhardt, H., Halder, D., Kundu, A.K., Chatterjee, D.,

Berner, Z. and Bhattacharya, P. (2014) Role of competing ions in the mobilization of arsenic in groundwater of Bengal Basin: Insight from surface complexation modeling. *Water Research* **55**, 30-39.

Biswas, A., Majumder, S., Neidhardt, H., Halder, D., Bhowmick, S., Mukherjee-Goswami, A., Kundu, A., Saha, D., Berner, Z. and Chatterjee, D. (2011) Groundwater chemistry and redox processes: Depth dependent arsenic release mechanism. *Applied Geochemistry* **26**(4), 516-525.

Bolan, N., Mahimairaja, S., Kunhikrishnan, A. and Choppala, G. (2013) Phosphorus-arsenic interactions in variable-charge soils in relation to arsenic mobility and bioavailability. *Science of The Total Environment* **463**, 1154-1162.

Borba, R.P., Figueiredo, B.R., Rawlins, B. and Matschullat, J. (2003) Geochemical distribution of arsenic in waters, sediments and weathered gold mineralized rocks from Iron Quadrangle, Brazil. *Environmental Geology* **44**(1), 39-52.

Bordoloi, S., Nath, S.K., Gogoi, S. and Dutta, R.K. (2013) Arsenic and iron removal from groundwater by oxidation–coagulation at optimized pH: Laboratory and field studies. *Journal of Hazardous Materials* **260**, 618-626.

Bose, P. and Sharma, A. (2002) Role of iron in controlling speciation and mobilization of arsenic in subsurface environment. *Water Research* **36**(19), 4916-4926.

Bostick, B.C. and Fendorf, S. (2003) Arsenite sorption on troilite (FeS) and pyrite (FeS2). *Geochimica et Cosmochimica Acta* **67**(5), 909-921.

Brammer, H. and Ravenscroft, P. (2009) Arsenic in groundwater: A threat to sustainable agriculture in South and South-east Asia. *Environment International* **35**(3), 647-654.

Brannon, J.M. and Patrick, W.H. (1987) Fixation, transformation, and mobilization of arsenic in sediments. *Environmental Science & Technology* **21**(5), 450-459.

Bundschuh, J., Litter, M.I., Parvez, F., Román-Ross, G., Nicolli, H.B., Jean, J.-S., Liu, C.-W., López, D., Armienta, M.A., Guilherme, L.R.G., Cuevas, A.G., Cornejo, L., Cumbal, L. and Toujaguez, R. (2012) One century of arsenic exposure in Latin America: A review of history and occurrence from 14 countries. *Science of The Total Environment* **429**, 2-35.

Buschmann, J., Kappeler, A., Lindauer, U., Kistler, D., Berg, M. and Sigg, L. (2006) Arsenite and arsenate binding to dissolved humic acids: Influence of pH, type of humic acid, and aluminum. *Environmental Science & Technology* **40**(19), 6015-6020.

Campbell, K.M., Malasarn, D., Saltikov, C.W., Newman, D.K. and Hering, J.G. (2006) Simultaneous microbial reduction of iron(III) and arsenic(V) in suspensions of hydrous ferric oxide. *Environmental Science & Technology* **40**(19), 5950-5955.

Carpenter, A.W., de Lannoy, C.F. and Wiesner, M.R. (2015) Cellulose Nanomaterials in Water Treatment Technologies. *Environmental Science & Technology* **49**(9), 5277-5287.

Chandra, V., Park, J., Chun, Y., Lee, J.W., Hwang, I.-C. and Kim, K.S. (2010) Water-Dispersible Magnetite-Reduced Graphene Oxide Composites for Arsenic Removal. *ACS Nano* **4**(7), 3979-3986.

Charlet, L., Morin, G., Rose, J., Wang, Y.H., Auffan, M., Burnol, A. and Fernandez-Martinez, A. (2011) Reactivity at (nano)particle-water interfaces, redox processes, and arsenic transport in the environment. *Comptes Rendus Geoscience* **343**(2-3), 123-139.

Chen, W., Parette, R., Zou, J., Cannon, F.S. and Dempsey, B.A. (2007) Arsenic removal by iron-modified activated carbon. *Water Research* **41**(9), 1851-1858.

Choong, T.S.Y., Chuah, T.G., Robiah, Y., Gregory Koay, F.L. and Azni, I. (2007a) Arsenic toxicity, health hazards and removal techniques from water: an overview. *Desalination* **217**(1), 139-166.

Choong, T.S.Y., Chuah, T.G., Robiah, Y., Koay, F.L.G. and Azni, I. (2007b) Arsenic toxicity, health hazards and removal techniques from water: an overview. *Desalination* **217**(1-3), 139-166.

Chowdhury, S.R. and Yanful, E.K. (2010) Arsenic and chromium removal by mixed magnetite–maghemite nanoparticles and the effect of phosphate on removal. *Journal of Environmental Management* **91**(11), 2238-2247.

Chowdhury, T.R., Basu, G.K., Mandal, B.K., Biswas, B.K., Samanta, G., Chowdhury, U.K., Chanda, C.R., Lodh, D., Roy, S.L., Saha, K.C., Roy, S., Kabir, S., Quamruzzaman, Q. and Chakraborti, D. (1999) Arsenic poisoning in the Ganges delta. *Nature* **401**(6753), 545-546.

Chowdhury, U.K., Biswas, B.K., Chowdhury, T.R., Samanta, G., Mandal, B.K., Basu, G.C., Chanda, C.R., Lodh, D., Saha, K.C., Mukherjee, S.K., Roy, S., Kabir, S., Quamruzzaman, Q. and Chakraborti, D. (2000) Groundwater arsenic contamination in Bangladesh and West Bengal, India. *Environmental Health Perspectives* **108**(5), 393-397.

Chwirka, J.D., Colvin, C., Gomez, J.D. and Mueller, P.A. (2004) Arsenic removal from drinking water using the coagulation/microfiltration process. *Journal (American Water Works Association)* **96**(3), 106-114.

Chwirka, J.D., Thomson, B.M. and Stomp III, J.M. (2000) Removing arsenic from groundwater. *Journal-American Water Works Association* **92**(3), 79-88.

Ciardelli, M.C., Xu, H.F. and Sahai, N. (2008) Role of Fe(II), phosphate, silicate, sulfate, and carbonate in arsenic uptake by coprecipitation in synthetic and natural groundwater. *Water Research* **42**(3), 615-624.

Clifford, D., Ceber, L. and Chow, S. (1983) Arsenic (III)/As (V) Separation by Chloride-Form Ion-Exchange Resins.

Clifford, D.A. (1999) Ion exchange and inorganic adsorption. *Water quality and treatment* **4**, 561-564.

Coleman, N.T., McClung, A.C. and Moore, D.P. (1956) Formation Constants for Cu(II)-Peat Complexes. *Science* **123**(3191), 330.

Copeland, R.C., Lytle, D.A. and Dionysious, D.D. (2007) Desorption of arsenic from drinking water distribution system solids. *Environmental Monitoring and Assessment* **127**(1), 523-535.

Cullen, W.R. and Reimer, K.J. (1989) Arsenic speciation in the environment. *Chemical Reviews* **89**(4), 713-764.

Cummings, D.E., Caccavo, F., Fendorf, S. and Rosenzweig, R.F. (1999) Arsenic Mobilization by the Dissimilatory Fe(III)-Reducing Bacterium Shewanella alga BrY. *Environmental Science & Technology* **33**(5), 723-729.

Cundy, A.B., Hopkinson, L. and Whitby, R.L. (2008a) Use of iron-based technologies in contaminated land and groundwater remediation: a review. *Science of The Total Environment* **400**(1), 42-51.

Cundy, A.B., Hopkinson, L. and Whitby, R.L.D. (2008b) Use of iron-based technologies in contaminated land and groundwater remediation: A review. *Science of The Total Environment* **400**(1-3), 42-51.

Dai, Z.X., Keating, E., Bacon, D., Viswanathan, H., Stauffer, P., Jordan, A. and Pawar, R. (2014) Probabilistic evaluation of shallow groundwater resources at a hypothetical carbon sequestration site. *Scientific Reports* **4**.

Das, D., Samanta, G., Mandal, B.K., Roy Chowdhury, T., Chanda, C.R., Chowdhury, P.P., Basu, G.K. and Chakraborti, D. (1996) Arsenic in groundwater in six districts of West Bengal, India. *Environmental Geochemistry and Health* **18**(1), 5-15.

Das, N., Paul, S., Chatterjee, D., Banerjee, N., Majumder, N.S., Sarma, N., Sau, T.J., Basu, S., Banerjee, S., Majumder, P., Bandyopadhyay, A.K., States, J.C. and Giri, A.K. (2012) Arsenic exposure through drinking water increases the risk of liver and cardiovascular diseases in the population of West Bengal, India. *Bmc Public Health* **12**.

Datta, S., Mailloux, B., Jung, H.-B., Hoque, M.A., Stute, M., Ahmed, K.M. and Zheng, Y. (2009a) Redox trapping of arsenic during groundwater discharge in sediments from the Meghna riverbank in Bangladesh. *Proceedings of the National Academy of Sciences* **106**(40), 16930-16935.

Datta, S., Mailloux, B., Jung, H.B., Hoque, M.A., Stute, M., Ahmed, K.M. and Zheng, Y. (2009b) Redox trapping of arsenic during groundwater discharge in sediments from the Meghna riverbank in Bangladesh. *Proceedings of the National Academy of Sciences of the United States of America* **106**(40), 16930-16935.

Daus, B., Wennrich, R. and Weiss, H. (2004) Sorption materials for arsenic removal from water:: a comparative study. *Water Research* **38**(12), 2948-2954.

Dixit, S. and Hering, J.G. (2003) Comparison of Arsenic(V) and Arsenic(III) Sorption onto Iron Oxide Minerals: Implications for Arsenic Mobility. *Environmental Science & Technology* **37**(18), 4182-4189.

Dixit, S. and Hering, J.G. (2006) Sorption of Fe(II) and As(III) on goethite in single- and dual-sorbate systems. *Chemical Geology* **228**(1), 6-15.

Duker, A.A., Carranza, E.J. and Hale, M. (2005) Arsenic geochemistry and health. *Environ Int* **31**(5), 631-641.

Farquhar, M.L., Charnock, J.M., Livens, F.R. and Vaughan, D.J. (2002) Mechanisms of Arsenic Uptake from Aqueous Solution by Interaction with Goethite, Lepidocrocite, Mackinawite, and Pyrite: An X-ray Absorption Spectroscopy Study. *Environmental Science & Technology* **36**(8), 1757-1762.

Fendorf, S. and Kocar, B.D. (2009a) Advances in Agronomy, Volume 104, pp. 137-164.

Fendorf, S. and Kocar, B.D. (2009b) Chapter 3 Biogeochemical Processes Controlling the Fate and Transport of Arsenic. *Advances in Agronomy* **104**, 137-164.

Fendorf, S., Michael, H.A. and van Geen, A. (2010) Spatial and Temporal Variations of Groundwater Arsenic in South and Southeast Asia. *Science* **328**(5982), 1123.

Frank, P. and Clifford, D.A. (1986) Arsenic (III) oxidation and removal from drinking water, Water Engineering Research Laboratory, Office of Research and Development, US Environmental Protection Agency.

Gadd, G.M. and Ravenscroft, K. (2009) Arsenic Pollution: A Global Synthesis. *Experimental Agriculture* **45**(4), 509.

Ghurye, G., Clifford, D. and Tripp, A. (2004) Iron coagulation and direct microfiltration to remove arsenic from groundwater. *Journal (American Water Works Association)* **96**(4), 143-152.

Goh, K.-H. and Lim, T.-T. (2005) Arsenic fractionation in a fine soil fraction and influence of various anions on its mobility in the subsurface environment. *Applied Geochemistry* **20**(2), 229-239.

Goldberg, S. and Johnston, C.T. (2001) Mechanisms of Arsenic Adsorption on Amorphous Oxides Evaluated Using Macroscopic Measurements, Vibrational Spectroscopy, and Surface Complexation Modeling. *Journal of Colloid and Interface Science* **234**(1), 204-216.

Grimalt, J.O., Ferrer, M. and Macpherson, E. (1999) The mine tailing accident in Aznalcollar. *Science of The Total Environment* **242**(1–3), 3-11.

Guan, X.H., Du, J.S., Meng, X.G., Sun, Y.K., Sun, B. and Hu, Q.H. (2012) Application of titanium dioxide in arsenic removal from water: A review. *Journal of Hazardous Materials* **215**, 1-16.

Guo, H.M., Yang, S.Z., Tang, X.H., Li, Y. and Shen, Z.L. (2008) Groundwater geochemistry and its implications for arsenic mobilization in shallow aquifers of the Hetao Basin, Inner Mongolia. *Science of The Total Environment* **393**(1), 131-144.

Guo, X. and Chen, F. (2005) Removal of Arsenic by Bead Cellulose Loaded with Iron Oxyhydroxide from Groundwater. *Environmental Science & Technology* **39**(17), 6808-6818.

Han, B., Runnells, T., Zimbron, J. and Wickramasinghe, R. (2002) Arsenic removal

from drinking water by flocculation and microfiltration. *Desalination* **145**(1), 293-298.

Han, C., Li, H., Pu, H., Yu, H., Deng, L., Huang, S. and Luo, Y. (2013) Synthesis and characterization of mesoporous alumina and their performances for removing arsenic (V). *Chemical Engineering Journal* **217**, 1-9.

Harvey, C.F., Ashfaque, K.N., Yu, W., Badruzzaman, A.B.M., Ali, M.A., Oates, P.M., Michael, H.A., Neumann, R.B., Beckie, R., Islam, S. and Ahmed, M.F. (2006) Groundwater dynamics and arsenic contamination in Bangladesh. *Chemical Geology* **228**(1-3), 112-136.

He, Y.T., Fitzmaurice, A.G., Bilgin, A., Choi, S., O'Day, P., Horst, J., Harrington, J., Reisinger, H.J., Burris, D.R. and Hering, J.G. (2010) Geochemical processes controlling arsenic mobility in groundwater: A case study of arsenic mobilization and natural attenuation. *Applied Geochemistry* **25**(1), 69-80.

Hering Janet, G., Chen, P.-Y., Wilkie Jennifer, A. and Elimelech, M. (1997) Arsenic Removal from Drinking Water during Coagulation. *Journal of Environmental Engineering* **123**(8), 800-807.

Hering, J.G., Pen-Yuan, C., Wilkie, J.A., Elimelech, M. and Sun, L. (1996) Arsenic removal by ferric chloride. *American Water Works Association. Journal* **88**(4), 155.

Hingston, J.A., Collins, C.D., Murphy, R.J. and Lester, J.N. (2001) Leaching of chromated copper arsenate wood preservatives: a review. *Environmental Pollution* **111**(1), 53-66.

Ho, Y.-S. (2006) Review of second-order models for adsorption systems. *Journal of Hazardous Materials* **136**(3), 681-689.

Ho, Y.S. and McKay, G. (1999) Pseudo-second order model for sorption processes. *Process Biochemistry* **34**(5), 451-465.

Ho, Y.S., Ng, J.C.Y. and McKay, G. (2000) KINETICS OF POLLUTANT SORPTION BY BIOSORBENTS: REVIEW. *Separation and Purification Methods* **29**(2), 189-232.

Hokkanen, S., Repo, E., Lou, S. and Sillanpää, M. (2015) Removal of arsenic(V) by magnetic nanoparticle activated microfibrillated cellulose. *Chemical Engineering Journal* **260**, 886-894.

Holm, T.R. (2002) Effects of CO32-/bicarbonate, Si, and PO43- on arsenic sorption to HFO. *Journal American Water Works Association* **94**(4), 174-181.

Hong, Y.-S., Song, K.-H. and Chung, J.-Y. (2014) Health Effects of Chronic Arsenic Exposure. *Journal of Preventive Medicine and Public Health* **47**(5), 245-252.

Hopp, L., Peiffer, S. and Durner, W. (2006) Spatial variability of arsenic and chromium in the soil water at a former wood preserving site. *Journal of Contaminant Hydrology* **85**(3), 159-178.

Hsiao-Wen, C., Frey, M.M., Clifford, D., McNeill, L.S. and Edwards, M. (1999) Arsenic treatment considerations. *American Water Works Association. Journal*

91(3), 74.

Hu, X., Ding, Z.H., Zimmerman, A.R., Wang, S.S. and Gao, B. (2015) Batch and column sorption of arsenic onto iron-impregnated biochar synthesized through hydrolysis. *Water Research* **68**, 206-216.

Hughes, M.F. (2002) Arsenic toxicity and potential mechanisms of action. *Toxicology Letters* **133**(1), 1-16.

Hunt, K.M., Srivastava, R.K., Elmets, C.A. and Athar, M. (2014) The mechanistic basis of arsenicosis: Pathogenesis of skin cancer. *Cancer Letters* **354**(2), 211-219.

IARC (1980) An Evaluation of Chemicals and Industrial Processes Associated with Cancer in Humans Based on Human and Animal Data: IARC Monographs Volumes 1 to 20. *Cancer Research* **40**(1), 1.

Islam, F.S., Gault, A.G., Boothman, C., Polya, D.A., Charnock, J.M., Chatterjee, D. and Lloyd, J.R. (2004) Role of metal-reducing bacteria in arsenic release from Bengal delta sediments. *Nature* **430**(6995), 68-71.

Itai, T., Takahashi, Y., Seddique, A.A., Maruoka, T. and Mitamura, M. (2010) Variations in the redox state of As and Fe measured by X-ray absorption spectroscopy in aquifers of Bangladesh and their effect on As adsorption. *Applied Geochemistry* **25**(1), 34-47.

Jain, C.K. and Ali, I. (2000) Arsenic: occurrence, toxicity and speciation techniques. *Water Research* **34**(17), 4304-4312.

Janet, G.H., Pen-Yuan, C., Jennifer, A.W. and Menachem, E. (1997) Arsenic Removal from Drinking Water during Coagulation. *Journal of Environmental Engineering* **123**(8), 800-807.

Jiang, J., Bauer, I., Paul, A. and Kappler, A. (2009) Arsenic Redox Changes by Microbially and Chemically Formed Semiquinone Radicals and Hydroquinones in a Humic Substance Model Quinone. *Environmental Science & Technology* **43**(10), 3639-3645.

Johnson, D.L. and Pilson, M.E.Q. (1975) The Oxidation of Arsenite in Seawater. *Environmental Letters* **8**(2), 157-171.

Johnston, S.G., Keene, A.F., Burton, E.D., Bush, R.T. and Sullivan, L.A. (2011) Iron and Arsenic Cycling in Intertidal Surface Sediments during Wetland Remediation. *Environmental Science & Technology* **45**(6), 2179-2185.

Kanel, S.R., Manning, B., Charlet, L. and Choi, H. (2005) Removal of Arsenic(III) from Groundwater by Nanoscale Zero-Valent Iron. *Environmental Science & Technology* **39**(5), 1291-1298.

Khan, B.I., Jambeck, J., Solo-Gabriele, H.M., Townsend, T.G. and Cai, Y. (2006a) Release of arsenic to the environment from CCA-treated wood. 2. Leaching and speciation during disposal. *Environmental Science & Technology* **40**(3), 994-999.

Khan, B.I., Solo-Gabriele, H.M., Dubey, B.K., Townsend, T.G. and Cai, Y. (2004)

Arsenic speciation of solvent-extracted leachate from new and weathered CCA-treated wood. *Environmental Science & Technology* **38**(17), 4527-4534.

Khan, B.I., Solo-Gabriele, H.M., Townsend, T.G. and Cai, Y. (2006b) Release of arsenic to the environment from CCA-treated wood. 1. Leaching and speciation during service. *Environmental Science & Technology* **40**(3), 988-993.

Kim, K., Moon, J.T., Kim, S.H. and Ko, K.S. (2009) Importance of surface geologic condition in regulating As concentration of groundwater in the alluvial plain. *Chemosphere* **77**(4), 478-484.

Kim, M.-J. and Nriagu, J. (2000) Oxidation of arsenite in groundwater using ozone and oxygen. *Science of The Total Environment* **247**(1), 71-79.

Kim, Y., Kim, C., Choi, I., Rengaraj, S. and Yi, J. (2004) Arsenic Removal Using Mesoporous Alumina Prepared via a Templating Method. *Environmental Science & Technology* **38**(3), 924-931.

Kirk, M.F., Roden, E.E., Crossey, L.J., Brearley, A.J. and Spilde, M.N. (2010) Experimental analysis of arsenic precipitation during microbial sulfate and iron reduction in model aquifer sediment reactors. *Geochimica et Cosmochimica Acta* **74**(9), 2538-2555.

Knobeloch, L.M., Zierold, K.M. and Anderson, H.A. (2006) Association of arsenic-contaminated drinking-water with prevalence of skin cancer in Wisconsin's Fox River Valley. *Journal of Health, Population and Nutrition*, 206-213.

Kuila, T., Bose, S., Mishra, A.K., Khanra, P., Kim, N.H. and Lee, J.H. (2012) Chemical functionalization of graphene and its applications. *Progress in Materials Science* **57**(7), 1061-1105.

Labrenz, M., Druschel, G.K., Thomsen-Ebert, T., Gilbert, B., Welch, S.A., Kemner, K.M., Logan, G.A., Summons, R.E., De Stasio, G., Bond, P.L., Lai, B., Kelly, S.D. and Banfield, J.F. (2000) Formation of sphalerite (ZnS) deposits in natural biofilms of sulfate-reducing bacteria. *Science* **290**(5497), 1744-1747.

Langmuir, I. (1918) The adsorption of gases on plane surfaces of glass, mica and platinum. *Journal of the American Chemical society* **40**(9), 1361-1403.

Lata, S. and Samadder, S.R. (2016) Removal of arsenic from water using nano adsorbents and challenges: A review. *Journal of Environmental Management* **166**, 387-406.

Leiva, E.D., Ramila, C.D.P., Vargas, I.T., Escauriaza, C.R., Bonilla, C.A., Pizarro, G.E., Regan, J.M. and Pasten, P.A. (2014) Natural attenuation process via microbial oxidation of arsenic in a high Andean watershed. *Science of The Total Environment* **466**, 490-502.

Leybourne, M.I. and Cameron, E.M. (2008) Source, transport, and fate of rhenium, selenium, molybdenum, arsenic, and copper in groundwater associated with porphyry-Cu deposits, Atacama Desert, Chile. *Chemical Geology* **247**(1-2), 208-228.

Li, X., He, K., Pan, B.C., Zhang, S.J., Lu, L. and Zhang, W.M. (2012) Efficient

As(III) removal by macroporous anion exchanger-supported Fe-Mn binary oxide: Behavior and mechanism. *Chemical Engineering Journal* **193**, 131-138.

Lin, H.-J., Sung, T.-I., Chen, C.-Y. and Guo, H.-R. (2013) Arsenic levels in drinking water and mortality of liver cancer in Taiwan. *Journal of Hazardous Materials* **262**, 1132-1138.

Lin, T.-F. and Wu, J.-K. (2001) Adsorption of Arsenite and Arsenate within Activated Alumina Grains: Equilibrium and Kinetics. *Water Research* **35**(8), 2049-2057.

Liu, Y. (2008) New insights into pseudo-second-order kinetic equation for adsorption. *Colloids and Surfaces A: Physicochemical and Engineering Aspects* **320**(1), 275-278.

Liu, Z., Shen, J., Carbrey, J.M., Mukhopadhyay, R., Agre, P. and Rosen, B.P. (2002) Arsenite transport by mammalian aquaglyceroporins AQP7 and AQP9. *Proceedings of the National Academy of Sciences* **99**(9), 6053-6058.

Lokuge, K.M., Smith, W., Caldwell, B., Dear, K. and Milton, A.H. (2004) The Effect of Arsenic Mitigation Interventions on Disease Burden in Bangladesh. *Environmental Health Perspectives* **112**(11), 1172-1177.

Madhavan, N. and Subramanian, V. (2000) Sulphide mining as a source of arsenic in the environment. *Current Science* **78**(6), 702-709.

Mailloux, B.J., Alexandrova, E., Keimowitz, A.R., Wovkulich, K., Freyer, G.A., Herron, M., Stolz, J.F., Kenna, T.C., Pichler, T., Polizzotto, M.L., Dong, H.L., Bishop, M. and Knappett, P.S.K. (2009) Microbial Mineral Weathering for Nutrient Acquisition Releases Arsenic. *Applied and Environmental Microbiology* **75**(8), 2558-2565.

Mandal, B.K. and Suzuki, K.T. (2002) Arsenic round the world: a review. *Talanta* **58**(1), 201-235.

Manning, B. (2005) Arsenic speciation in As(III)- and As(V)-treated soil using XANES spectroscopy. *Microchimica Acta* **151**(3-4), 181-188.

Masuda, H., Yamatani, Y. and Okai, M. (2005) Transformation of arsenic compounds in modern intertidal sediments of Iriomote Island, Japan. *Journal of Geochemical Exploration* **87**(2), 73-81.

Matisoff, G., Khourey, C.J., Hall, J.F., Varnes, A.W. and Strain, W.H. (1982) The Nature and Source of Arsenic in Northeastern Ohio Ground Watera. *Ground Water* **20**(4), 446-456.

Matschullat, J. (2000) Arsenic in the geosphere — a review. *Science of The Total Environment* **249**(1), 297-312.

Mazumder, D.G. and Dasgupta, U.B. (2011) Chronic arsenic toxicity: Studies in West Bengal, India. *Kaohsiung Journal of Medical Sciences* **27**(9), 360-370.

Mazumder, D.N.G. (2007) Arsenic and non-malignant lung disease. *Journal of Environmental Science and Health Part a-Toxic/Hazardous Substances & Environmental Engineering* **42**(12), 1859-1867.

McArthur, J.M., Banerjee, D.M., Sengupta, S., Ravenscroft, P., Klump, S., Sarkar, A., Disch, B. and Kipfer, R. (2010) Migration of As, and H-3/(3) He ages, in groundwater from West Bengal: Implications for monitoring. *Water Research* **44**(14), 4171-4185.

McArthur, J.M., Ravenscroft, P., Safiulla, S. and Thirlwall, M.F. (2001) Arsenic in groundwater: Testing pollution mechanisms for sedimentary aquifers in Bangladesh. *Water Resources Research* **37**(1), 109-117.

McClintock, T.R., Chen, Y., Bundschuh, J., Oliver, J.T., Navoni, J., Olmos, V., Lepori, E.V., Ahsan, H. and Parvez, F. (2012) Arsenic Exposure in Latin America: Biomarkers, Risk Assessments and Related Health Effects. *The Science of the total environment* **429**, 76-91.

McLaren, R.G., Naidu, R., Smith, J. and Tiller, K.G. (1998) Fractionation and distribution of arsenic in soils contaminated by cattle dip. *Journal of Environmental Quality* **27**(2), 348-354.

Mehta, D., Mazumdar, S. and Singh, S.K. (2015) Magnetic adsorbents for the treatment of water/wastewater—A review. *Journal of Water Process Engineering* **7**, 244-265.

Meng, X.G., Jing, C.Y. and Korfiatis, G.P. (2003) Biogeochemistry of Environmentally Important Trace Elements, pp. 70-83.

Meng, X.G., Korfiatis, G.P., Jing, C.Y. and Christodoulatos, C. (2001) Redox transformations of arsenic and iron in water treatment sludge during aging and TCLP extraction. *Environmental Science & Technology* **35**(17), 3476-3481.

Mladenov, N., Zheng, Y., Miller, M.P., Nemergut, D.R., Legg, T., Simone, B., Hageman, C., Rahman, M.M., Ahmed, K.M. and McKnight, D.M. (2010) Dissolved Organic Matter Sources and Consequences for Iron and Arsenic Mobilization in Bangladesh Aquifers. *Environmental Science & Technology* **44**(1), 123-128.

Mohan, D. and Pittman, C.U. (2007) Arsenic removal from water/wastewater using adsorbents—A critical review. *Journal of Hazardous Materials* **142**(1), 1-53.

Mohan, D. and Pittman Jr, C.U. (2007) Arsenic removal from water/wastewater using adsorbents—A critical review. *Journal of Hazardous Materials* **142**(1–2), 1-53.

Mok, W.M. and Wai, C.M. (1990) Distribution and mobilization of arsenic and antimony species in the Coeur d'Alene River, Idaho. *Environmental Science & Technology* **24**(1), 102-108.

Molinari, A., Guadagnini, L., Marcaccio, M., Straface, S., Sanchez-Vila, X. and Guadagnini, A. (2013) Arsenic release from deep natural solid matrices under experimentally controlled redox conditions. *Science of The Total Environment* **444**, 231-240.

Mondal, P., Bhowmick, S., Chatterjee, D., Figoli, A. and Van der Bruggen, B. (2013) Remediation of inorganic arsenic in groundwater for safe water supply: A critical assessment of technological solutions. *Chemosphere* **92**(2), 157-170.

Mondal, P., Majumder, C.B. and Mohanty, B. (2006) Laboratory based approaches for arsenic remediation from contaminated water: Recent developments. *Journal of Hazardous Materials* **137**(1), 464-479.

Morin, G. and Calas, G. (2006) Arsenic in soils, mine tailings, and former industrial sites. *Elements* **2**(2), 97-101.

Muñoz, J.A., Gonzalo, A. and Valiente, M. (2002) Arsenic Adsorption by Fe(III)-Loaded Open-Celled Cellulose Sponge. Thermodynamic and Selectivity Aspects. *Environmental Science & Technology* **36**(15), 3405-3411.

Muniz, G., Fierro, V., Celzard, A., Furdin, G., Gonzalez-Sánchez, G. and Ballinas, M. (2009) Synthesis, characterization and performance in arsenic removal of iron-doped activated carbons prepared by impregnation with Fe (III) and Fe (II). *Journal of Hazardous Materials* **165**(1), 893-902.

Murphy, E.A. and Aucott, M. (1998) An assessment of the amounts of arsenical pesticides used historically in a geographical area. *Science of The Total Environment* **218**(2–3), 89-101.

Nelson, K.W. (1977) Industrial contributions of arsenic to the environment. *Environmental Health Perspectives* **19**, 31-34.

Neumann, R.B., Ashfaque, K.N., Badruzzaman, A.B.M., Ashraf Ali, M., Shoemaker, J.K. and Harvey, C.F. (2010) Anthropogenic influences on groundwater arsenic concentrations in Bangladesh. *Nature Geosci* **3**(1), 46-52.

Nickson, R., McArthur, J., Burgess, W., Ahmed, K.M., Ravenscroft, P. and Rahmann, M. (1998) Arsenic poisoning of Bangladesh groundwater. *Nature* **395**(6700), 338-338.

Nickson, R.T., McArthur, J.M., Ravenscroft, P., Burgess, W.G. and Ahmed, K.M. (2000) Mechanism of arsenic release to groundwater, Bangladesh and West Bengal. *Applied Geochemistry* **15**(4), 403-413.

Nordstrom, D.K. (2002) Worldwide Occurrences of Arsenic in Ground Water. *Science* **296**(5576), 2143.

O'Day, P.A., Vlassopoulos, D., Root, R. and Rivera, N. (2004) The influence of sulfur and iron on dissolved arsenic concentrations in the shallow subsurface under changing redox conditions. *Proceedings of the National Academy of Sciences of the United States of America* **101**(38), 13703-13708.

Oremland, R.S. and Stolz, J.F. (2003) The Ecology of Arsenic. *Science* **300**(5621), 939.

Petrusevski, B., van der Meer, W., Baker, J., Kruis, F., Sharma, S.K. and Schippers, J.C. (2007) Innovative approach for treatment of arsenic contaminated groundwater in Central Europe. *Water Science and Technology: Water Supply* **7**(3), 131.

Pichler, T., Veizer, J. and Hall, G.E.M. (1999) Natural Input of Arsenic into a Coral-Reef Ecosystem by Hydrothermal Fluids and Its Removal by Fe(III) Oxyhydroxides. *Environmental Science & Technology* **33**(9), 1373-1378.

Pierce, M.L. and Moore, C.B. (1982) Adsorption of arsenite and arsenate on amorphous iron hydroxide. *Water Research* **16**(7), 1247-1253.

Polizzotto, M.L., Harvey, C.F., Sutton, S.R. and Fendorf, S. (2005) Processes conducive to the release and transport of arsenic into aquifers of Bangladesh. *Proceedings of the National Academy of Sciences of the United States of America* **102**(52), 18819-18823.

Polizzotto, M.L., Kocar, B.D., Benner, S.G., Sampson, M. and Fendorf, S. (2008) Near-surface wetland sediments as a source of arsenic release to ground water in Asia. *Nature* **454**(7203), 505-508.

Qiu, W. and Zheng, Y. (2007) Arsenate removal from water by an alumina-modified zeolite recovered from fly ash. *Journal of Hazardous Materials* **148**(3), 721-726.

Rahman, M.M., Chowdhury, U.K., Mukherjee, S.C., Mondal, B.K., Paul, K., Lodh, D., Biswas, B.K., Chanda, C.R., Basu, G.K., Saha, K.C., Roy, S., Das, R., Palit, S.K., Quamruzzaman, Q. and Chakraborti, D. (2001) Chronic arsenic toxicity in Bangladesh and West Bengal, India - A review and commentary. *Journal of Toxicology-Clinical Toxicology* **39**(7), 683-700.

Rahman, M.M., Dong, Z.M. and Naidu, R. (2015) Concentrations of arsenic and other elements in groundwater of Bangladesh and West Bengal, India: Potential cancer risk. *Chemosphere* **139**, 54-64.

Rajaković, L.V. (1992) The sorption of arsenic onto activated carbon impregnated with metallic silver and copper. *Separation Science and Technology* **27**(11), 1423-1433.

Ray, P.Z. and Shipley, H.J. (2015) Inorganic nano-adsorbents for the removal of heavy metals and arsenic: a review. *RSC Advances* **5**(38), 29885-29907.

Reza, A., Jean, J.S., Lee, M.K., Liu, C.C., Bundschuh, J., Yang, H.J., Lee, J.F. and Lee, Y.C. (2010) Implications of organic matter on arsenic mobilization into groundwater: Evidence from northwestern (Chapai-Nawabganj), central (Manikganj) and southeastern (Chandpur) Bangladesh. *Water Research* **44**(19), 5556-5574.

Rhine, E.D., Onesios, K.M., Serfes, M.E., Reinfelder, J.R. and Young, L.Y. (2008) Arsenic transformation and mobilization from minerals by the arsenite oxidizing strain WAO. *Environmental Science & Technology* **42**(5), 1423-1429.

Rice, K.C., Conko, K.M. and Hornberger, G.M. (2002) Anthropogenic Sources of Arsenic and Copper to Sediments in a Suburban Lake, Northern Virginia. *Environmental Science & Technology* **36**(23), 4962-4967.

Rittle, K.A., Drever, J.I. and Colberg, P.J.S. (1995) PRECIPITATION OF ARSENIC DURING BACTERIAL SULFATE REDUCTION. *Geomicrobiology Journal* **13**(1), 1-11.

Roberts, L.C., Hug, S.J., Dittmar, J., Voegelin, A., Kretzschmar, R., Wehrli, B., Cirpka, O.A., Saha, G.C., Ali, M.A. and Badruzzaman, A.B.M. (2010)

Arsenic release from paddy soils during monsoon flooding. *Nature Geoscience* **3**(1), 53-59.

Robertson, F.N. (1989) Arsenic in ground-water under oxidizing conditions, south-west United States. *Environmental Geochemistry and Health* **11**(3), 171-185.

Robinson, G.R. and Ayotte, J.D. (2006) The influence of geology and land use on arsenic in stream sediments and ground waters in New England, USA. *Applied Geochemistry* **21**(9), 1482-1497.

Robinson Jr, G.R. and Ayuso, R.A. (2004) Use of spatial statistics and isotopic tracers to measure the influence of arsenical pesticide use on stream sediment chemistry in New England, USA. *Applied Geochemistry* **19**(7), 1097-1110.

Rodríguez-Lado, L., Sun, G., Berg, M., Zhang, Q., Xue, H., Zheng, Q. and Johnson, C.A. (2013) Groundwater Arsenic Contamination Throughout China. *Science* **341**(6148), 866.

Roussel, C., Néel, C. and Bril, H. (2000) Minerals controlling arsenic and lead solubility in an abandoned gold mine tailings. *Science of The Total Environment* **263**(1), 209-219.

Sankar, M.S., Vega, M.A., Defoe, P.P., Kibria, M.G., Ford, S., Telfeyan, K., Neal, A., Mohajerin, T.J., Hettiarachchi, G.M., Barua, S., Hobson, C., Johannesson, K. and Datta, S. (2014) Elevated arsenic and manganese in groundwaters of Murshidabad, West Bengal, India. *Science of The Total Environment* **488**, 574-583.

Sarkar, A. and Paul, B. (2016) The global menace of arsenic and its conventional remediation - A critical review. *Chemosphere* **158**, 37-49.

Saunders, J.A., Mohammad, S., Korte, N.E., Lee, M.K., Fayek, M., Castle, D. and Barnett, M.O. (2005) Advances in Arsenic Research: Integration of Experimental and Observational Studies and Implications for Mitigation, pp. 191-205.

Seyler, P. and Martin, J.M. (1989) Biogeochemical processes affecting arsenic species distribution in a permanently stratified lake. *Environmental Science & Technology* **23**(10), 1258-1263.

Sharma, A.K., Tjell, J.C., Sloth, J.J. and Holm, P.E. (2014) Review of arsenic contamination, exposure through water and food and low cost mitigation options for rural areas. *Applied Geochemistry* **41**, 11-33.

Sharma, P., Rolle, M., Kocar, B., Fendorf, S. and Kappler, A. (2011) Influence of Natural Organic Matter on As Transport and Retention. *Environmental Science & Technology* **45**(2), 546-553.

Sharma, V.K. and Sohn, M. (2009) Aquatic arsenic: Toxicity, speciation, transformations, and remediation. *Environment International* **35**(4), 743-759.

Sherman, D.M. and Randall, S.R. (2003) Surface complexation of arsenic(V) to iron(III) (hydr)oxides: structural mechanism from ab initio molecular geometries and EXAFS spectroscopy. *Geochimica et Cosmochimica Acta* **67**(22), 4223-4230.

Shi, X., Lei, T., Yan, Y. and Zhang, F. (2016) Determination and impact factor analysis of hydrodynamic dispersion coefficient within a gravel layer using an electrolyte tracer method. *International Soil and Water Conservation Research* **4**(2), 87-92.

Singh, R., Singh, S., Parihar, P., Singh, V.P. and Prasad, S.M. (2015) Arsenic contamination, consequences and remediation techniques: A review. *Ecotoxicology and Environmental Safety* **112**(Supplement C), 247-270.

Singh, T.S. and Pant, K.K. (2004) Equilibrium, kinetics and thermodynamic studies for adsorption of As(III) on activated alumina. *Separation and Purification Technology* **36**(2), 139-147.

Smedley, P.L. and Edmunds, W.M. (2002) Redox patterns and trace-element behavior in the East Midlands Triassic Sandstone Aquifer, UK. *Ground Water* **40**(1), 44-58.

Smedley, P.L. and Kinniburgh, D.G. (2002) A review of the source, behaviour and distribution of arsenic in natural waters. *Applied Geochemistry* **17**(5), 517-568.

Smith, A.H., Lingas, E.O. and Rahman, M. (2000) Contamination of drinking-water by arsenic in Bangladesh: a public health emergency. *Bulletin of the World Health Organization* **78**(9), 1093-1103.

Smith, A.H. and Steinmaus, C.M. (2009) Health Effects of Arsenic and Chromium in Drinking Water: Recent Human Findings. *Annual review of public health* **30**, 107-122.

Smith, E., Smith, J., Smith, L., Biswas, T., Correll, R. and Naidu, R. (2003) Arsenic in Australian Environment: An Overview. *Journal of Environmental Science and Health, Part A* **38**(1), 223-239.

Smith, S.C. and Rodrigues, D.F. (2015) Carbon-based nanomaterials for removal of chemical and biological contaminants from water: A review of mechanisms and applications. *Carbon* **91**, 122-143.

Sorlini, S. and Gialdini, F. (2010) Conventional oxidation treatments for the removal of arsenic with chlorine dioxide, hypochlorite, potassium permanganate and monochloramine. *Water Research* **44**(19), 5653-5659.

Sracek, O., Bhattacharya, P., Jacks, G., Gustafsson, J.-P. and Brömssen, M.v. (2004) Behavior of arsenic and geochemical modeling of arsenic enrichment in aqueous environments. *Applied Geochemistry* **19**(2), 169-180.

Su, S.M., Zeng, X.B., Bai, L.Y., Li, L.F. and Duan, R. (2011) Arsenic biotransformation by arsenic-resistant fungi Trichoderma asperellum SM-12F1, Penicillium janthinellum SM-12F4, and Fusarium oxysporum CZ-8F1. *Science of The Total Environment* **409**(23), 5057-5062.

Sun, H.-J., Rathinasabapathi, B., Wu, B., Luo, J., Pu, L.-P. and Ma, L.Q. (2014) Arsenic and selenium toxicity and their interactive effects in humans. *Environment International* **69**(Supplement C), 148-158.

Szramek, K., Walter, L.M. and McCall, P. (2004) Arsenic mobility in groundwater/surface water systems in carbonate-rich Pleistocene glacial drift

aquifers (Michigan). *Applied Geochemistry* **19**(7), 1137-1155.

Tian, Y., Wu, M., Liu, R., Wang, D., Lin, X., Liu, W., Ma, L., Li, Y. and Huang, Y. (2011) Modified native cellulose fibers—A novel efficient adsorbent for both fluoride and arsenic. *Journal of Hazardous Materials* **185**(1), 93-100.

Toride, N., Leij, F.J. and van Genuchten, M.T. (1993) A comprehensive set of analytical solutions for nonequilibrium solute transport with first-order decay and zero-order production. *Water Resources Research* **29**(7), 2167-2182.

Townsend, T., Dubey, B., Tolaymat, T. and Solo-Gabriele, H. (2005) Preservative leaching from weathered CCA-treated wood. *Journal of Environmental Management* **75**(2), 105-113.

Van Geen, A., Rose, J., Thoral, S., Garnier, J.M., Zheng, Y. and Bottero, J.Y. (2004) Decoupling of As and Fe release to Bangladesh groundwater under reducing conditions. Part II: Evidence from sediment incubations. *Geochimica et Cosmochimica Acta* **68**(17), 3475-3486.

van Geen, A., Zheng, Y., Goodbred, S., Horneman, A., Aziz, Z., Cheng, Z., Stute, M., Mailloux, B., Weinman, B., Hoque, M.A., Seddique, A.A., Hossain, M.S., Chowdhury, S.H. and Ahmed, K.M. (2008) Flushing History as a Hydrogeological Control on the Regional Distribution of Arsenic in Shallow Groundwater of the Bengal Basin. *Environmental Science & Technology* **42**(7), 2283-2288.

Vanbroekhoven, K., Van Roy, S., Gielen, C., Maesen, M., Ryngaert, A., Diels, L. and Seuntjens, P. (2007) Microbial processes as key drivers for metal (im)mobilization along a redox gradient in the saturated zone. *Environmental Pollution* **148**(3), 759-769.

Wang, C., Liu, X., Chen, J.P. and Li, K. (2015) Superior removal of arsenic from water with zirconium metal-organic framework UiO-66. *Scientific Reports* **5**, 16613.

Wang, S.L. and Mulligan, C.N. (2006) Effect of natural organic matter on arsenic release from soils and sediments into groundwater. *Environmental Geochemistry and Health* **28**(3), 197-214.

Welch, A.H., Lico, M.S. and Hughes, J.L. (1988) Arsenic in Ground Water of the Western United States. *Ground Water* **26**(3), 333-347.

Welch, A.H., Westjohn, D.B., Helsel, D.R. and Wanty, R.B. (2000) Arsenic in Ground Water of the United States: Occurrence and Geochemistry. *Ground Water* **38**(4), 589-604.

Whitacre, D.M., Fernanda, M. and Gunther, F.A. (2012) Reviews of environmental contamination and toxicology, Springer.

Wilkie, J.A. and Hering, J.G. (1996) Adsorption of arsenic onto hydrous ferric oxide: effects of adsorbate/adsorbent ratios and co-occurring solutes. *Colloids and Surfaces A: Physicochemical and Engineering Aspects* **107**, 97-110.

Williams, M., Fordyce, F., Paijitprapapon, A. and Charoenchaisri, P. (1996) Arsenic contamination in surface drainage and groundwater in part of the southeast

Asian tin belt, Nakhon Si Thammarat Province, southern Thailand. *Environmental Geology* **27**(1), 16-33.

Winkel, L., Berg, M., Amini, M., Hug, S.J. and Annette Johnson, C. (2008) Predicting groundwater arsenic contamination in Southeast Asia from surface parameters. *Nature Geosci* **1**(8), 536-542.

Wu, Z., Li, W., Webley, P.A. and Zhao, D. (2012) General and Controllable Synthesis of Novel Mesoporous Magnetic Iron Oxide@Carbon Encapsulates for Efficient Arsenic Removal. *Advanced Materials* **24**(4), 485-491.

Xie, X.J., Johnson, T.M., Wang, Y.X., Lundstrom, C.C., Ellis, A., Wang, X.L. and Duan, M.Y. (2013) Mobilization of arsenic in aquifers from the Datong Basin, China: Evidence from geochemical and iron isotopic data. *Chemosphere* **90**(6), 1878-1884.

Xu, J.H., Gao, N.Y., Deng, Y. and Xia, S.Q. (2013) Nanoscale iron hydroxide-doped granular activated carbon (Fe-GAC) as a sorbent for perchlorate in water. *Chemical Engineering Journal* **222**, 520-526.

Yan, X.P., Kerrich, R. and Hendry, M.J. (2000) Distribution of arsenic(III), arsenic(V) and total inorganic arsenic in porewaters from a thick till and clay-rich aquitard sequence, Saskatchewan, Canada. *Geochimica et Cosmochimica Acta* **64**(15), 2637-2648.

Yang, J., Zhang, H., Yu, M., Emmanuelawati, I., Zou, J., Yuan, Z. and Yu, C. (2014) High-Content, Well-Dispersed γ-Fe2O3 Nanoparticles Encapsulated in Macroporous Silica with Superior Arsenic Removal Performance. *Advanced Functional Materials* **24**(10), 1354-1363.

Yu, X., Tong, S., Ge, M., Zuo, J., Cao, C. and Song, W. (2013) One-step synthesis of magnetic composites of cellulose@iron oxide nanoparticles for arsenic removal. *Journal of Materials Chemistry A* **1**(3), 959-965.

Yuan, T., Luo, Q.-F., Hu, J.-Y., Ong, S.-L. and Ng, W.-J. (2003) A Study on Arsenic Removal from Household Drinking Water. *Journal of Environmental Science and Health, Part A* **38**(9), 1731-1744.

Zhang, G.S., Qu, J.H., Liu, H.J., Liu, R.P. and Wu, R.C. (2007) Preparation and evaluation of a novel Fe-Mn binary oxide adsorbent for effective arsenite removal. *Water Research* **41**(9), 1921-1928.

Zhang, H. and Selim, H.M. (2008) Advances in Agronomy, Vol 98, pp. 45-115.

Zhao, Y., Huang, M., Wu, W. and Jin, W. (2009) Synthesis of the cotton cellulose based Fe(III)-loaded adsorbent for arsenic(V) removal from drinking water. *Desalination* **249**(3), 1006-1011.

Zheng, Y., Stute, M., van Geen, A., Gavrieli, I., Dhar, R., Simpson, H.J., Schlosser, P. and Ahmed, K.M. (2004) Redox control of arsenic mobilization in Bangladesh groundwater. *Applied Geochemistry* **19**(2), 201-214.

Zhu, H., Jia, Y., Wu, X. and Wang, H. (2009) Removal of arsenic from water by supported nano zero-valent iron on activated carbon. *Journal of Hazardous Materials* **172**(2), 1591-1596.